

4 PLATES

(This table of contents just added for convenience to understand the new chapter structure, to be cut in final version)

4	PLATES	1
4.1	INTRODUCTION.....	3
4.2	ELASTIC LOCAL BUCKLING OF FLAT PLATES	5
4.2.1	Uniform Compression.....	5
4.2.2	Compression and Bending	7
4.2.3	Shear	9
4.2.4	Shear and Compression	11
4.2.5	Shear and Bending	12
4.2.6	Biaxially Compressed	14
4.2.7	Longitudinally varying Compression	14
4.2.8	Plates on one-way foundations	15
4.2.9	Singly curved plates.....	16
4.2.10	Square Plate with a Central Hole	16
4.2.11	Rectangular Plate with Multiple Holes	17
4.3	INELASTIC BUCKLING, POST-BUCKLING, AND STRENGTH OF FLAT PLATES	21
4.3.1	Inelastic buckling.....	22
4.3.2	Post-buckling	22
4.3.3	Strength and Effective Width.....	24
4.3.4	Strength in shear and combined loadings with shear	32
4.3.5	Strength of biaxially compressed plates.....	33
4.3.6	Average stress and strength of aluminum plates.....	34
4.3.7	Yield-line analysis and plastic buckling of plates.....	35
4.3.8	Energy dissipation (steel plate shear wall).....	36
4.4	BUCKLING, POST-BUCKLING AND STRENGTH OF STIFFENED PLATES	38
4.4.1	Compression: Buckling.....	38
4.4.2	Compression: Post-buckling and Strength.....	43
4.4.3	Compression and Shear: Buckling.....	47
4.4.4	Compression and Shear: Post-buckling and Strength.....	49
4.4.5	Laterally Loaded plates in compression.....	49
4.5	BUCKLING OF ORTHOTROPIC PLATES	51
4.5.1	Compression	52
4.5.2	Biaxial compression.....	53
4.5.3	Shear	55
4.6	INTERACTION BETWEEN PLATE ELEMENTS	58
4.6.1	Buckling Modes of a Plate Assembly	58
4.6.2	Local Buckling of a Plate Assembly.....	60
4.6.3	Post-buckling of a Plate Assembly	62
4.7	REFERENCES.....	63

List of Figures

Fig. 4.1 Compression or flexural members.....	3
Fig. 4.2 Local plate buckling coefficient, k of Eq. 4.1, for plates in compression with varied boundary conditions ...	6
Fig. 4.3 Plate buckling coefficient, k , as a function of normalized plate length ($\beta=a/b$) for different boundary conditions, m =number of buckled half-waves along the length of the plate (after Yu and Schafer (2007)) ...	7
Fig. 4.4 Plate buckling coefficients for long plates under compression and bending (Brockenbrough and Johnston, 1974; Bijlaard, 1957).....	8
Fig. 4.5 Plate buckling coefficients for unstiffened elements in compression and bending, after (Bambach and Rasmussen 2004a).....	9
Fig. 4.6 Plate buckling coefficients for plates in pure shear. (Side b is the short side.).....	10
Fig. 4.7 Interaction curve for buckling of flat plates under shear and uniform compression.	12
Fig. 4.8 Buckling coefficients for plates in combined bending and shear.	13
Fig. 4.9 Interaction curve for buckling of flat plates under shear, compression, and bending.	14
Fig. 4.10 Simply supported plate subject to a longitudinal stress gradient (note shear stresses are required for equilibrium, after (Yu and Schafer 2007))	15
Fig. 4.11 Simply supported and clamped plates with hole under shear loading (Rockey et al., 1969).....	17
Fig. 4.12 Illustration of unstiffened strips adjacent to a hole.....	18
Fig. 4.13 Critical shear stress for webs with holes (Michael, 1960).....	19
Fig. 4.14 Perforated rectangular plate under combined action of shear and bending.	20
Fig. 4.15 Simple model for post-buckling of a flat plate in uniform compression (after AISI 2007).....	23
Fig. 4.16 Post-buckling stiffness of plates having simply supported edges (Allen and Bulson, 1980)	24
Fig. 4.17 Longitudinal stress after buckling and definition of effective width.....	25
Fig. 4.18 Chart for determining σ_e/σ_y	28
Fig. 4.19 Nondimensional buckling curves for plates under uniform edge compression (adapted from Brockenbrough and Johnston, 1974).	29
Fig. 4.20 Distributing effective width in plates under a stress gradient, after (Schafer and Peköz 1999)	31
Fig. 4.21 Shear and tension fields (square plate).	33
Fig. 4.22 Equations for buckling stress and ultimate strength of plates used in Aluminum Association specifications (AA, 1994).	35
Fig. 4.23 Hysteretic response of a steel plate shear wall under cyclic loading (Lubell et al. 2000)	36
Fig. 4.24 Hysteretic response of steel plate shear walls with cutouts (Hitaka and Matsui 2003)	37
Fig. 4.25 Stiffened plate panels; (a) panel with longitudinal stiffeners; (b) panel with transverse stiffeners.	38
Fig. 4.26 Buckling of columns with elastic supports.....	42
Fig. 4.27 Initial and final buckled shapes	44
Fig. 4.28 Column curve for stiffened panels.....	45
Fig. 4.29 Column chart by Gerard and Becker (1957/1958).	45
Fig. 4.30 Longitudinally stiffened plate under combined compression and shear stresses.....	48
Fig. 4.31 Analytical interaction relations for infinitely wide stiffened plate under combined compression and shearing stresses.	48
Fig. 4.32 Analytically predicted elastic and inelastic interaction curves for an integrally stiffened panel.	49
Fig. 4.33 Idealized beam-column.	50
Fig. 4.34 Plate subjected to axial and shear stress.	51
Fig. 4.35 Function f_1 in Eq. 4.5.....	52
Fig. 4.36 Functions f_2 and f_3 in Eq. 4.52.	53
Fig. 4.37 Buckling coefficients for orthotropic plates.	54
Fig. 4.38 Interaction curve for orthotropic plates.	55
Fig. 4.39 Shear buckling coefficients for orthotropic plates. [Adapted from Johns (1971), printed with the permission of Her Majesty's Stationery Office.].....	56
Fig. 4.40 Stability response of an I-beam in major axis bending using the finite strip method (a) half-wavelength vs. buckling stress, (b) buckling mode shapes, (c) plate buckling coefficient (Hancock 1978).....	59
Fig. 4.41 Plate buckling coefficients for plate assemblies (Kroll et al., 1943)	61

Tables

Table 4.1 Coefficients for plate buckling under longitudinal stress gradients.....	15
Table 4.2 Limiting Values of gamma for Transverse Stiffeners.....	42

4.1 INTRODUCTION

Metal compression or flexural members (Fig. 4.1, excepting Fig. 4.1a) typically employ cross-sectional shapes which may be idealized as a composition of elements, or flat plates. When a plate element is subjected to direct compression, bending, shear, or a combination of these stresses in its plane, the plate may buckle locally before the member as a whole becomes unstable or before the yield stress of the material is reached. Such local buckling behavior is characterized by distortion of the cross-section of the member. Contrary to the notion of buckling being a sudden or discontinuous phenomena, the almost inevitable presence of initial out-of-planeness (imperfections) results in a gradual growth of this cross-sectional distortion with no sudden discontinuity in real behavior at the theoretical critical load.

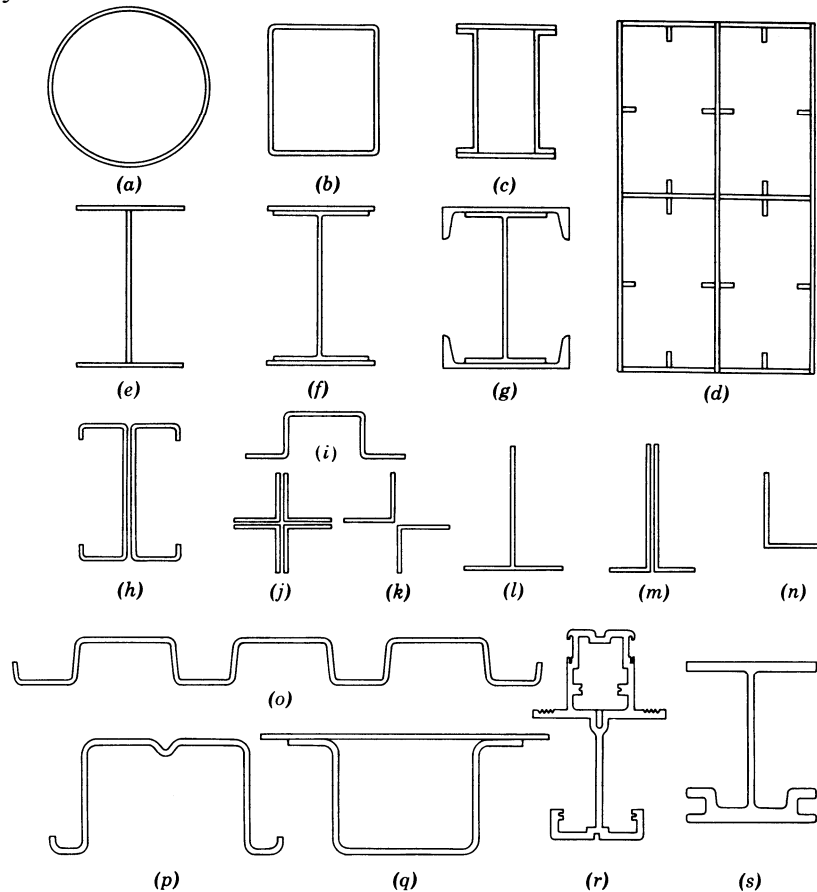


Fig. 4.1 Compression or flexural members

The theoretical, or elastic critical local buckling load is not on its own a satisfactory basis for design. Ultimate strength of plates may be less than the critical local buckling load due to yielding, or may be in excess of the critical local buckling load due to beneficial post-buckling reserve. For example, a slender plate loaded in uniaxial compression, with both longitudinal edges supported, will undergo stress redistribution as well as develop transverse tensile membrane stresses after buckling that provide post-buckling reserve. Thus, additional load may often be applied without structural damage. Initial imperfections in such a plate may cause deformations to begin below the buckling load, yet unlike an initially imperfect column, the plate may sustain loads greater than the theoretical buckling load. Despite its limitations the critical

local buckling load typically forms the basis for an initial evaluation of plates and is the focus of the first section of this Chapter.

After considering elastic local buckling of flat plates in Section 4.2, the inelastic buckling, post-buckling, and ultimate strength of flat plates is discussed in Section 4.3. Particular attention is paid to the effective width method, which is an approximate method for ultimate strength determination which is still in wide use in design today. Flat plates are often augmented with stiffeners, both longitudinally and transversally, these stiffeners improve and complicate the response as detailed in Section 4.4. One common approximation for stiffened plates is to treat the stiffened plate as a flat plate with orthotropic properties, this approximation is detailed in Section 4.5. Finally, in Section 4.6, the concluding section of this chapter, the interaction of plate elements which make up cross-sections such as those of Fig. 4.1 are discussed along with the three modes of cross-section instability: local, distortional, and global buckling inherent to most thin-walled members. Significant additional material related to the topics examined in this chapter are provided in Chapters 6, 7 and 13 of this Guide.

4.2 ELASTIC LOCAL BUCKLING OF FLAT PLATES

An examination of the buckling behavior of a single plate supported along its edges is an essential preliminary step toward the understanding of local buckling behavior of plate assemblies. The buckling stresses are obtained from the concept of bifurcation of an initially perfect structure. In practice, the response of the structure is continuous, due to the inevitable presence of initial imperfections. Thus the critical stress is best viewed as a useful index to the behavior, as slender plates can continue to carry additional loads well after initial buckling. Post-buckling and strength of plates is discussed in Section 4.3.

When the member cross section is composed of various connected elements (see Fig. 4.1) a lower bound of the critical stress can be determined by assuming, for each plate element, a simple support condition for each edge attached to another plate element or a free condition for any edge not so attached. The smallest value of the critical stress found for any of the elements is a lower bound of the critical stress for the cross section. This lower bound approximation may be excessively conservative for many practical design situations, more thorough methods are discussed in Section 4.3.8.

4.2.1 Uniform Compression

Long Rectangular Plates. In 1891, Bryan (1891) presented the analysis of the elastic critical stress for a rectangular plate simply supported along all edges and subjected to a uniform longitudinal compressive stress. The elastic critical stress of a long plate segment is determined by the plate width-to-thickness ratio b/t , by the restraint conditions along the longitudinal boundaries, and by the elastic material properties (elastic modulus, E , and Poisson's ratio ν). The elastic critical stress, σ_c , is expressed as

$$\sigma_c = k \frac{\pi^2 E}{12(1-\nu^2)(b/t)^2} \quad (4.1)$$

in which k is a *plate buckling coefficient* determined by a theoretical critical-load analysis; k is a function of plate geometry and boundary conditions such as those shown in Fig. 4.2.

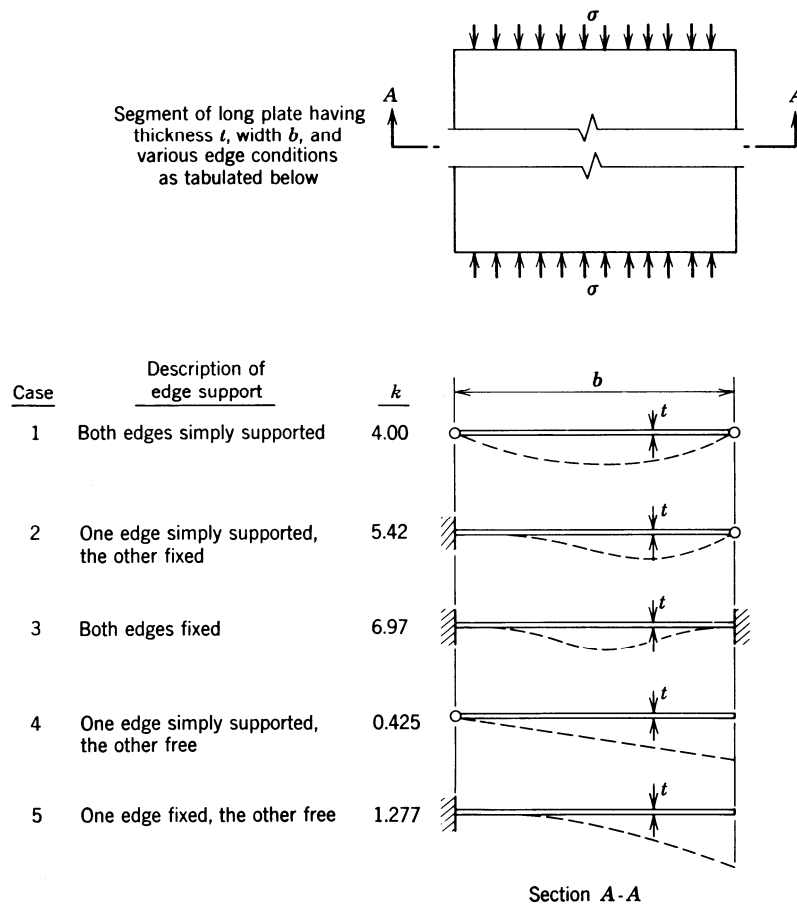


Fig. 4.2 Local plate buckling coefficient, k of Eq. 4.1, for plates in compression with varied boundary conditions

Short Plates. When a plate element is relatively short in the direction of the compressive stress there may exist an influence in the elastic buckling stress due to the fact that the buckled half-waves which take integer values are forced into a finite length plate. Fig. 4.3 demonstrates how k varies as a function of normalized plate length; the variation is a function of the plate boundary conditions and the loading. Full analytical solutions for k as a function of a/b and m may be found in Timoshenko and Gere (1961), Allen and Bulson (1980) and others. When a plate element is very short in the direction of the compressive stress (i.e. $a/b \ll 1$), the critical stress may be conservatively estimated by assuming that a unit width of plate behaves like a column.

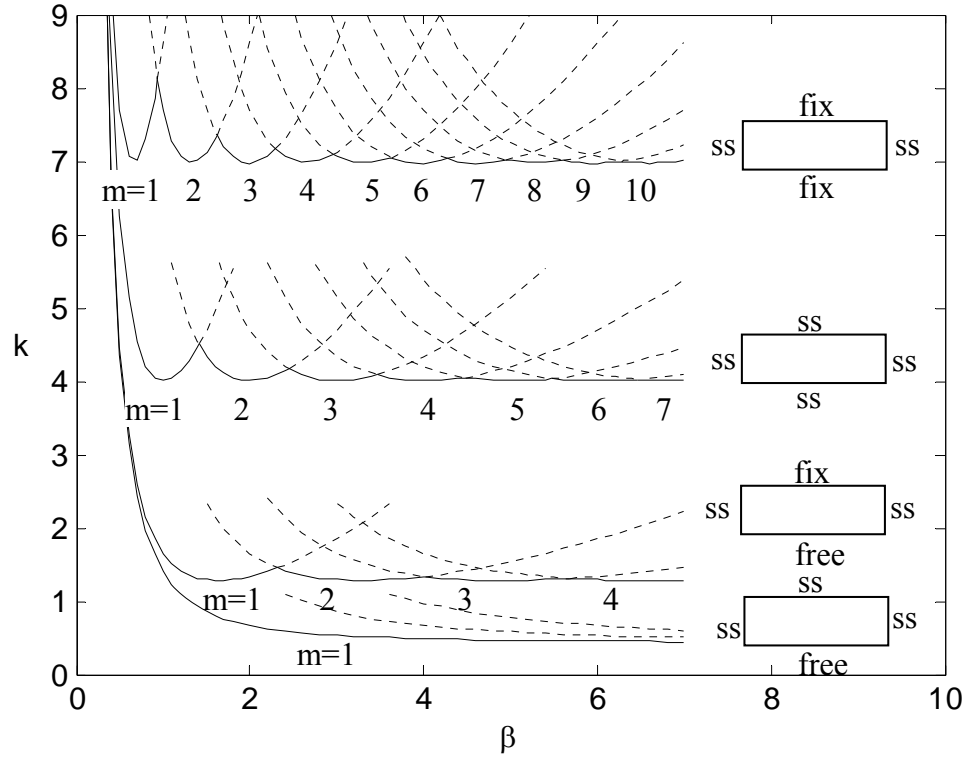
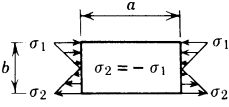
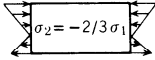
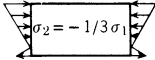
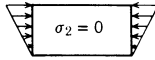
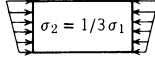
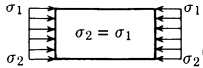


Fig. 4.3 Plate buckling coefficient, k , as a function of normalized plate length ($\beta=a/b$) for different boundary conditions, m =number of buckled half-waves along the length of the plate (after Yu and Schafer (2007))

4.2.2 Compression and Bending

When compression plus bending loads are applied to a structural member, plate elements of the member can be subjected to in-plane stresses which vary along the loaded edges of the plate, from a maximum compressive stress, σ_1 , to a minimum stress, σ_2 , as shown in Fig. 4.4. For this situation, elastic critical plate stresses are dependent on the edge-support conditions and the ratio of bending stress to uniform compression stress. Long plate values of k_c that can be substituted for k in Eq. 4.1 are tabulated in Fig. 4.4 for several cases. For plates with a free edge the k_c values vary slightly with Poisson's ratio.

Loading	Ratio of Bending Stress to Uniform Compression Stress σ_{cb}/σ_c	Minimum Buckling Coefficient, $*k_c$					
		Unloaded Edges Simply Supported	Unloaded Edges Fixed	Top Edge Free		Bottom Edge Free	
				Bottom Edge Simply Supported	Bottom Edge Fixed	Top Edge Simply Supported	Top Edge Fixed
 $\sigma_2 = -\sigma_1$ (pure bending)	∞	23.9	39.6	0.85	2.15		
 $\sigma_2 = -2/3 \sigma_1$	5.00	15.7					
 $\sigma_2 = -1/3 \sigma_1$	2.00	11.0					
 $\sigma_2 = 0$	1.00	7.8	13.6	0.57	1.61	1.70	5.93
 $\sigma_2 = 1/3 \sigma_1$	0.50	5.8					
 $\sigma_2 = \sigma_1$ (pure compression)	0.0	4.0	6.97	0.42	1.33	0.42	1.33

*Values given are based on plates having loaded edges simply supported and are conservative for plates having loaded edges fixed.

Fig. 4.4 Plate buckling coefficients for long plates under compression and bending (Brockenbrough and Johnston, 1974; Bijlaard, 1957).

Beyond the k values provided in Fig. 4.4 closed-form expressions also exist for the compression and bending case. For plates simply supported on all four sides k may be found based on the work of Peköz (1987) to be:

$$k_c = 4 + 2(1 - \psi)^3 + 2(1 - \psi) \quad (4.2)$$

where $\psi = \sigma_1/\sigma_2$. For plates with one longitudinal edge free Bambach and Rasmusen (2004a) provide a series of solutions summarized in Fig. 4.5. These closed-form expressions for k are employed in the AISI (2007) Specification. Diagrams for buckling coefficients for rectangular plates under combined bending and compressive stresses in two perpendicular directions are given by Yoshizuka and Naruoka (1971).

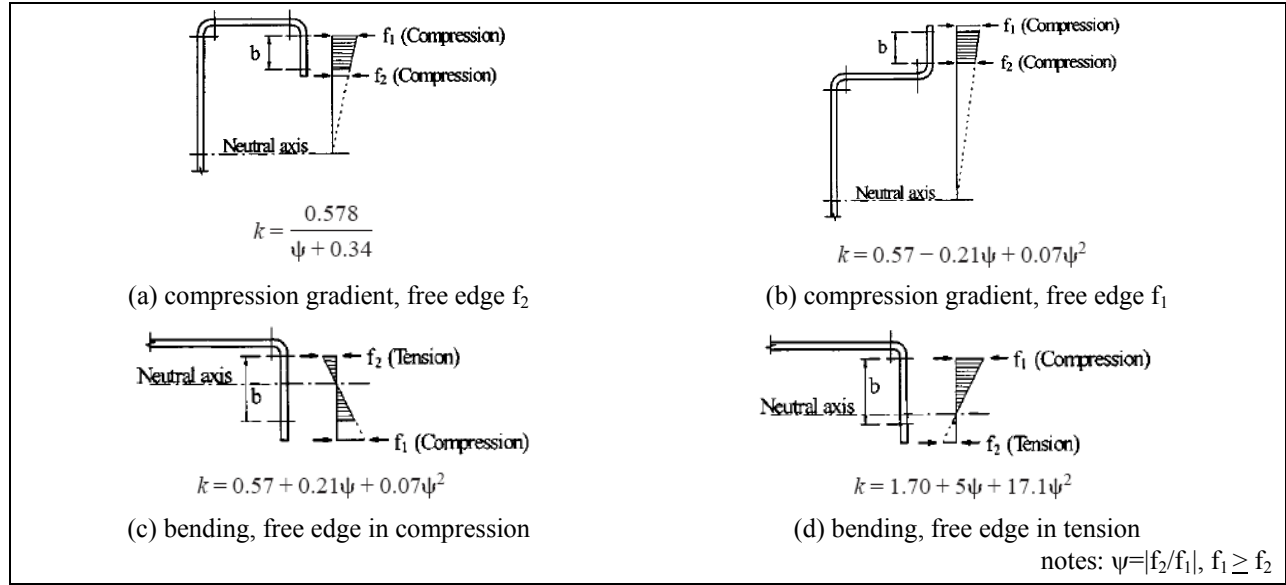


Fig. 4.5 Plate buckling coefficients for unstiffened elements in compression and bending, after (Bambach and Rasmussen 2004a)

4.2.3 Shear

When a plate is subjected to edge shear stresses as shown in Fig. 4.6, it is said to be in a state of *pure shear*. The critical shear buckling stress can be obtained by substituting τ_c and k_s , for σ_c and k in Eq. 4.1, in which k_s is the buckling coefficient for shear buckling stress. Critical stress coefficients, k_s , for plates subjected to pure shear have been evaluated for three conditions of edge support. In Fig. 4.9 these are plotted with the side b , as used in Eq. 4.1, always assumed to be shorter than side a . Thus α is always greater than 1 and by plotting k_s in terms of $1/\alpha$, the complete range of k_s can be shown and the magnitude of k_s remains manageable for small values of α . However, for application to plate-girder design it is convenient to define b (or h in plate-girder applications) as the vertical dimension of the plate-girder web for a horizontal girder. Then α may be greater or less than unity and empirical formulas for k_s together with source data are as follows:

Plate Simply Supported on Four Edges. Solutions developed by Timoshenko (1910), Bergmann and Reissner (1932), and Seydel (1933) are approximated by Eqs. 4.3a and 4.3b, in which $\alpha = a/b$:

$$k_s = \begin{cases} 4.00 + \frac{5.34}{\alpha^2} & \text{for } \alpha \leq 1 \\ 5.34 + \frac{4.00}{\alpha^2} & \text{for } \alpha \geq 1 \end{cases} \quad (4.3a)$$

$$k_s = \begin{cases} 4.00 + \frac{5.34}{\alpha^2} & \text{for } \alpha \leq 1 \\ 5.34 + \frac{4.00}{\alpha^2} & \text{for } \alpha \geq 1 \end{cases} \quad (4.3b)$$

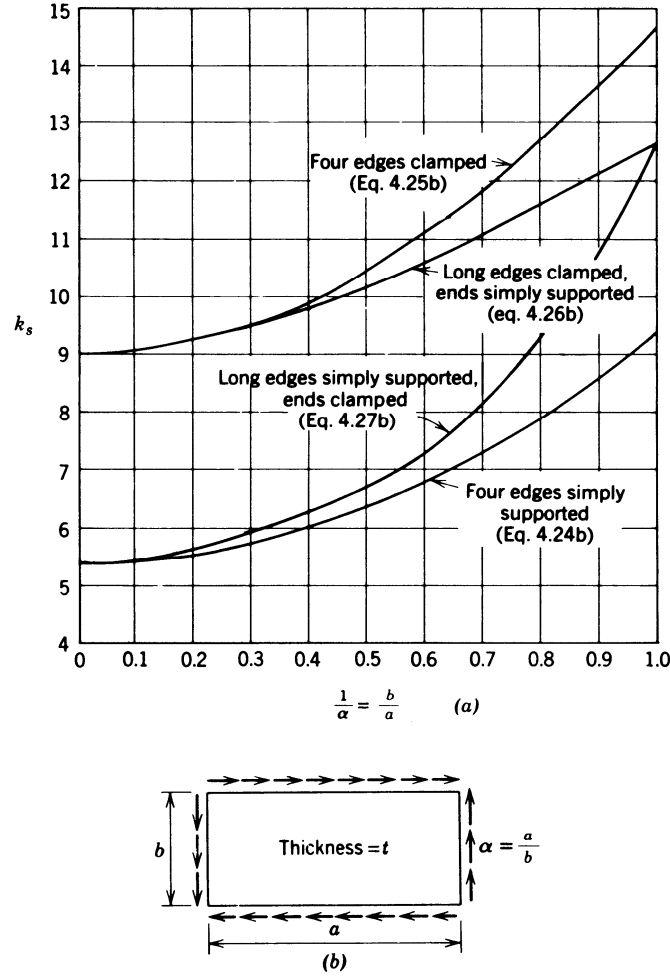


Fig. 4.6 Plate buckling coefficients for plates in pure shear. (Side b is the short side.)

Plate Clamped on Four Edges. In 1924, Southwell and Skan obtained $k_s = 8.98$ for the case of the infinitely long rectangular plate with clamped edges. For the finite-length rectangular plate with clamped edges, Moheit (1939) obtained

$$k_s = \begin{cases} 5.6 + \frac{8.98}{\alpha^2} & \text{for } \alpha \leq 1 \\ 8.98 + \frac{5.6}{\alpha^2} & \text{for } \alpha \geq 1 \end{cases} \quad (4.4a)$$

$$k_s = \begin{cases} 5.6 + \frac{8.98}{\alpha^2} & \text{for } \alpha \leq 1 \\ 8.98 + \frac{5.6}{\alpha^2} & \text{for } \alpha \geq 1 \end{cases} \quad (4.4b)$$

Plate Clamped on Two Opposite Edges and Simply Supported on the Other Two Edges. A solution for this problem has been given by Iguchi (1938) for the general case, and by Leggett (1941) for the case of the square plate. Cook and Rockey (1963) later obtained solutions considering the antisymmetric buckling mode which was not considered by Iguchi. The expressions below were obtained by fitting a polynomial equation to the Cook and Rockey results as shown in Fig. 2.36 of the book by Bulson (1970).

For long edges clamped,

$$k_s = \begin{cases} \frac{8.98}{\alpha^2} + 5.61 - 1.99\alpha & \text{for } \alpha \leq 1 \\ 8.98 + \frac{5.61}{\alpha^2} - \frac{1.99}{\alpha^3} & \text{for } \alpha \geq 1 \end{cases} \quad (4.5a)$$

$$k_s = \begin{cases} \frac{8.98}{\alpha^2} + 5.61 - 1.99\alpha & \text{for } \alpha \leq 1 \\ 8.98 + \frac{5.61}{\alpha^2} - \frac{1.99}{\alpha^3} & \text{for } \alpha \geq 1 \end{cases} \quad (4.5b)$$

and for short edges clamped,

$$k_s = \begin{cases} \frac{5.34}{\alpha^2} + \frac{2.31}{\alpha} - 3.44 + 8.39\alpha & \text{for } \alpha \leq 1 \\ 5.34 + \frac{2.31}{\alpha} - \frac{3.44}{\alpha^2} + \frac{8.39}{\alpha^3} & \text{for } \alpha \geq 1 \end{cases} \quad (4.6a)$$

$$k_s = \begin{cases} \frac{5.34}{\alpha^2} + \frac{2.31}{\alpha} - 3.44 + 8.39\alpha & \text{for } \alpha \leq 1 \\ 5.34 + \frac{2.31}{\alpha} - \frac{3.44}{\alpha^2} + \frac{8.39}{\alpha^3} & \text{for } \alpha \geq 1 \end{cases} \quad (4.6b)$$

Curves for $\alpha \geq 1$ are plotted in Fig. 4.6. Tension and compression stresses exist in the plate, equal in magnitude to the shear stress and inclined at 45° . The destabilizing influence of compressive stresses is resisted by tensile stresses in the perpendicular direction, often referred to as ‘tension field action’ in the literature. Unlike the case of edge compression, the buckling mode is composed of a combination of several waveforms and this is part of the difficulty in the buckling analysis for shear.

4.2.4 Shear and Compression

The case of shear combined with longitudinal compression, with all sides simply supported, was treated by Iguchi (1938). His results are approximated by the following interaction equation, also shown graphically in Fig. 4.7:

$$\frac{\sigma_c}{\sigma_c^*} + \left(\frac{\tau_c}{\tau_c^*} \right)^2 = 1 \quad (4.7)$$

where σ_c^* and τ_c^* denote critical stress, respectively, under compression or shear alone.

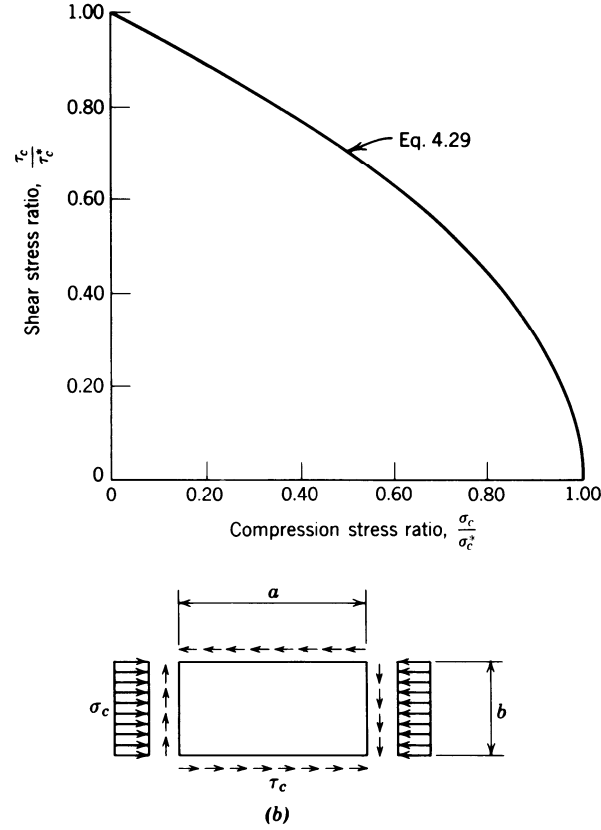


Fig. 4.7 Interaction curve for buckling of flat plates under shear and uniform compression.

Equation 4.7, shown in Fig. 4.7, is for ratios of a/b greater than unity. Batdorf and associates (Batdorf and Houbolt, 1946; Batdorf and Stein, 1947) have shown that when the loaded side b is more than twice as long as a , Eq. 4.29 becomes overly conservative. This situation is the exception in actual practice, and Eq. 4.7 may be accepted for engineering design purposes.

4.2.5 Shear and Bending

For a plate simply supported on four sides, under combined bending and pure shear, Timoshenko (1934) obtained a reduced k_c as a function of τ_c / τ_c^* for values of $\alpha = 0.5, 0.8$, and 1.0 , where τ_c is the actual shearing stress and τ_c^* is the buckling stress for pure shear. This problem was also solved by Stein (1936) and Way (1936), whose results for four values of α are plotted in Fig. 4.8. Chwalla (1936a) suggested the following approximate interaction formula, which agrees well with the graphs of Fig. 4.8.

$$\left(\frac{\sigma_{cb}}{\sigma_{cb}^*} \right)^2 + \left(\frac{\tau_c}{\tau_c^*} \right)^2 = 1 \quad (4.8)$$

For a plate simply supported on four sides, under combined bending and direct stress at the ends (of dimension b), combined with shear, an approximate evaluation of the critical combined load is obtained by use of a three-part interaction formula, Eq. 4.9 (Gerard and Becker, 1957/1958).

$$\frac{\sigma_c}{\sigma_c^*} + \left(\frac{\sigma_{cb}}{\sigma_{cb}^*} \right)^2 + \left(\frac{\tau_c}{\tau_c^*} \right)^2 = 1 \quad (4.9)$$

The foregoing problem, with the further addition of vertical compressive force along the top and bottom edges of length a , has been treated by McKenzie (1964) with results given in the form of interaction graphs. The results are in good agreement with the special case of Eq. 4.9. Interaction equation 4.9, valid when a/b is greater than unity, is shown graphically in Fig. 4.9, as presented in Brockenbrough and Johnston (1974).

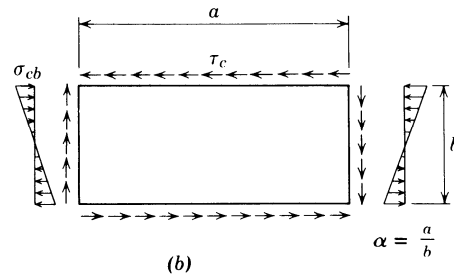
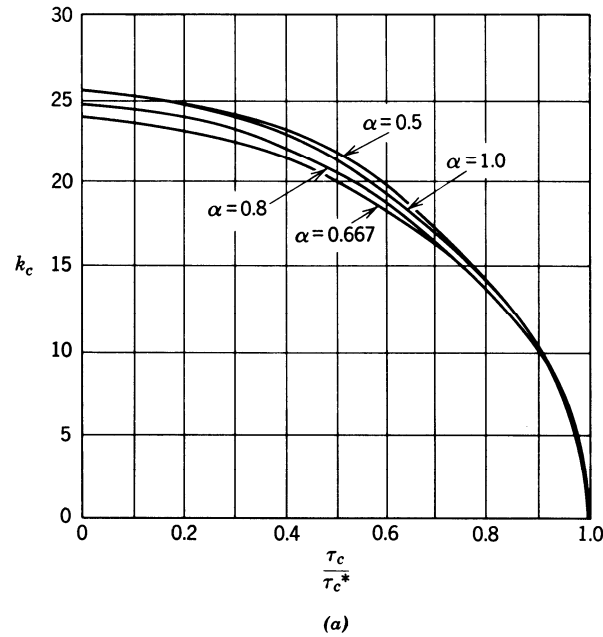


Fig. 4.8 Buckling coefficients for plates in combined bending and shear.

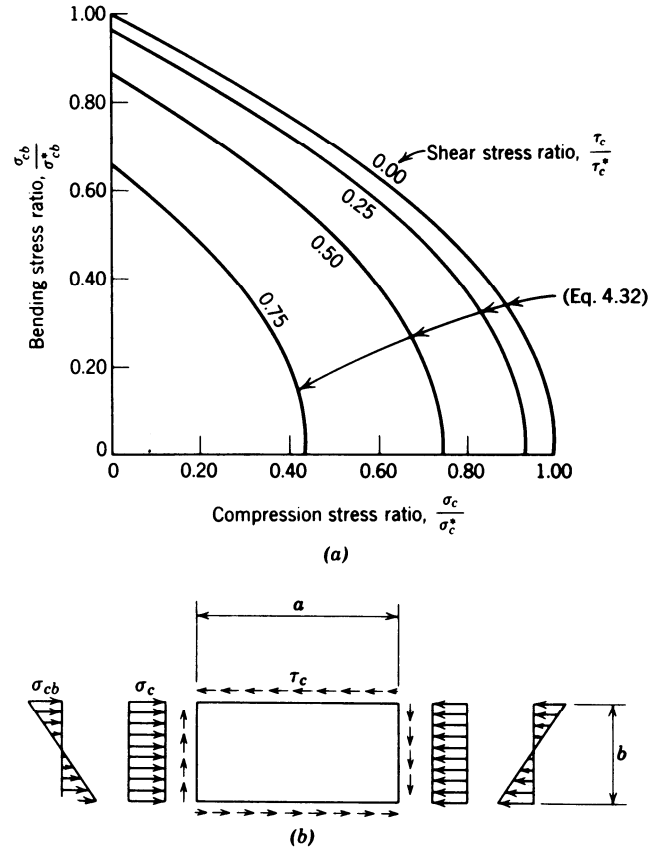


Fig. 4.9 Interaction curve for buckling of flat plates under shear, compression, and bending.

4.2.6 Biaxially Compressed

Pavlovic and Baker (1989) presented an exact solution for the stability of a rectangular plate under biaxial compression. The case when both longitudinal and transverse stresses were uniform was used as a starting point to investigate the much more complex problem of partial loading on two opposite edges. A parametric study was carried out covering different plate geometrics, load ratios, and varying edge lengths over which the applied load acted. The limiting cases of very long and very wide plates were considered in the study, as was the problem in which two opposite edges were subjected to concentrated forces.

4.2.7 Longitudinally varying Compression

When members such as those of Fig. 4.1 are used as beams they are typically exposed to a moment gradient. Under a moment gradient, the plate which comprises the compression flange is subject to a longitudinal variation in the compression force, as shown in Fig. 4.10.

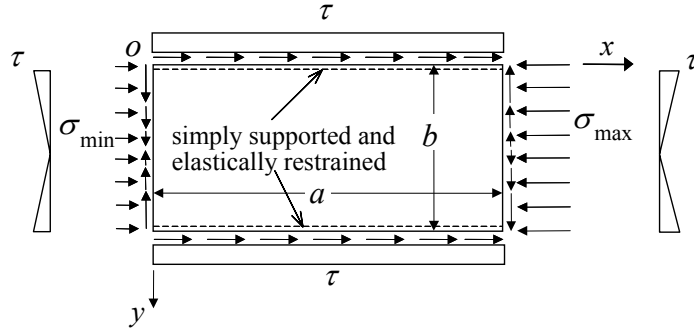


Fig. 4.10 Simply supported plate subject to a longitudinal stress gradient (note shear stresses are required for equilibrium, after (Yu and Schafer 2007))

This case was first treated by Libove, Ferdman et al. (1949), recently Yu and Schafer (2007) provided a closed-form expression for k :

$$k = k_{\infty} + \frac{\alpha_1 r + \alpha_2}{\alpha_3 r + \alpha_4 + \beta^{\alpha_5}} \quad (4.10)$$

where, k_{∞} is the traditional plate buckling coefficient (i.e., k for pure compression as the plate length tends to infinity), r is the stress gradient ($\sigma_{\min}/\sigma_{\max}$), β is the plate aspect ratio (a/b), and α_1 through α_5 are empirical coefficients dependent on the plate boundary conditions along the unloaded longitudinal edges. Table 4.1 summarizes those coefficients.

Table 4.1 Coefficients for plate buckling under longitudinal stress gradients

	k_{∞}	α_1	α_2	α_3	α_4	α_5
ss-ss	4.000	-1.70	1.70	0.20	-0.20	0.75
fix-fix	6.970	-2.20	2.20	0.20	-0.20	0.65
ss-free	0.425	-0.80	1.00	0.00	-0.60	0.95
fix-free	1.277	-0.60	0.60	0.00	-0.65	0.60

Note: applicable for $1 \leq \beta \leq 30$ and $-1 \leq r \leq 1$, ss = simply supported

4.2.8 Plates on one-way foundations

Often, one way considered to constrain local buckling in metal plates is to have the thin plate adjacent to a foundation of some sort, for example thin steel plate may be adjacent to a concrete beam, or the bottom flange of a beam may rest against a floor, foundation, or the ground. If the foundation is two-way (i.e. works in tension and compression) then the buckling load essentially follows the foundation stiffness, and traditional methods such as those of Timoshenko and Gere (1961) may readily be used, the energy from the foundation simply needs to be included in the formulation. The more common case is a foundation that is only engaged when the thin plate buckles into the foundation, this is known as a tensionless or one-way foundation. The elastic critical local buckling load for this case has seen some study, in particular the work of Smith, Bradford et al. (1999) provide plate buckling coefficients, k , for one-way foundations in compression, bending, shear, and combinations thereof. An important practical finding that may be gleaned from Shahwan and Waas (1998) is that the increase in the elastic critical local buckling load, even for a rigid one-way foundation is limited. For instance, in uniform compression the increase in k due to a rigid one-way foundation is only to 5.33 (from 4.0). Thus suggesting that one-way foundations only provide a limited relief from local buckling.

4.2.9 Singly curved plates

It is not uncommon that one of the members of Fig. 4.1 may be curved either in plan or profile. In such a case the plates making up the cross-section are singly curved. Featherston and Ruiz (1998) provide a summary of the fundamental work in this area as well as additional testing to verify the available plate buckling coefficients. A common application for this situation is the horizontally curved steel I-girder treated in Chapter 9 of this Guide. Recent work on elastic buckling of plates in I-girders (Davidson et al. 1999) is detailed in Chapter 9.

4.2.10 Square Plate with a Central Hole

Designers frequently find it necessary to introduce openings in the webs of girders and other large plate structures. The introduction of an opening changes the stress distribution within the member and will, in many instances, also change the mode of failure. Buckling is a key aspect in the behavior of thin perforated plates. This section covers the case of a square plate with a single hole, while the following section covers the case of a rectangular plate with multiple holes.

Compression: Though limited in many respects the first problem to see significant study in this area was that of a square plate with a central hole and either simply supported or clamped-edge conditions, research includes: Levy et al. (1947), Kumai (1952), Schlack (1964), Kawai and Ohtsubo (1968), and Fujita et al. (1970). The work indicates reductions in the plate buckling coefficient of 25% from the unperforated k for holes on the order of 50% of the width of the square plate. Square holes are shown to result in greater reductions than round holes of the same diameter (Yang, 1969). Uniform stress loading is shown to be more critical than uniform displacement loading on the member edges. Also, it has been demonstrated that by suitably reinforcing the hole, it is possible to increase the critical stress beyond that of the unperforated plate (Levy et al., 1947).

Shear: The buckling of a square plate with a central circular cutout has been examined by Rockey et al. (1969) using the finite element method. The relationship between the buckling stress of the plate and the relative size of the hole (d/b) was obtained for both simply supported and clamped-edge conditions. Rockey's work suggests a simple linear relationship between the critical stress and the d/b ratio in the form

$$\tau_{cp} = \tau_c \left(1 - \frac{d}{b} \right) \quad (4.11)$$

where τ_{cp} and τ_c are the critical stresses for the perforated plate and unperforated plate, respectively. The relationship holds for both clamped and simply supported end conditions (Fig. 4.11). Shear buckling of square perforated plates was also investigated by Grosskurth et al. (1976) using the finite element approach. They considered the case of uniform shear deformation instead of uniform shear stress and obtained critical stresses that were in closer agreement with, although higher than, the experimental values.

The behavior of plates with cutouts reinforced by a ring formed by a pressing process was also studied by Rockey, both analytically and experimentally (Rockey, 1980). It was found that the buckling stress increases with t_r/t , the ratio of the depth of the lip to the plate thickness, and the larger the hole, the greater must be the t_r/t ratio to achieve a buckling strength equal to that of the unperforated plate.

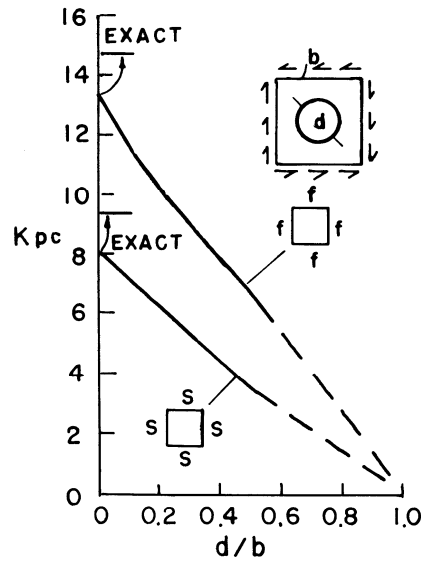


Fig. 4.11 Simply supported and clamped plates with hole under shear loading (Rockey et al., 1969).

Combined loads: Elastic buckling of square plates with holes under combined loads: compression, bending, and shear are considered by Brown and Yettram (1986).

4.2.11 Rectangular Plate with Multiple Holes

Compression: Recent research on elastic buckling of rectangular plates with holes under compression loading provide a more nuanced picture than the early results on square plates detailed in the previous section. In a square plate with a hole the buckling mode shape is constricted to the width of the plate, in rectangular plates longer buckling mode shapes are possible and likely. Research employing thin shell finite element analysis shows that the presence of holes can either increase or decrease the critical elastic buckling stress as well as change the length and quantity of the buckled half-waves, depending upon the quantity of hole material removed relative to the size of the plate, as well as the hole spacing (May and Ganaba 1988, Brown 1990, Brown and Yettram 2000; El-Sawy and Nazmy 2001; Moen and Schafer 2006).

However, the research on square plates with holes, in particular Kawai and Ohtsubo (1968), did lead to a useful approximation of elastic buckling stress for rectangular plates with holes, based on assuming the strips adjacent to the hole act as unstiffened elements (i.e., plates with one free edge) in compression (see Fig. 4.12). For a plate in uniform compression the “unstiffened strip” buckling stress uses Eq. 4.1 with h_A or h_B replacing b and $k=0.425$ per Fig. 4.2. case 4.

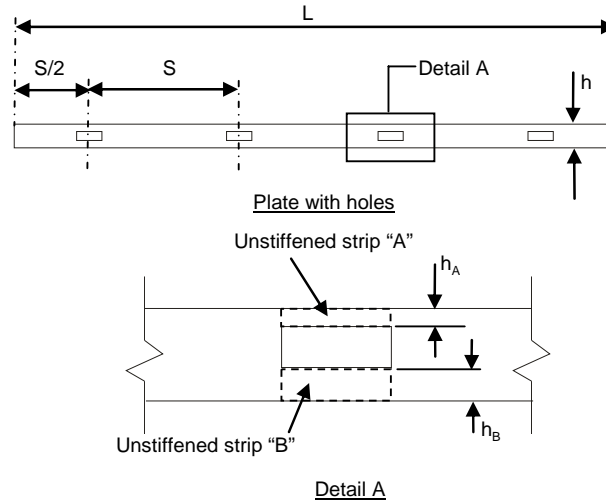


Fig. 4.12 Illustration of unstiffened strips adjacent to a hole

The unstiffened strip approximation is useful, but one must also consider the possibility of buckling away from the hole. In addition the length of the hole, as well as its width, can influence the results. Moen and Schafer (2008) provide expressions for the plate buckling coefficient, k , that account for these effects. Further, their work also covers the case of a rectangular plate with holes in which one longitudinal edge is supported and the other free.

Bending: The problem of a rectangular plate with holes in bending has seen little attention, in part due to the fact that shear is often more critical in this situation. Moen and Schafer (2008) provide plate buckling coefficients for stiffened and unstiffened elements under bending with holes present along the length of the plate.

Shear: The problem of a long shear web with holes has been examined by Michael (1960); he suggested semiempirical expressions for the critical stress in terms of d/a and a/b (notation indicated in Fig. 4.16). These are plotted graphically in Fig. 4.16 and are applicable for the web fixed along the top and bottom edges.

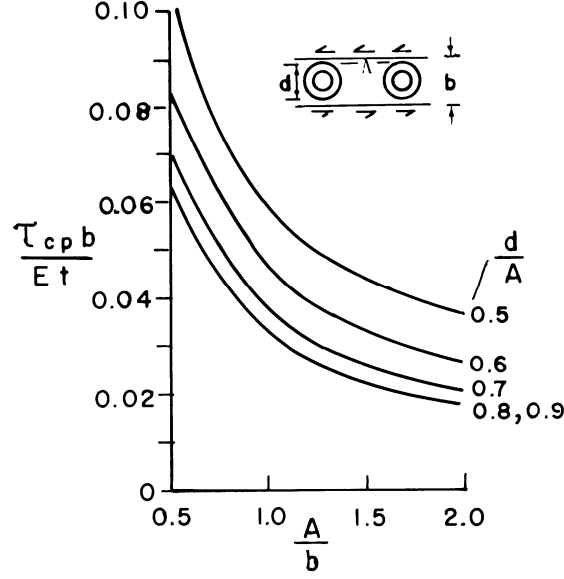


Fig. 4.13 Critical shear stress for webs with holes (Michael, 1960).

Combined loading: Redwood and Uenoya (1979) have investigated the problem of webs with holes subjected to combined bending and shear. They studied the problem of shear webs with aspect ratios from 1.5 to 2.5 with circular or rectangular holes. They suggested a classic circular interaction formula for τ_c and σ_{cb} (critical values of the maximum shear and bending stresses, respectively) in the form:

$$\left(\frac{\tau_c}{\tau_{cp}} \right)^2 + \left(\frac{\sigma_{cb}}{\sigma_{cbp}} \right)^2 = 1.0 \quad (4.12)$$

in which τ_{cp} and σ_{cbp} are the pure shear and pure bending critical stresses of the plate with the hole. These, in turn, can be expressed in terms of the corresponding critical stresses of plates without holes (τ_c^*, σ_{cb}^*) and the relative sizes of the holes with respect to the plate dimensions. With the notation indicated in Fig. 4.17, the expressions for plates with rectangular holes take the form

$$\sigma_{cbp} = \left[1.02 - 0.04 \left(\frac{a}{H} \right) \right] \sigma_{cb}^* \quad \text{but } \leq \sigma_{cb}^* \quad (4.13a)$$

$$\tau_{cp} = \left[1.24 - 1.16 \left(\frac{2H}{h} \right) - 0.17 \left(\frac{a}{H} \right) \right] \tau_c^* \quad \text{but } \leq \tau_c^* \quad (4.13b)$$

and for circular holes,

$$\sigma_{cbp} = \sigma_{cb}^* \quad (4.14a)$$

$$\tau_{cp} = \left[1.15 - 1.05 \left(\frac{2R}{h} \right) \right] \tau_c^* \quad \text{but } \leq \tau_c^* \quad (4.14b)$$

where R is the radius of the hole.

The values of σ_{cb}^* and τ_c^* can be obtained from a knowledge of the aspect ratio and boundary conditions of the plate. For example, for a simply supported plate with an aspect ratio of 2, these stresses are given with sufficient accuracy by the following expressions

$$\sigma_{cb}^* = 23.90 \sigma_c^* \quad (4.15a)$$

$$\tau^* = 6.59 \sigma_c^* \quad (4.15b)$$

in which

$$\sigma_c^* = \frac{\pi^2 E}{12(1-\nu^2)} \left(\frac{t}{h} \right)^2 \quad (4.15c)$$

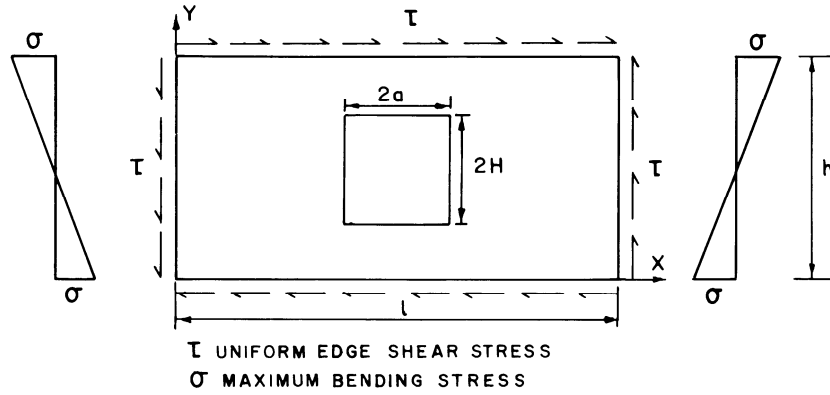


Fig. 4.14 Perforated rectangular plate under combined action of shear and bending.

4.3 INELASTIC BUCKLING, POST-BUCKLING, AND STRENGTH OF FLAT PLATES

The elastic critical plate buckling stresses, or corresponding plate buckling coefficients (k 's), provided in the previous section represent an important benchmark for understanding the behavior of thin plates. However, such elastic critical buckling stresses do not directly indicate the actual behavior that may occur in such a thin plate. In thin plates loaded to failure material and geometric effects complicate the response.

It is common, though artificial, to use the elastic critical buckling stress as a benchmark for delineating different forms of plate buckling: if material yielding occurs prior to the elastic critical buckling stress this is known as inelastic buckling; strength at magnitudes greater than the elastic critical buckling stress, and the associated deformations that occur under such loading, are referred to as post-buckling and may be either elastic or inelastic. Finally, ultimate strength refers to the maximum load the plate may carry, typically independent of deformation, which may indeed be quite large.

Actual plate response under load is more complicated than the simple notions of inelastic buckling and post-buckling, this is due in part to unavoidable imperfections. In an imperfect plate out-of-plane deformations begin immediately upon loading, such deformations lead to second order (geometrically nonlinear) forces (and strains) that must be accounted for throughout the loading/deformation, and thus the notions of buckling and post-buckling are not definitively distinct. Under load the stress field response of a thin plate is complicated and varies along the length, across the width, and through the thickness of the plate. Residual stresses that may exist in the plate further complicate the response. A plate with an applied stress well below the elastic critical plate buckling stress may still have portions of the plate yielding; thus determining a definitive regime where a plate enters inelastic buckling is difficult. For gradual yielding metals (e.g., aluminum, stainless steel) the distinction between elastic and inelastic buckling becomes even more difficult.

Currently, inelastic buckling, post-buckling, and the strength of thin plates (and plate assemblages such as Fig. 4.1) are most robustly examined through the use of numerical methods such as finite element analysis. Finite element models for stability critical structures are discussed further in Chapter 21, but key considerations for plates include: the manner in which shear in the plate is handled (namely Kirchhoff vs. Mindlin plate theory), the material stress-strain relation including residual stresses and strains, the yield criterion (von Mises is by far the most common in metals), the hardening law (isotropic hardening is the most common for static loading, but is inadequate if large strain reversals are present), magnitude and distribution of geometric imperfections, inclusion of higher-order strain terms in the development of the plate stiffness, enforcement of equilibrium on the deformed geometry, details of the boundary conditions, and for finite elements the order of the elements and the discretization of the plate both in terms of element density and element aspect ratio. Finite element analysis is not the only method able to provide post-buckling and collapse analysis of plates, finite strip (Bradford and Azhari 1995; Kwon and Hancock 1991; Lau and Hancock 1986; Lau and Hancock 1989), and recently generalized beam theory (Goncalves and Camotim 2007; Silvestre and Camotim 2002) have proven to be able to provide reliable solutions.

For typical design, fully nonlinear numerical collapse analysis of thin plates remains too involved of a task; in this situation one turns to classical and semi-empirical approaches. These design approximations are the focus of this section. In particular, the effective width method, has

wide use as an approximate technique for determining ultimate strength of plates that accounts for inelastic buckling and post-buckling and is discussed in detail.

4.3.1 Inelastic buckling

The notion of “inelastic buckling” is an attempt to extend the elastic critical buckling approximations of Section 4.2 to situations where material yielding has already occurred. Bleich (1952) generalized the expression for the critical stress of a flat plate under uniform compressive stress in either the elastic or inelastic range in the following manner:

$$\sigma_c = k \frac{\pi^2 E \sqrt{\eta}}{12(1-\nu^2)(b/t)^2} \quad (4.16)$$

in which $\eta = E_i/E$. This modification of Eq. 4.1 to adapt it to a stress higher than the proportional limit is a conservative approximation to the solution of a complex problem that involves a continuous updating of the constitutive relations depending on the axial stress carried (Stowell, 1948; Bijlaard, 1949, 1950).

In combined loading the work of Stowell (1949) and Peters (1954) suggest that the inelastic buckling interaction is not the same as the elastic buckling interaction. Under combined compressive and shear stress for loads applied in constant ratio Peters found that a circular stress-ratio interaction formula as expressed by Eq. 4.17 was conservative and agreed better with test results than Eq. 4.7 which was provided for elastic buckling interaction.

$$\left(\frac{\sigma_c}{\sigma_c^*} \right)^2 + \left(\frac{\tau_c}{\tau_c^*} \right)^2 = 1 \quad (4.17)$$

4.3.2 Post-buckling

Post-buckling of plates may readily be understood through an analogy to a simple grillage model, as shown in Fig. 4.15. In the grillage model the continuous plate is replaced by vertical columns and horizontal ties. Under edge loading the vertical columns will buckle, if they were not connected to the ties they would buckle at the same load and no post-buckling reserve would exist. However, the ties are stretched as the columns buckle outward, thus restraining the motion and providing post-buckling reserve.

In an actual plate the tension in the transverse ties is represented by membrane tension and shear. Note also that the columns nearer to the supported edge are restrained by the ties more than those in the middle. This too occurs in a real plate, as more of the longitudinal membrane compression is carried near the edges of the plate than in the center. Thus, the grillage model provides a working analogy for both the source of the post-buckling reserve and its most important result, re-distribution of longitudinal membrane stresses.

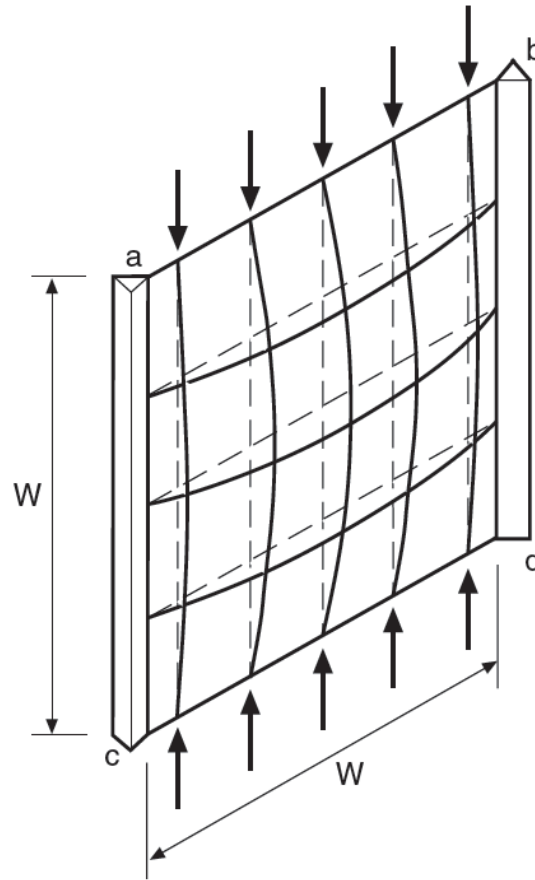


Fig. 4.15 Simple model for post-buckling of a flat plate in uniform compression (after AISI 2007)

Elastic post-buckling stiffness may be measured in terms of the apparent modulus of elasticity E^* (the ratio of the average stress carried by the plate to average strain) (see Fig. 4.16). The values of E^* for long plates ($a \gg b$) for some typical longitudinal edge conditions are given by Allen and Bulson (1980). The values given below are sufficiently accurate up to twice the critical stress.

Simply supported longitudinal edges.

Sides straight but free to move laterally:

$$E^* = 0.5E \quad (4.18a)$$

Sides free to move:

$$E^* = 0.408E \quad (4.18b)$$

Clamped longitudinal edges.

Sides straight but free to move laterally:

$$E^* = 0.497E \quad (4.18c)$$

One longitudinal edge simply supported, the other free

$$E^* = 0.444E \quad (4.18d)$$

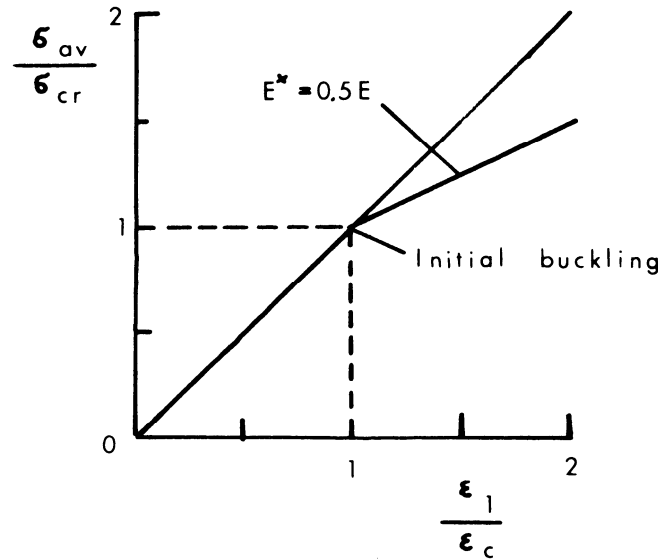


Fig. 4.16 Post-buckling stiffness of plates having simply supported edges (Allen and Bulson, 1980)

Another means for accounting for the loss in stiffness in the post-buckling regime is to assume a correlation between the strength loss of the plate and the stiffness loss. The effective width of the plate (as defined in the following section) is used in place of the actual width for determining cross-section moment of inertia. This method is employed in the cold-formed steel specification (AISI 2007) and discussed further in Chapter 13.

Nemeth and Michael (1990) presented an experimental study of the buckling and post-buckling behavior of square and rectangular compression-loaded aluminum plates with centrally located circular, square, and elliptical cutouts. The results indicated that the plates exhibit overall trends of increasing buckling strain and decreasing initial post-buckling stiffness with increasing cutout width. Results showed that the reduction in initial post-buckling stiffness due to a cutout generally decreases as the plate aspect ratio increases. Also, the square plates with elliptical cutouts having large cutout width/plate width ratio generally lose pre-buckling and initial post-buckling stiffness as the cutout height increases.

4.3.3 Strength and Effective Width

4.3.3.1 Uniform Compression

Local buckling causes a loss of stiffness and a redistribution of stresses (see the previous section). Uniform edge compression in the longitudinal direction results in a nonuniform stress distribution after buckling (Fig. 4.17) and the buckled plate derives almost all of its stiffness from the longitudinal edge supports. It is worth noting that the longitudinal stress distribution of Fig. 4.17 is an idealization of the membrane stress at the cross-section where the buckling wave is at maximum deformation; the longitudinal membrane stress varies along the length of the plate and the bending stress at the face of the plate provide a wholly different picture than Fig. 4.17.

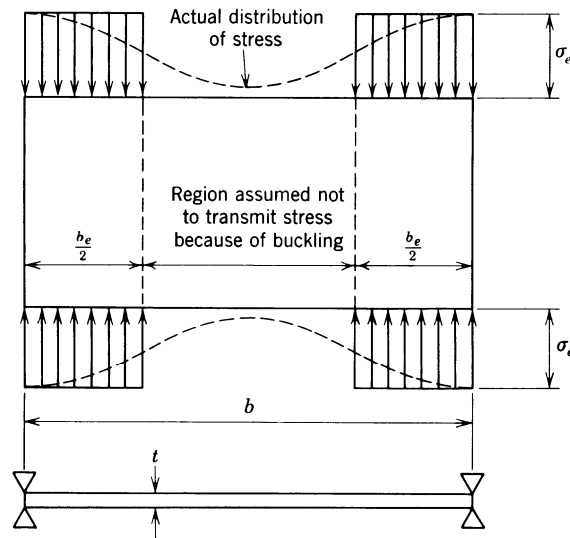


Fig. 4.17 Longitudinal stress after buckling and definition of effective width

An important semiempirical method of estimating the maximum strength of plates is by the use of the *effective width* concept. The fact that much of the load is carried by the region of the plate in the close vicinity of the edges suggests the simplifying assumption that the maximum edge stress acts uniformly over two “strips” of plate and the central region is unstressed (Fig. 4.17). Thus, only a fraction of the width is considered effective in resisting applied compression. The concept of effective width is, however, not confined to calculation of post-buckling strength of uniformly compressed plates but has become the means of allowing for local buckling effects in columns, panels, or flexural members that have the dual function of supporting loads and acting as walls, partitions, bulkheads, floors, or roof decking. In a plate structure, use of the effective width leads to an effective cross section consisting of portions of members meeting along a junction. It is near these junctions that the plates will begin to yield preceding failure.

The effective-width concept has been used in design specifications for many years. Specifications of the AISI (2007), the Aluminum Association (2005), and the AISC (2005) all permit the use of an effective width in the design of members having plate elements with b/t ratios greater than the limits for full effectiveness. Though implementations of the effective width method vary greatly for the three design specifications.

The effective-width concept seems to have had its origin in the design of ship plating (Murray, 1946). It had been found that longitudinal bending moments in ships caused greater deflections than those calculated using section properties based on the gross area of the longitudinal members. Deflections could be calculated more accurately by considering only a strip of plate over each stiffener having a width of 40 or 50 plate thicknesses as effective in acting with the stiffeners in resisting longitudinal bending.

The advent of all-metal aircraft construction provided another opportunity for the use of the effective-width concept, since it was advantageous to consider some of the metal skin adjacent to stiffeners as being part of the stiffener in calculating the strength of aircraft components. Cold-formed members used in steel buildings also provide useful applications of stiffened-sheet construction. A thorough discussion of the effective-width concept as applied to cold-formed steel design has been prepared by Winter (1983).

Tests by Schuman and Back (1930) of plates supported in V-notches along their unloaded edges demonstrated that, for plates of the same thickness, increasing the plate width beyond a certain value did not increase the ultimate load that the plate could support. It was observed that wider plates acted as though narrow side portions or effective load-carrying areas took most of the load. Newell (1930) and others were prompted by these tests to develop expressions for the ultimate strength of such plates. The first to use the effective-width concept in handling this problem was von Kármán (1932). He derived an approximate formula for the effective width of simply supported plates, and in an appendix to his paper, Sechler and Donnell derived another formula based on slightly different assumptions. Subsequently, many other effective-width formulas have been derived, some empirical, based on approximate analyses, and some based on the large-deflection plate-bending theory, employing varying degrees of rigor.

For plates under uniform compression, stiffened along both edges parallel to the direction of the applied compression stress, von Kármán (1932) developed the following approximate formula for effective width, based on the assumption that two strips along the sides, each on the verge of buckling, carry the entire load:

$$b_e = \left[\frac{\pi}{\sqrt{3(1-\nu^2)}} \sqrt{\frac{E}{\sigma_e}} \right] t \quad (4.19)$$

Combining Eqs. 4.19 and 4.1, for $k = 4$ (simple edge supports), the formula suggested by Ramberg et al. (1939) is obtained (see Fig. Fig. 4.17 for notation):

$$\frac{b_e}{b} = \sqrt{\frac{\sigma_c}{\sigma_e}} \quad (4.20)$$

From Fig. 4.17, the average stress is

$$\sigma_{av} = \frac{b_e}{b} \sigma_e \quad (4.21)$$

Substituting Eq. 4.20 into Eq. 4.21 with the edge stress equal to the yield stress ($\sigma_e = \sigma_y$) gives us

$$\sigma_{av} = \sqrt{\sigma_c \sigma_y} \quad (4.22)$$

As a result of many tests and studies of post-buckling strength, Winter (1947) and Winter et al. (1950) suggested the formula for effective width that was adopted in the 1946 through 1962 editions of the AISI specifications for cold-formed steel members:

$$\frac{b_e}{t} = 1.9 \sqrt{\frac{E}{\sigma_e}} \left(1 - 0.475 \sqrt{\frac{E}{\sigma_e}} \frac{t}{b} \right) \quad (4.23)$$

or, alternatively, in the form of Eq. 4.5,

$$\frac{b_e}{b} = \sqrt{\frac{\sigma_c}{\sigma_e}} \left(1 - 0.25 \sqrt{\frac{\sigma_c}{\sigma_e}} \right) \quad (4.24)$$

Equations 4.23 and 4.24 are basically the same as Eqs. 4.19 and 4.20, respectively, but include a correction coefficient determined from tests and reflecting the total effect of various imperfections, including initial deviations from planeness. Equation 4.23 was found to be satisfactory also for austenitic stainless steel in the annealed and flattened condition (Johnson and Winter, 1966) and for quarter- and half-hard type 301 stainless steel (Wang, 1969; Wang et al., 1975).

Introducing the coefficient $B = b/t\sqrt{\sigma_e/E}$, Winter's formula, Eq. 4.23, can be written as

$$\frac{b_e}{b} = \frac{1.90}{B} - \frac{0.90}{B^2} \quad (4.25)$$

A formula proposed by Conley et al. (1963) is nearly the same as that proposed by Winter and can be expressed as

$$\frac{b_e}{b} = \frac{1.82}{B} - \frac{0.82}{B^2} \quad (4.26)$$

A useful form of Eq. 4.25 or 4.26 is obtained by introducing the material yield strength into the dimensionless parameter B . If \bar{B} is defined as

$$\bar{B} = B \sqrt{\frac{\sigma_y}{\sigma_e}} = \frac{b}{t} \sqrt{\frac{\sigma_y}{E}} \quad (4.27)$$

and if σ_{av}/σ_e is substituted for b_e/b , and both sides of the equation are multiplied by σ_e/σ_y , Eq. 4.26 can be written as

$$\frac{\sigma_{av}}{\sigma_y} = \frac{1.82}{B} \sqrt{\frac{\sigma_e}{\sigma_y}} - \frac{0.82}{\bar{B}^2} \quad (4.28)$$

By introducing discrete values of \bar{B} into Eq. 4.28, the relationships shown in Fig. 4.18 between σ_{av}/σ_y and σ_e/σ_y for B values greater than 1.0 were determined. It was assumed that there would be no loss of plate effectiveness for values of $\bar{B} \leq 1.0$ and thus the straight line from (0, 0) to (1.0, 1.0) was drawn for $\bar{B} = 1.0$. Lines of constant \bar{B} when plotted fully are tangent to the $\bar{B} = 1.0$ line, and only their upper portions are shown. Thus for any given strength level of plate steel, a relationship between average stress after buckling and the maximum or edge stress of the plate panel is established as a function of the actual b/t ratio. This relationship is valid for stiffened plates in which the ratio of stiffener cross-sectional area to plate-panel cross-sectional area is small. If the cross section of a structural member includes a buckled plate, the effective-width approach should be used in computing deflections, in determining the location of the neutral axis, or in other calculations where the effective moment of inertia or radius of gyration of the member is important.

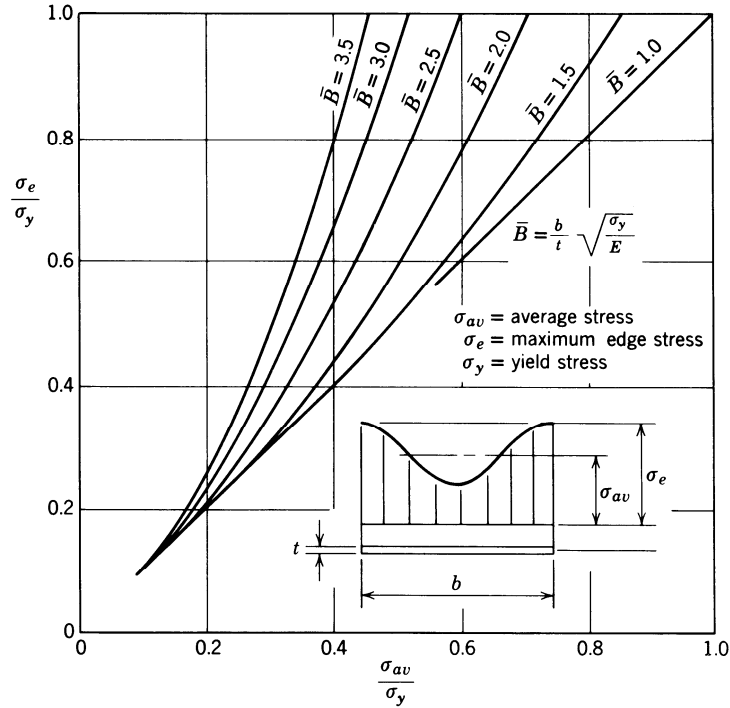


Fig. 4.18 Chart for determining σ_e/σ_y

In the 1968 and later editions of the AISI specification for cold-formed steel members (e.g., AISI 2007) the coefficients in Eqs. 4.23 and 4.24 were reduced slightly, giving the following expressions for effective width:

$$\frac{b_e}{t} = 1.9 \sqrt{\frac{E}{\sigma_e}} \left(1.0 - 0.415 \sqrt{\frac{E}{\sigma_e}} \frac{t}{b} \right) \quad (4.29)$$

or

$$\frac{b_e}{b} = \sqrt{\frac{\sigma_c}{\sigma_e}} \left(1.0 - 0.22 \sqrt{\frac{\sigma_c}{\sigma_e}} \right) \quad (4.30)$$

The limiting value of b/t when all of the width is considered to be effective is obtained by setting b_e equal to b . The AISI value thus obtained from Eq. 4.14 is $(b/t)_{\lim} = 221/\sqrt{\sigma}$. AISC values of effective width (2005) remain slightly more liberal than those of AISI. (See Section 4.3.3.5 for further information on width-to-thickness limits.)

In the calculation of the ultimate compression load for plates supported along the two unloaded edges, σ_e is taken equal to the compressive yield stress for steel. For aluminum alloys and magnesium alloys, σ_e is taken as 0.7 times the yield strength, as determined by the offset method. However, if the buckling stress σ_c exceeds 0.7 times the yield strength, the load capacity as determined by inelastic plate-buckling analysis may be taken as $bt\sigma_c$ in which σ_c is determined by Eq. 4.16 (inelastic buckling) and the effective width need not be calculated. The use of the ultimate compressive buckling load in specifications for aluminum structures is discussed later in this section.

Equation 4.30 can be used to determine a nondimensional ultimate-strength curve for steel plates in the post-buckling range. The average stress on the plate at ultimate load, σ_{av} , is the ultimate load divided by the total area. From Eq. 4.30,

$$\sigma_{av} = \frac{P_{ult}}{bt} = \sqrt{\sigma_c \sigma_y} \left(1.0 - 0.22 \sqrt{\frac{\sigma_c}{\sigma_y}} \right) \quad (4.31)$$

In Fig. 4.19 the average stress at ultimate load, by Eq. 4.31, is compared with the uniform-edge compression stresses to cause buckling. A method for predicting the strength of simply supported plates, taking into account initial out-of-flatness, is given by Abdel Sayed (1969) and Dawson and Walker (1972). Out-of-flatness, residual stress, and strain hardening are considered by Dwight and Ratcliffe (1968).

(delete equation numbers in figure or replace with new numbers 4.7→4.22, 4.16→4.31, 4.18→4.33 (4.1 remains the same))

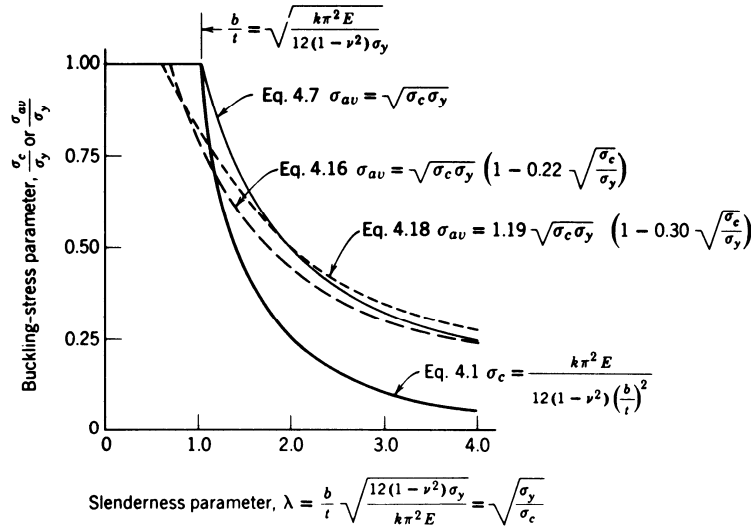


Fig. 4.19 Nondimensional buckling curves for plates under uniform edge compression (adapted from Brockenbrough and Johnston, 1974).

For a plate supported along only one longitudinal edge, the effective width has been experimentally determined by Winter as

$$\frac{b_c}{b} = 1.19 \sqrt{\frac{\sigma_c}{\sigma_e}} \left(1 - 0.30 \sqrt{\frac{\sigma_c}{\sigma_e}} \right) \quad (4.32)$$

This equation has also been confirmed by an analysis carried out by Kalyanaraman (Kalyanaraman et al., 1977; Kalyanaraman and Peköz, 1978). The average stress at ultimate load can then be expressed as

$$\sigma_{av} = 1.19 \sqrt{\sigma_c \sigma_y} \left(1 - 0.30 \sqrt{\frac{\sigma_c}{\sigma_y}} \right) \quad (4.33)$$

Equation 4.33 is also shown in Fig. 4.19. This curve actually falls above and to the right of Eq. 4.31, but it must be remembered that in the elastic range σ_c for a plate supported on both longitudinal edges is about eight times as large as that for the same plate supported along only one longitudinal edge.

Considering that Eq. 4.29 is an appropriate formula for determining the effective design width of stiffened compression elements with a k value of 4.0, a generalized formula for different stiffened compression elements with various rotational edge restraints can be written as follows:

$$\frac{b_e}{t} = 0.95 \sqrt{\frac{kE}{\sigma_e}} \left(1 - 0.209 \sqrt{\frac{kE}{\sigma_e}} \frac{t}{b} \right) \quad (4.34)$$

In fact Eq. 4.34 has also been extended to unstiffened elements. For example to determine the effective width of a plate simply supported on only one longitudinal edge, the engineer would use $k=0.425$ of Fig. 4.2 in Eq. 4.15. This basic approach where an appropriate k value is used to determine the strength regardless of the boundary conditions (or loading) is known as the unified method and has been shown to provide adequate strength predictions for a variety of conditions (Peköz 1987) and forms the basis for the cold-formed steel specification discussed further in Chapter 13.

Jombock and Clark (1962) list 14 effective-width formulas, along with their sources, and discuss the assumptions on which they are based. Since the effective-width concept is also well developed in current specifications and commentaries, it is suggested that reference be made thereto for further information on this topic.

Certain box-girder-bridge structural failures in the early 1970s have interjected a warning due to designers of plate structures that many aspects of plate behavior need further investigation. For example, the concepts of effective width and average stress at failure consider plate strains only up to the maximum plate capacity—that is, the ultimate load as characterized by reaching the yield stress at the edge. Research has shown that inelastic strains beyond the point may lead to a sudden and substantial reduction of the plate's load-carrying capacity (Dwight and Moxham, 1969; Dwight, 1971).

4.3.3.2 Compression and Bending

One approach to determining the ultimate strength of a plate in bending, or compression and bending, is to use the plate buckling coefficients from Section 4.2.2 applied in Winter's effective width formula, i.e. Eq. 4.34. One difficulty that remains after determination of the effective width, b_e , is how to distribute b_e to the plate edges. For example, for a simply supported plate in bending if b_e/b is designated as ρ , Fig. 4.20 provides a rational method for distributing the effective width based on maintaining force and moment equilibrium in the effective plate based on the work of Schafer and Peköz (1999). Other alternatives exist, for example LaBoube and Yu (1982), Peköz (1987), and Usami (1982). For plates with one longitudinal edge free the plate buckling coefficients of Fig. 4.5 may be used with Eq. 4.34 to provide effective width predictions. Distribution of the effective width is provided by Bambach and Rasmussen (2004b) and has been adopted in AISI (2007).

A direct solution for the ultimate strength of plates under compression and bending without recourse to effective width was studied and proposed by Rhodes and Harvey (1971, 1976, 1977). In the case of simply supported plates under eccentric loading P , the failure loads for plates with various loading eccentricities can be accurately predicted by a simple expression of the form (Rhodes and Harvey, 1977).

$$\bar{P}_{ult} = \frac{pb}{\pi^2 D} = \frac{\bar{\sigma}_y + 11.4}{b(e/b) + 0.85} \quad (4.35)$$

where $D = Et^3/12(1 - \nu^2)$, $\bar{\sigma}_y = \sigma_y(b^2t/\pi^2 D)$, and e is the distance from the point of load application to the remote edge of the plate.

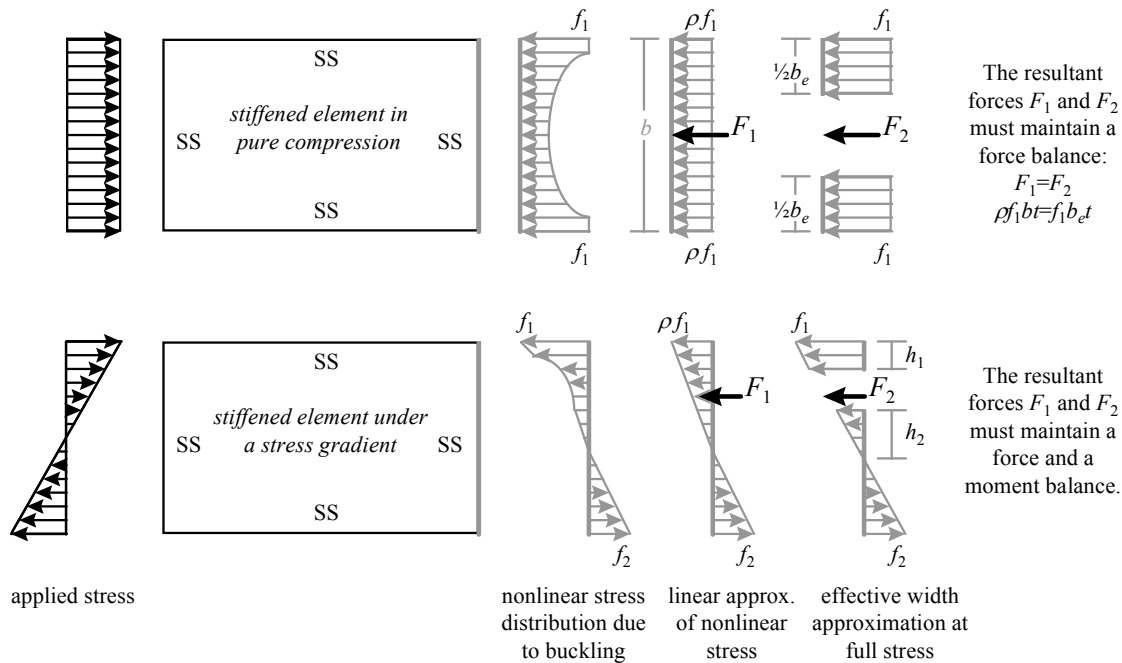


Fig. 4.20 Distributing effective width in plates under a stress gradient, after (Schafer and Peköz 1999)

4.3.3.3 Longitudinally varying Compression

It has been demonstrated that the use of the plate buckling coefficients of Section 4.2.7 in Winter's effective width formula lead to reliable and conservative predictions of the strength of plates under longitudinally varying compression, as occurs in the compression flange of members subjected to moment gradient (Yu and Schafer 2006).

4.3.3.4 Plates with holes

The simplest means for determining the ultimate strength and effective width of plates with holes is to adopt the "unstiffened strip" approach described in Section 4.2.11, in particular Fig. 4.12. The strips of plate material adjacent to the hole are treated as plates with one longitudinal edge free, i.e., unstiffened strips; the plate buckling coefficient may then be determined like any other plate with one edge free (e.g., Fig. 4.2), and the effective width calculated using Winter's formula. This approach, which was developed by Vann (1971), Yu and Davis (1973), and Miller and Peköz (1994), is essentially that adopted in AISI (2007).

4.3.3.5 Width-to-thickness limits

In plastic design of steel structures, it is necessary that the moment capacity of the member not be impaired by local buckling until the required rotation is achieved. This can be achieved by limiting the width-to-thickness ratios of elements that are vulnerable to local buckling in the inelastic range. Such limiting width-to-thickness ratios have been proposed for flanges of I-beams by Lay (1965). Further studies of this topic can be found in the following references: Dawe and Kulak (1984, 1986), Kuhlmann (1989) and Kemp, (1996). Such provisions are also available in design specifications (AISC 2005). Additional width-to-thickness limits have also been adopted for seismic applications where cyclic inelasticity must be considered (AISC 2005b). (Earls 1999) shows that care must be taken in the use of these limits particularly as new high strength materials are introduced and the buckling limit states may not follow the simple empirical criteria previously employed.

4.3.4 Strength in shear and combined loadings with shear

The initial mode of buckling in pure shear, which takes the form of a half wave in the tension direction and at least one full wave in the compression direction (Fig. 4.10a), undergoes a change in the advanced post-buckling range, eventually taking the form of a family of diagonal folds (Fig. 4.10b). These folds carry significant tensile stresses developed in the post-buckling range and the displacement pattern is called a *tension field*. The dominance of this tension field behavior has lead to methods other than effective width for determining the strength of thin plates in shear.

The maximum shear load that can be applied before failure occurs due to a breakdown of the material in the tension field, and it is influenced by the rigidity of the edge members supporting the plate. This problem is dealt with in greater detail in Chapter 6 for bridge applications and is discussed further in Section 4.3.8 below within the context of steel plate shear walls for buildings.

For a plate with infinitely stiff edge members, the maximum shear strength can be estimated by the formula (Allen and Bulson, 1980)

$$\bar{V}_u = \tau_c bt + \frac{1}{2} \sigma_{ty} bt \quad (4.36)$$

where

$$\sigma_{ty} = \sqrt{\sigma_y^2 - 0.75\tau_c^2} - 1.5\tau_c \quad \text{provided that } \tau_c \leq \sigma_y \quad \tau_c < \sigma_y \quad (4.37)$$

Stein and Manue (1989) presented buckling and post-buckling results for plates loaded by in-plane shear. The buckling results had been plotted to show the effects of thickness on the stress coefficient for aluminum plates. Results were given for various length-to-width ratios. Post-buckling results for thin plates with transverse shearing flexibility were compared to results from classical theory. The plates were considered to be long with side edges simply supported, with various in-plane edge conditions and the plates were subjected to a constant shearing displacement along the side edges.

Elangovan and Prinsze (1992) carried out a numerical investigation, using a finite element buckling analysis to determine the critical shear stress of flat rectangular plates with two opposite edges free. Plate sizes and the boundary conditions at the two edges loaded in shear were the parameters considered in their study. Results showed a considerable difference in the buckling strength of plates if the in-plane displacement normal to the loaded edges were restrained either at one or at both of those edges.

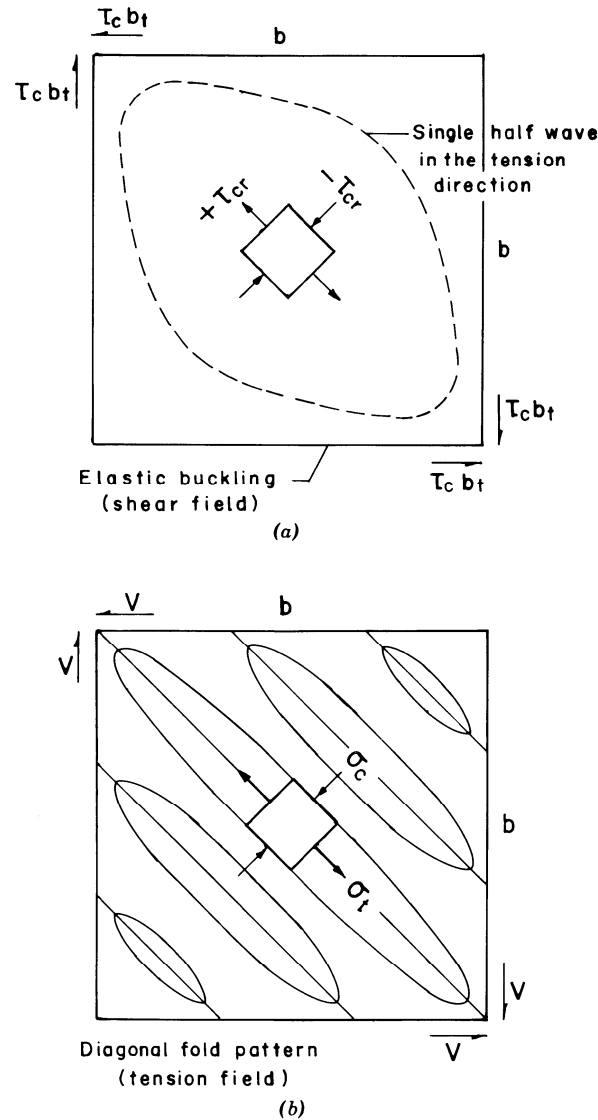


Fig. 4.21 Shear and tension fields (square plate).

Information on the post-buckling strength of plate elements subjected to the combined action of shear and compression is limited. A semiempirical method for the determination of stress levels at which permanent buckles occur in a long plate with simply supported edges under the combined action of uniform axial compression and shear has been suggested by Zender and Hall (1960). Additional information on post-buckling strength of plates subjected to the combined action of shear and bending can be found in Chapters 6 and 7.

4.3.5 Strength of biaxially compressed plates

Few simplified design methods exist for post-buckling and strength prediction of biaxially compressed plates. For example, the effective width method for plates under biaxial compression has seen little study. Isami and Hidenori (1989) employed mechanism analysis methods (see Section 4.3.7) to provide predictions for biaxially compressed plates. Post-buckling and strength prediction relies primarily on geometric and material nonlinear finite element

analysis. For example biaxial compression of ship plates with particular attention paid to the role of initial imperfections in determining the ultimate strength is studied by (Paik et al. 2004). In addition, they show that the collapse behavior of biaxially compressed plates can vary significantly from those under only longitudinal compression.

4.3.6 Average stress and strength of aluminum plates

As an alternative to the effective width concept for wide, thin plates, another approach is to use the average stress at failure and the actual (unreduced) plate width. This is the basis for allowable stresses on thin sections in the Aluminum Association specifications (AA, 1994). In applying these specifications the designer does not, in general, calculate an effective width but uses instead an allowable stress that has been derived by applying a factor of safety to the average stress at failure for plate elements. For plates that buckle in the inelastic stress range, the average stress at failure is considered to be the same as the local-buckling stress, since plates of these proportions have little post-buckling strength (Jomback and Clark, 1968). Inelastic local-buckling strength for aluminum plates is represented in the specifications by the following straight-line approximation to Eq. 4.1 (Clark and Rolf, 1966):

$$\sigma_c = B_p - D_p \kappa_1 \frac{b}{t} \quad (4.38)$$

where

$$B_p = \sigma_y \left[1 + \frac{(\sigma_y)^{1/3}}{k_2} \right] \quad (4.39)$$

$$D_p = \frac{(B_p)^{3/2}}{k_3 (E)^{1/2}} \quad (4.40)$$

$$\kappa_1 = \sqrt{\frac{12(1-\nu^2)}{k}} \quad (4.41)$$

For aluminum alloys that are artificially aged (temper designations beginning with T5, T6, T7, T8, or T9), $k_2 = 11.4 \text{ ksi}^{1/3}$ ($78.6 \text{ MPa}^{1/3}$) and $k_3 = 10$. For other aluminum alloys (temper designations beginning with 0, H, T1, T2, T3, or T4), $k_2 = 7.6 \text{ ksi}^{1/3}$ ($52.4 \text{ MPa}^{1/3}$) and $k_3 = 10\sqrt{2/3}$. Equation 4.20 has been shown to agree well with the results of tests on aluminum plate elements (Clark and Rolf, 1966; Jomback and Clark, 1968). For plates that buckle elastically, the average stress at failure is represented for purposes of the aluminum specification as

$$\sigma_{av} = \sqrt{\sigma_e \sigma_c} \quad (4.42)$$

Equation 4.42 corresponds to Eq. 4.22. Jomback and Clark (1968) demonstrated that the edge stress at failure σ_e for aluminum plates could be represented by a function of the intercept B_p in Eq. 4.38. This results in a simple relationship between the ultimate-strength curves corresponding to elastic and inelastic buckling. Generally, this edge stress at failure for aluminum alloys is about $0.7\sigma_y$.

The formulas used in the Aluminum Association specifications (AA, 1994) are illustrated in Fig. 4.7. Comparisons with test results were published by Jomback and Clark (1968). The use in these specifications of the average stress at failure for thin sections results in some simplification, since the designer does not have to calculate an effective width. However, it sacrifices some of the flexibility of the effective-width approach. For example, the average stress-at-failure method does not treat the change in moment of inertia of a member when its

compression elements are in the post-buckling range, and hence does not readily lend itself to calculation of deflections. Therefore, the Aluminum Association specifications include an effective-width formula to be used in calculating deflections in the post-buckling range. See Chapter 13 for further discussion.

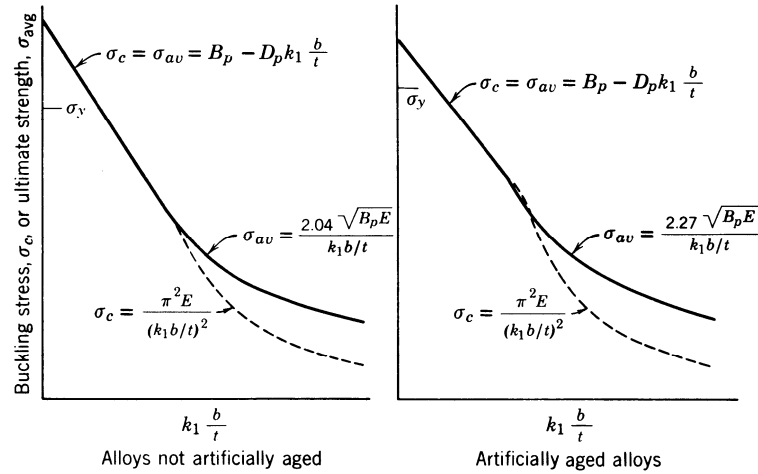


Fig. 4.22 Equations for buckling stress and ultimate strength of plates used in Aluminum Association specifications (AA, 1994).

The Aluminum Association specifications (AA, 1994) treat post-buckling strength of webs in bending by means of an average stress approach similar to that used for plates in compression. This approach is compared with test results by Jombock and Clark (1968).

4.3.7 Yield-line analysis and plastic buckling of plates

Yield-line analysis represents the extension of concentrated plasticity such as plastic hinge analysis in beams to two-dimensional structures. For out-of-plane loading (applied loads on floor slabs, etc) yield-line analysis has a long history; however for in-plane loading such as that which has been the focus of this chapter the use is less widespread. One of the primary difficulties with the extension to in-plane loads is that yielding mechanisms for in-plane loaded plates typically involve yielded zones (membrane extension), as well as yield lines (where bending and twist) occur. Successful applications include connection design, particularly for tubular and HSS sections (Kosteski et al. 2003), determination of the limiting rotation for beams (Gioncu and Petcu 1997; Shi et al. 1996), and patch loading or crippling of webs. Use of yield-line analysis for generalized collapse analysis of plates is not widespread, Bambach (2008) represents a recent summary and the most complete treatment still remains Murray and Khoo (1981), Murray (1984).

Inoue et al. (1993) studied an analytical evaluation of the effective plastic shear modulus of fully yielded steel plates at the instant of buckling. It was assumed that yielding of steel was to follow the Tresca yield criterion and that plastic deformation of a steel plate was to be caused by slips. The Tresca yield criterion provides lower bending stiffnesses than those obtained from the von Mises yield criterion, but it does not lower the plastic shear modulus of the material at any point on the yield plateau. They proposed a new theory that assumes a nonuniform distribution of slips depending on the orientation of an infinite number of possible slip planes at each point in the plate. The twisting of the plate is then accompanied by distortion of its sectional shape, and this mode of buckling is shown to provide a considerable reduction in the effective plastic shear modulus. Applying these sectional stiffnesses and solving differential equilibrium equations

leads to a lower bifurcation strength, which provides much better correlations with experimental results than those of previous predictions.

4.3.8 Energy dissipation (steel plate shear wall)

The collapse of metal plate structures generally involve either fracture or stability limit states. Stability limit states, such as inelastic local plate buckling are typically preferred over fracture limit states, because they provide some post-buckling resistance, and hence greater ductility and the potential for energy dissipation. For seismic design energy dissipation is a fundamental need for most structures, rather than rely on inherent or assumed energy dissipation, modern designs often attempt to explicitly use specific element(s) for energy dissipation. Properly designed and detailed a thin plate undergoing post-buckling may provide reliable energy dissipation.

Steel plate shear walls are an important example of the application of metal plate structures for the purposes of energy dissipation. Utilizing the post-buckling response of plates in the shear experimental tests under cyclic load have been used to verify the potential energy dissipation of unstiffened steel plate shear walls, as shown in Fig. 4.23. (Caccese et al. 1993) (Elgaaly et al. 1993) (Elgaaly 1998) (Lubell et al. 2000). Currently phenomenological models are favored for characterizing the response of steel plate shear walls, while such models have limitations, they are readily implemented in nonlinear dynamic analysis allowing the influence of steel plate shear walls on full structural systems to be studied (Roberts and Sabouri-Ghomi 1992; Sabouri-Ghomi and Roberts 1992). Recent and ongoing research indicates that perforated steel plates may offer further advantages for energy dissipation as shown in Fig. 4.24 (Hitaka and Matsui 2003).

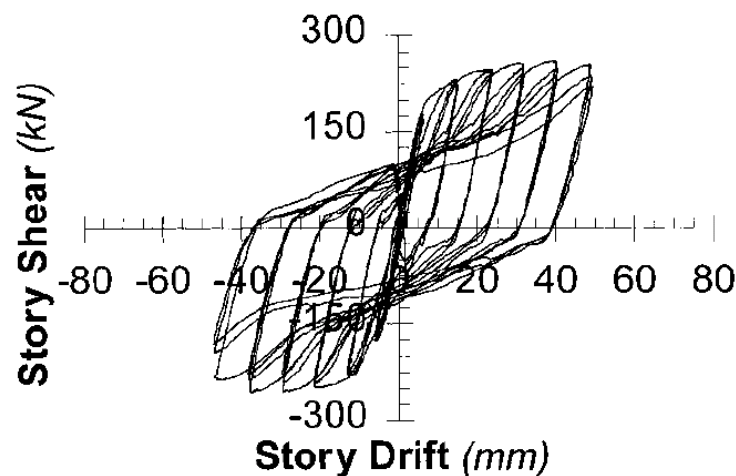
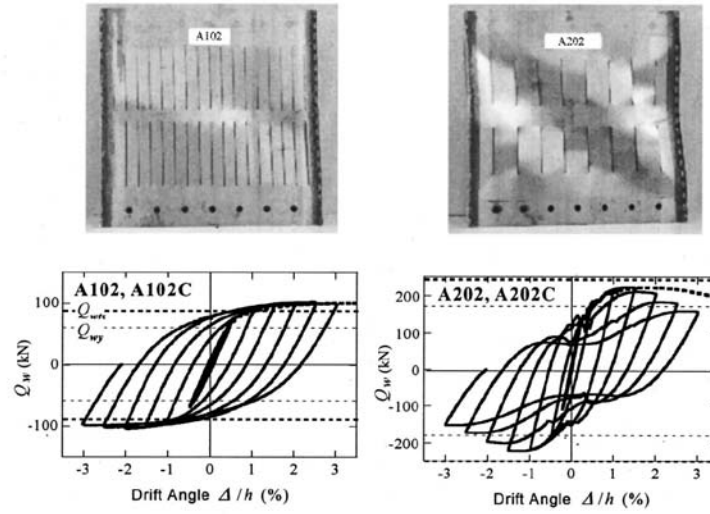


Fig. 4.23 Hysteretic response of a steel plate shear wall under cyclic loading (Lubell et al. 2000)



a) Behavior of Stiffener- Stiffened 102 and 202-Type

Fig. 4.24 Hysteretic response of steel plate shear walls with cutouts (Hitaka and Matsui 2003)

4.4 BUCKLING, POST-BUCKLING AND STRENGTH OF STIFFENED PLATES

This section deals with the buckling and ultimate strength of stiffened flat plates under various combinations of loadings. The behavior of the stiffened plate as a unit is emphasized rather than the stability of its individual elements. However, in design, the structural properties of all of the components must be considered.

Stiffened plates can fail through instability in essentially two different ways. In one, overall buckling (also referred to as stiffener buckling or distortional buckling in the literature), the stiffeners buckle along with the plate, and in the other, local buckling, the stiffeners form nodal lines and the plate panels buckle between the stiffeners. In either case the stiffness of the combination may be such that initial buckling takes place at fairly low stress levels. Nevertheless, a significant amount of post-buckling strength may remain in the stiffened plate, provided that proper attention is given to the design and fabrication of the structural details. A great deal of information on this subject can be found in the *Handbook of Structural Stability* (CRCJ, 1971) and in a book by Troitsky (1976).

Finally, as discussed in the introduction to Section 4.3, today it is becoming increasingly common to study buckling, post-buckling, and strength through geometric and material nonlinear finite element analysis using plate or shell elements. Such models provide the capability to accurately include boundary conditions, imperfections, residual stresses, etc. and are a powerful tool in the study of stiffened plates. For the most part, the discussion provided herein focuses on analytical methods and tools that can be used with far greater expediency than a complete nonlinear finite element analysis. For further discussion on stiffened plates see Chapters 6, 7 and 13, and for further discussion on finite element modeling for stability problems see Chapter 21.

4.4.1 Compression: Buckling

It is often economical to increase the compressive strength of a plate element by introducing longitudinal and/or transverse stiffeners (Fig. 4.25). In the following paragraphs methods are presented for determining the compressive strength of stiffened plate panels. The edges of the plate are assumed to be simply supported in all cases, and it is also assumed that individual elements of the panel and stiffeners are not subject to instability.

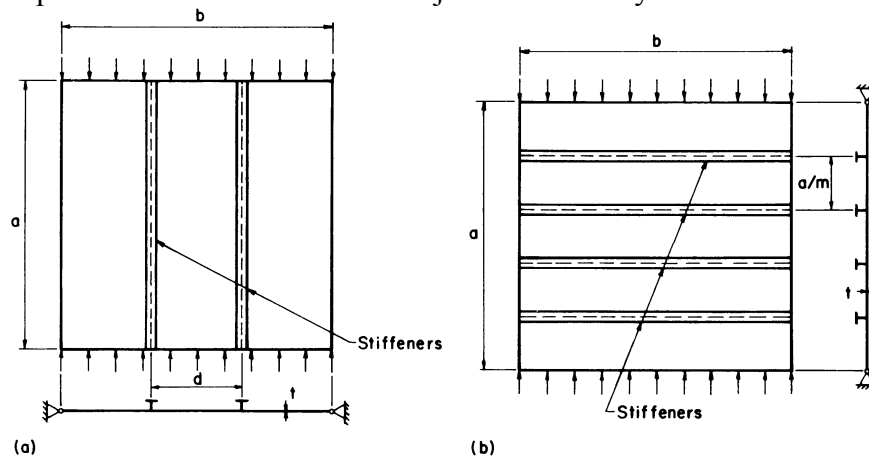


Fig. 4.25 Stiffened plate panels; (a) panel with longitudinal stiffeners; (b) panel with transverse stiffeners.

4.4.1.1 Longitudinal Stiffeners

Seide and Stein (1949), Bleich and Ramsey (1951), and Timoshenko and Gere (1961) have presented charts and tables for determining the critical stress of plates simply supported on all edges and having one, two, or three equally spaced longitudinal stiffeners parallel to the direction of the applied compressive load. The solutions of Seide and Stein are also useful for other numbers of equally spaced stiffeners. In all of these solutions the stiffeners are assumed to have zero torsional rigidity. If we consider only overall buckling with $m=1$ then this classical solution may be provided in a compact form (Schafer and Peköz 1998) where:

$$f_{cr} = k_{cr} \frac{\pi^2 D}{b_o^2 t} \quad (4.43)$$

$$\gamma_i = \frac{EI_i}{b_o D} \quad \delta_i = \frac{(A_s)_i}{b_o t} \quad \alpha_i = \frac{c_i}{b_o} \quad D = \frac{Et^3}{12(1-\nu^2)} \quad (4.44)$$

$$\gamma_i = \frac{EI_i}{b_o D} \quad \delta_i = \frac{(A_s)_i}{b_o t} \quad \alpha_i = \frac{c_i}{b_o} \quad D = \frac{Et^3}{12(1-\nu^2)} \quad (4.45)$$

$$\gamma_i = \frac{EI_i}{b_o D} \quad \delta_i = \frac{(A_s)_i}{b_o t} \quad \alpha_i = \frac{c_i}{b_o} \quad D = \frac{Et^3}{12(1-\nu^2)} \quad (4.46)$$

and I is the stiffener moment of inertia, b_o the plate width, A_s the stiffener area, and c_i the distance the stiffener is from the edge, this form of the expressions is adopted in AISI (2007).

A conservative method of analysis proposed by Sharp (1966) divides the analysis of the stiffened plate into two parts: one applying to short panels in which the buckled configuration takes the form of a single half-wave in both the longitudinal and transverse directions and another applying to long panels in which several longitudinal waves may occur along with a single half-wave in the transverse direction. In very short panels, the stiffener and a width of plate equal to the stiffener spacing, d , are analyzed as a column of length, a , with a slenderness ratio

$$\left(\frac{L}{r} \right)_{eq} = \frac{\alpha}{r_e} \quad (4.47)$$

where r_e is the radius of gyration of the section consisting of a stiffener plus a width of plate equal to d .

In long panels the critical stress is larger than that calculated by the use of Eq. 4.47. In this case an equivalent slenderness ratio is defined for use in column strength formulas,

$$\frac{L}{r_{eq}} = \sqrt{6(1-\nu^2)} \frac{b}{t} \sqrt{\frac{1 + (A_s / bt)}{1 + \sqrt{(EI_e / bD)} + 1}} \quad (4.48)$$

where

$b = Nd$ = overall width of longitudinally stiffened panel

N = number of panels into which the longitudinal stiffeners divide the plate

I_e = moment of inertia of section consisting of the stiffener plus a width of plate equal to d

A_s = cross-sectional area of stiffener

$$D = \frac{Et^3}{12(1-\nu^2)}$$

The smaller of the values from Eqs. 4.47 and 4.48 is used in the analysis, and it is assumed that the plate is fully effective over the panel width d . For greater values of d , buckling of the stiffeners and of the plate between the stiffeners would need consideration.

A flat aluminum sheet with multiple longitudinal stiffeners, or a formed stiffened sheet, subjected to a uniform longitudinal compression (Sherbourne et al., 1971) will buckle into waves of length Ψb , in which b is the plate width and $\Psi = 1.8(I_x/t^3)^{1/4}$, where I_x is the moment of inertia in the strong direction and t is the plate thickness. For a formed aluminum stiffened sheet this becomes $\Psi = 1.8(\rho r_x/t)^{1/2}$, in which ρ is the ratio of the developed sheet width to the net width, and r_x is the radius of gyration in the strong direction. If the spacing, a , of transverse supports is less than Ψb , the elastic critical stress is given approximately by

$$\frac{\sigma_c = \pi^2 E [1 + (a/\Psi b)^4]}{(a/r_x)^2} \quad (4.49a)$$

If the spacing exceeds Ψb , then

$$\frac{\sigma_c = 2\pi^2 E}{(\Psi b/r_x)^2} \quad (4.49b)$$

The Canadian standard (CSA, 1983), using this method, reduces the design procedure to determining the equivalent slenderness ratios, which are, respectively, for the two cases,

$$\lambda = \frac{a/r_x}{[1 + (a/\Psi b)^4]^{1/2}} \quad (4.50a)$$

$$= \frac{0.7\Psi b}{r_x} \quad (4.50b)$$

4.4.1.2 Transverse Stiffeners

The required size of transverse stiffeners for plates loaded in uniaxial compression has been defined by Timoshenko and Gere (1961) for one, two, or three equally spaced stiffeners, and by Klitchieff (1949) for any number of stiffeners. The stiffeners as sized provide a nodal line for the buckled plate and thus prohibit overall buckling of the stiffened panel. The strength of the stiffened panel would be limited to the buckling strength of the plate between stiffeners. These authors also give formulas for calculating the buckling strength for smaller stiffeners. The required minimum value of γ given by Klitchieff is

$$\gamma = \frac{(4m^2 - 1)[(m^2 - 1)^2 - 2(m^2 + 1)\beta^2 + \beta^4]}{2m5m^2 + 1 - \beta^2\alpha^3} \quad (4.51)$$

where

$$\beta = \frac{\alpha^2}{m} \quad \alpha = \frac{a}{b} \quad \gamma = \frac{EI_s}{bD} \quad (4.52)$$

and m is the number of panels, $m - 1$ the number of stiffeners, and EI_s flexural rigidity of one transverse stiffener. These stiffener sizes should be understood as ideal stiffeners, in actuality unavoidable imperfections and the desire to avoid coupled instabilities will require designers to use stiffeners greater than those of Eq. 4.51.

An approximate analysis that errs on the conservative side but gives estimates of the required stiffness of transverse stiffeners for plates, either with or without longitudinal stiffeners,

may be developed from a consideration of the buckling of columns with elastic supports. Timoshenko and Gere (1961) show that the required spring constant, K , of the elastic supports for a column, for the supports to behave as if absolutely rigid, is given by

$$K = \frac{mP}{Ca} \quad (4.53)$$

where

$$P = \frac{m^2 \pi^2 (EI)_c}{\alpha^2} \quad (4.54)$$

and C is the constant depending on m , which decreases from 0.5 for $m = 2$ to 0.25 for infinitely large m , $(EI)_c$ the flexural stiffness of column, m the number of spans, and a the total length of column. In the case of a transversely stiffened plate (Fig. 4.25b), a longitudinal strip is assumed to act as a column which is elastically restrained by the transverse stiffeners. Assuming also that the loading from the strip to the stiffener is proportional to the deflection of the stiffener, the spring constant for each column support can be estimated. For a deflection shape of a half sine wave the spring constant is

$$K = \frac{\pi^4 (EI)_s}{b^4} \quad (4.55)$$

Equating Eqs. 4.53 and 4.55 and inserting the value given for P results in the following:

$$\frac{(EI)_s}{b(EI)_c} = \frac{m^3}{\pi^2 C (a/b)^3} \quad (4.56)$$

In the case of panels without longitudinal stiffeners $(EI)_c = D$ and the left side of Eq. 4.56 is γ . Values of C are tabulated by Timoshenko and Gere (1961) for $m \leq 11$. As shown by Fig. 4.26, these values are given approximately by

$$C = 0.25 + \frac{2}{m^3} \quad (4.57)$$

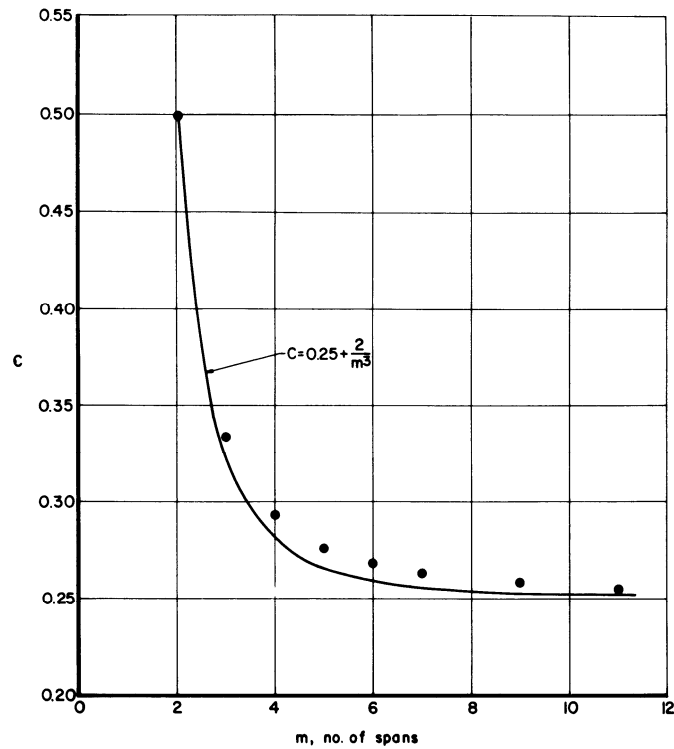


Fig. 4.26 Buckling of columns with elastic supports.

In Table 4.2 values calculated using Eq. 4.56 are compared to corresponding values tabulated by Timoshenko and Gere (1961) for one, two, and three stiffeners and to those calculated by Eq. 4.41 for 10 stiffeners. Equation 4.56 is always conservative and is highly accurate for cases in which several stiffeners subdivide the panel.

Table 4.2 Limiting Values of gamma for Transverse Stiffeners

a/b Ratio	One Stiffener		Two Stiffeners		Three Stiffeners		Ten Stiffeners	
	Timoshenko and Gere (1961)	Eq. 4.45	Timoshenko and Gere (1961)	Eq. 4.45	Timoshenko and Gere (1961)	Eq. 4.45	Eq. 4.42	Eq. 4.45
0.5	12.8	1.30	65.5	65.5	177.0	177.0	4170	4220
0.6	7.25	7.5	37.8	38.0	102.0	122.0	2420	2440
0.8	2.82	3.2	15.8	16.0	43.1	43.2	1020	1030
1.0	1.19	1.6	7.94	8.20	21.9	22.1	522	528
1.2	0.435	0.94	4.43	4.73	12.6	12.8	301	304
$\sqrt{2}$	0	0.57	2.53	2.90	7.44	7.85	185	187

4.4.1.3 Longitudinal and Transverse Stiffeners.

For a combination of longitudinal and transverse stiffeners, Gerard and Becker (1957/1958) give figures showing the minimum value of γ as a function of α for various combinations of equally stiff longitudinal and transverse stiffeners. The same procedure used to establish Eq. 4.56 can also be applied to this case. The difference in the development is that the spring constant, K , of the support is dependent on the number of longitudinal stiffeners as illustrated below. The flexural stiffness $(EI)_c$ in these cases is equal to the average stiffness per unit width of the plate-longitudinal stiffener combination.

Number and Spacing of Longitudinal Stiffeners	Spring Constant, K	$\frac{(EI)}{b(EI)_c} = \gamma$
One centrally located	$\frac{48(EI)_s}{b^3}$	$\frac{0.206m^3}{C(a/b)^3}$
Two equally spaced	$\frac{162}{5} \frac{(EI)_s}{b^3}$	$\frac{0.152m^3}{C(a/b)^3}$
Four equally spaced	$\frac{18.6(EI)_s}{b^3}$	$\frac{0.133m^3}{C(a/b)^3}$
Infinite number equally spaced	$\frac{\pi^4(EI)_s}{b^3}$	$\frac{m^3}{\pi^2 C(a/b)^3} = \frac{0.1013m^3}{C(a/b)^3}$

The required size of transverse stiffeners in a panel also containing longitudinal stiffeners is thus approximately

$$\frac{(EI)_s}{b(EI)_c} = \frac{m^3}{\pi^2 C(a/b)^3} \left(1 + \frac{1}{N-1} \right) \quad (4.58)$$

This formula yields essentially the same values as does the formula presented for aluminum panels in the *Alcoa Structural Handbook* (Aluminum Company of America, 1960). With this size of transverse stiffener the strength of the panel is limited to the buckling strength of the longitudinally stiffened panel between transverse stiffeners.

4.4.1.4 Stiffener Type

The methods of analysis described above are directly applicable to open-section stiffeners having negligible torsional stiffness and are conservative when applied to stiffeners with appreciable torsional stiffness. The influence of torsional stiffness on overall panel buckling has been studied by Kusuda (1959) for the case of one longitudinal or one transverse stiffener. Stiffeners with large torsional rigidity also provide partial or complete fixity of the edges of subpanel plating, thereby increasing their critical stresses.

It has been shown by Lind (1973) and Fukumoto et al. (1977) that the stiffener type affects the buckling mode as well as the ultimate carrying capacity of the stiffened plate. It has also been shown by Tvergaard (1973), and Fok et al. (1977) that local imperfections of stiffeners influence significantly the overall buckling behavior of stiffened plate panels.

4.4.2 Compression: Post-buckling and Strength

Buckling of a stiffened-plate panel may occur by primary instability with a half wavelength which is on the order of the panel length, or by local instability with a half-wavelength which is on the order of the width of plate elements of the plate and stiffeners. As plate panel length increases, the ultimate stress decreases, until at large slenderness ratio the panel fails in flexure as a long column. The ultimate strength in the long-column range can be predicted by the Euler column formula, where the radius of gyration is computed for the combined section of the stiffener and the effective width of the plating. At an intermediate slenderness ratio there is a transition in the mode of failure from the purely local mode to one dominated by overall panel failure. In the transition zone the panel fails through a combination of the primary buckling and flexural modes and may involve stiffener twisting.

It is well known that plates supported at their edges are often able to sustain compressive load far in excess of their buckling loads. The margin between the buckling load and the ultimate load in plates, known as the post-buckling strength, depends on whether the critical stress is reached below or above the proportional limit of the material. If the buckling stress is well below the proportional limit, the ultimate load may be many times greater than the buckling strength, depending on the aspect ratio, a/b , of the plate element. As the buckling stress approaches the yield strength of the material, the reserve strength in the post-buckling range approaches zero. See Section 4.3 for further discussion of the distinctions between elastic buckling, inelastic buckling, post-buckling and strength of plates.

Initial buckling modes of stiffened flat panels vary with the slenderness ratio of the panel and with the type of construction: monolithic or built-up. In the following, as a basis for evaluating post-buckling strength, a brief discussion is given regarding predictions of initial buckling stresses and ultimate strength.

4.4.2.1 Local Instability Mode

The initial buckled form has one transverse sinusoidal half-wave, with perhaps a number of longitudinal half-waves. As the compressive load is increased, the central portion of the transverse half-wave becomes flattened, and, as shown in Fig. 4.27 the transverse deformation is no longer a simple sinusoidal curve. The well-known effective-width approach to the analysis of the post-buckling strength of a flat plate is based on the stress distribution associated with this buckled form, as discussed in detail in Section 4.3.3.

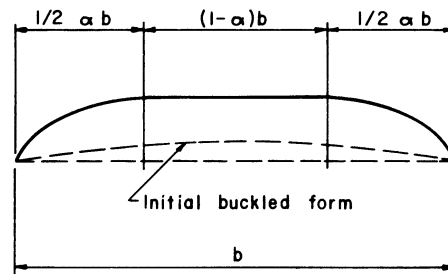


Fig. 4.27 Initial and final buckled shapes

Another change of buckled form is possible when a rectangular flat plate, simply supported on all sides, is subjected to uniform edge compression and is free to expand laterally. A dynamic snap from one buckled form to another may occur by a sudden change of wavelength of buckles along the direction of compression. The behavior of the flat plate in this sense is analogous to the elastic post-buckling of a column supported laterally by a nonlinear elastic medium (Tsien, 1942; Stein, 1959; Koiter, 1963). A column supported laterally by a finite number of nonlinear elastic restraints buckles initially into m sinusoidal half-waves over its length; then subsequently the buckled form may become unstable, and the column may snap into n half-waves, with n being greater than m . The exact analysis of transition between the two modes of buckling is not known at present. Sherbourne et al. (1971) determined the terminal wavelength for flat plates at the ultimate capacity.

4.4.2.2 Failure Strength of Very Short Stiffened Panels

For a short stiffened plate with the slenderness ratio smaller than 20, Gerard and Becker (1957/1958) note that the failure stress is independent of the panel length. The average stress at failure in this slenderness range is known as the crippling, crushing, or local-failure stress, and

will be represented by $\bar{\sigma}_f$. Gerard and Becker (1957/1958) present a method for determining the crippling stress of short longitudinally stiffened panels. However, for most cases, the yield stress of the material can be considered the failure stress for short stiffened panels.

4.4.2.3 Ultimate Strength of Intermediate and Long Stiffened Panels

Gerard and Becker (1957/1958) describe a method to predict the buckling failure of stiffened panels based on a curve analogous to the Johnson parabola shown in Fig. 4.28. At stresses lower than the local buckling stress σ_c and the proportional limit σ_{pl} , the Euler column equation is used. In the transition range between $L/r = 20$ and the long column, a parabola of the following form is used:

$$\bar{\sigma}_c = \bar{\sigma}_f \left[1 - \frac{\sigma_c}{\sigma_e} \left(1 - \frac{\sigma_c}{\bar{\sigma}_f} \right) \left(\frac{\sigma_{20}^{1/2} - \sigma_e^{1/2}}{\sigma_{20}^{1/2} - \sigma_c^{1/2}} \right)^2 \right] \quad (4.59)$$

where $\bar{\sigma}_c$ is the failure stress, $\sigma_e = \pi^2 E/(L/r)^2$ the Euler stress for the panel, $\bar{\sigma}_f$ the failure stress for a short stiffened panel, and σ_{20} the Euler stress evaluated at $L/r = 20$. Many direct-reading column charts have been prepared for panel ultimate strength. The type of plot is shown in Fig. 4.29. Gerard and Becker (1957/1958) have provided references and examples of this work.

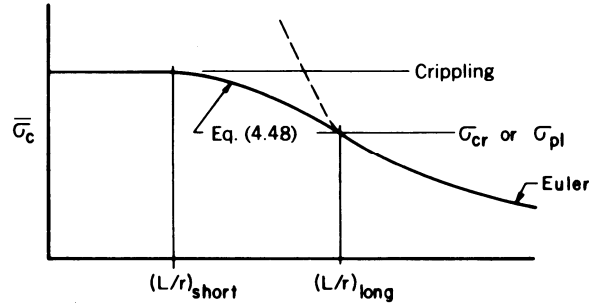


Fig. 4.28 Column curve for stiffened panels.

$$\bar{\sigma}_c = \frac{\sigma_c (A_{st} + 2b_c t_s)}{A_{st} + b_s t_s}$$

N = compressive force
per unit width

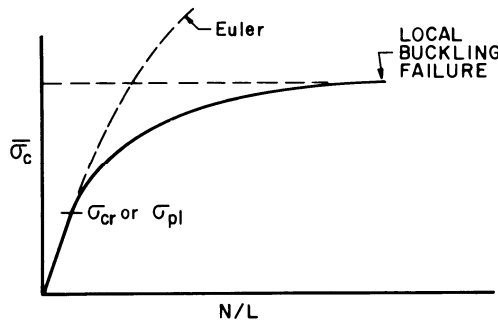


Fig. 4.29 Column chart by Gerard and Becker (1957/1958).

In the determination of panel strength it is necessary to estimate the effective column length of the plate-stiffener combinations as well as the effective width of plating that acts in conjunction with the stiffener. When the critical stress for the individual panel of plating between stiffeners is greater than the critical stress for the stiffened panel, the plating may be assumed

completely effective, and the effective column length of the panel is determined by the end conditions. When the critical stress for the individual plating panel is significantly less than that for the stiffened panel as a unit, the ultimate strength of the stiffened plate is considered to be the lesser of (1) the load that causes the stress at the juncture of plate and stiffener to reach the yield strength of the material, or (2) the column strength of the stiffener in conjunction with an effective width of plating that is less than the actual width of plating between stiffeners.

The application of the first criterion for ultimate strength assumes that the stiffener is stiff enough to allow the plate-edge stress to reach the yield stress before the stiffener buckles as a column and that the stress distribution across the buckled plate can be determined, while the second criterion assumes that the effective column length of the stiffener and the effective width of the associated plating can be properly determined and that residual stresses and distortions due to fabrication are properly accounted for with regard to column buckling. The effective-width concept is treated in Section 4.2.

To provide a better understanding of the behavior of stiffened plates, a theoretical study was carried out by Wittrick (1968). The collapse of box-girder bridges in the early 1970s precipitated a great interest in research on various aspects of box girders, especially the interactive buckling of an assembly of plates and the ultimate strength of a stiffened plate. The research efforts in many ways were centered around the Merrison Committee (1973). Murray (1975) reported on analysis and design procedure for the collapse load for the stiffened plates. Crisfield (1975) presented a finite element formulation for the large-deflection elastic-plastic full-range analysis of stiffened plating. A simple approach for the design of stiffened steel compression flanges was proposed by Dwight and Little (1976).

A theoretical and experimental study on the inelastic buckling strength of stiffened plates was reported by Fukumoto et al. (1977). Residual stresses were considered and the stiffened plates treated had relatively low width-to-thickness ratios and with relatively rigid stiffeners. It was found that partial yielding in the flat stiffeners considerably reduced the buckling strength of a stiffened plate. In the case of plates stiffened by T-type stiffeners, the strength reduction due to partial yielding in the stiffeners was much less pronounced. This is probably due to the fact that the T-stiffeners were more rigid and less susceptible to initial imperfections than were the flat stiffeners. Murray (1973) has indicated that based on experimental results there is often little margin of strength above the load at which yielding first occurs in a stiffener. This phenomenon can lead to a triggering effect which results in a sudden failure of the stiffened plate. Such a viewpoint is also shared by Horne and Narayanan (1977).

Horne and Narayanan (1975, 1977) have proposed a design method for the prediction of collapse loads of stiffened plates subjected to axial compression. They have compared the results obtained from their method, methods proposed by other researchers, and experiments. The results are all close to the observed strength. Horne and Narayanan's method is based on the British Perry–Robertson column formula and consists of analyzing the stiffened plates as a series of isolated columns comprising a stiffener and the associated effective width of plating. The criterion for plate failure is the attainment of yielding stress at the plate stiffener boundary. The criterion for the stiffener-initiated failure is by yielding or by instability of the stiffener.

Little (1976) and Elsharkawi and Walker (1980) have studied the effects of continuity of longitudinal stiffeners on the failure mode and strength of stiffened plates consisting of several bays between cross frames. Little has indicated that there is a tendency for longitudinal continuity to be strengthened where failure occurs in the plate, and weakened where failure

occurs in the stiffener. A simplified design method to account for the effects of continuity has been proposed by Elsharkawi and Walker (1980).

Nonlinear finite element analysis has been compared to tests and shown to provide reliable predictions of the ultimate strength of stiffened panels in a variety of limit states (Grondin et al. 1998). The same researchers went on to perform a wide ranging parametric study that resulted in design guidance for stiffened plates based on relevant plate and stiffener dimensions. (Grondin et al. 1999). The specific role of the stiffener geometry, particularly stiffener torsional stiffness has been the focus of tests (Ghavami 1994) as well as further nonlinear finite element analysis (Sheikh et al. 2003).

Desmond et al. (1981a,b) have presented an experimental study of edge-stiffened compression flanges and intermediately stiffened compression flanges. This work has been extended for edge stiffeners (Schafer and Peköz 1999) and intermediate stiffeners (Schafer and Peköz 1998). Effective width procedures for local and overall (distortional) buckling of the stiffened panels were proposed and have been adopted by AISI (2007). Nguyen and Yu (1982) have reported a study on longitudinally reinforced cold-formed steel beam webs. Based on the experimental results, an effective-width procedure is proposed to predict the ultimate strength of such members subjected to bending. Additional information on this subject matter is presented in Chapters 6, 7 and 13.

4.4.3 Compression and Shear: Buckling

4.4.3.1 Initial Buckling

Analytical and experimental results on the buckling behavior of stiffened plates under combined compression and shear are relatively scarce. Recourse is therefore usually made to data for unstiffened plates supplemented with whatever data are available for the type of longitudinally stiffened construction considered to be most important in practice, that is, that shown in Fig. 4.30. The case of unstiffened rectangular plates under combined compressive and shear stresses has been presented in Section 4.2.4, which showed that a simple parabolic relationship of the form of Eq. 4.60 was satisfactory for engineering purposes for all ranges of elastic restraint from free rotation to complete fixity. The relationship takes the form

$$R_c + R_s^2 = 1 \quad (4.60)$$

where R_c is the ratio of compressive stress when buckling occurs in combined shear and direct stress to compressive stress when buckling occurs in pure compression and R_s is the ratio of shear stress when buckling occurs in combined shear and direct stress to shear stress when buckling occurs in pure shear.

Johnson (1957) treated the problem of long plates with one and two stiffeners acted on by axial compression and shearing stresses. The stiffeners were assumed to have bending stiffness only and the resulting interaction curves show discontinuities which reflect the mode into which the plate buckles. When the bending stiffness ratio of the stiffener to that of the plate (EI/bD) is low, the buckle goes through the stiffener. However, when the stiffness ratio is increased so that nodal lines occur along the stiffener lengths, buckling takes place without deflection along the stiffeners. In this case another interaction relation exists between compressive and shearing stresses. Another somewhat more limited study of the interaction relationship of infinitely wide stiffened plates under compression and shearing stresses was reported by Harris and Pifko (1969). In this study the finite-element method was used. The stiffeners were assumed to have both bending and torsional stiffness, and the grid refinement used was judged to be adequate to ensure accurate results. The results shown in Fig. 4.31 were compared to the parabolic

expression (Eq. 4.49). Except for the case of assumed large torsional stiffness ratio ($GJ/bD = 10^6$) the analytical points follow the parabolic relationship very well.

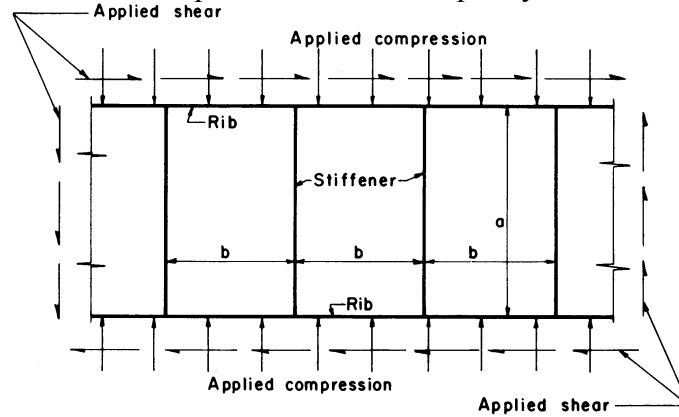
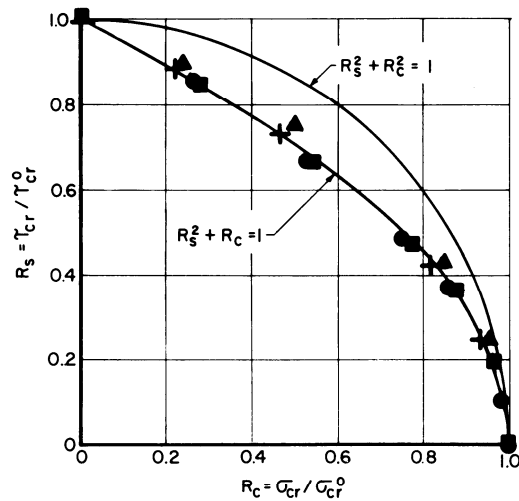
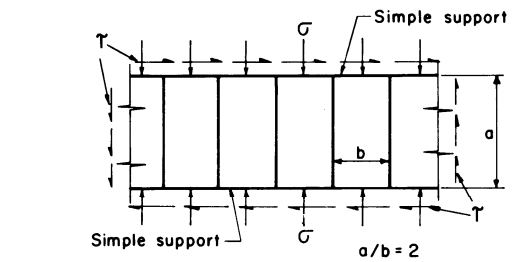


Fig. 4.30 Longitudinally stiffened plate under combined compression and shear stresses



A/bt	EI/bD	CJ/bD	Symbol
0.4	100	0	●
0.4	100	1	+
0.4	100	10^6	▲
0.4	1000	0	■

Fig. 4.31 Analytical interaction relations for infinitely wide stiffened plate under combined compression and shearing stresses.

4.4.3.2 Buckling in the Inelastic Range

Analytic prediction of the interaction relationship for stiffened panels which buckle in the inelastic range under combined compression and shear are practically nonexistent in the literature. One such computation reported by Harris and Pifko (1969) was made for an integrally stiffened panel made of aluminum 2024-T351 and having the dimensions shown in Fig. 4.26. The predicted interaction curves are shown in this figure for both the elastic case, which agrees very well with the parabolic relationship (Eq. 4.60), and the inelastic-buckling case. Because of the limited nature of the data, no general relationship for the inelastic-buckling case can be derived. However, it should be noted from Fig. 4.32 that the circular relationship lies above the analytical curve of the inelastic-buckling case.

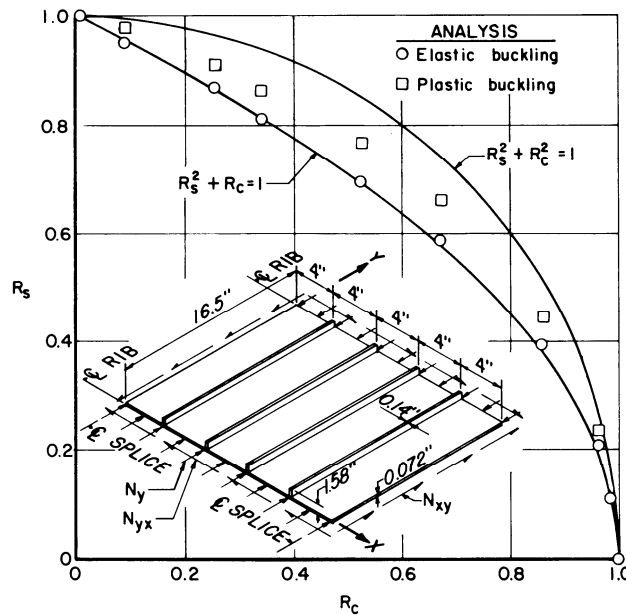


Fig. 4.32 Analytically predicted elastic and inelastic interaction curves for an integrally stiffened panel.

4.4.4 Compression and Shear: Post-buckling and Strength

Post-buckling behavior is complex, and exact treatment of the problem has not yet been achieved. Because of the importance of predicting the strength of stiffened panels loaded beyond initial buckling in the aircraft industry semiempirical methods have been in existence for many years. In the case of light stiffened plates under combined compression and shear, the structure will usually take a considerable load in excess of the initial buckling load of the plate. Chapter 6 covers the design aspects of using these post-buckling or tension-field theories; hence no further discussion of these methods is made here.

4.4.5 Laterally Loaded plates in compression

Plates with stiffeners in the direction of the axial load that are also subjected to a distributed lateral load are commonly encountered as the bottom plates in ships. A study based on a large-deflection post-buckling theory (Supple, 1980) shows that lateral pressure produces effects similar to initial geometric imperfections with a long buckling wavelength. It is shown that a sufficiently high pressure induces stable post-buckling in the long-wave mode.

The stiffened plating is supported on heavy transverse structural members which may be assumed to be rigid. The panels have width-to-length ratios of about 2.5 to 4.0, and there is essentially no interaction in the transverse direction and thus the panel undergoes cylindrical bending. It behaves as if it were a wide beam-column under axial and lateral loads. It is convenient to isolate one longitudinal stiffener together with a plate of the width equal to the spacing of the stiffeners, b , and to consider that all other stiffeners behave in a similar manner. Such a beam-column is shown in Fig. 4.33.

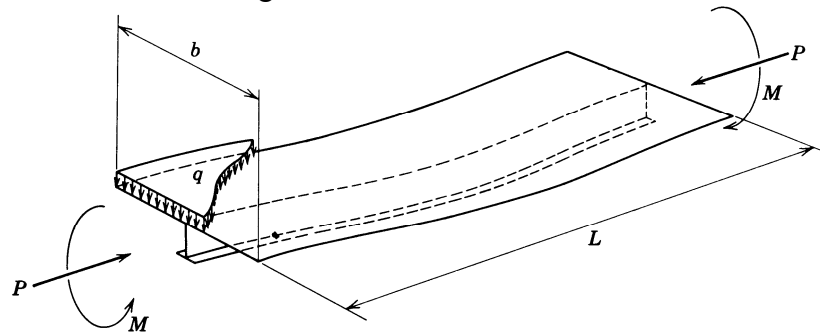


Fig. 4.33 Idealized beam-column.

Ultimate-strength analysis, that is, the determination of the maximum values of the lateral and axial loads that can be sustained by the member, requires a consideration of: 1. the yield strength of plate and stiffener materials, 2. Large-deflection theory, 3. Partial plastification of the section, and 4. Post-buckling and post-ultimate-strength behavior of the plate. The complexity of the problem, in particular, consideration of items 2, 3, and 4 suggests that numerical methods be used. Some solutions have been obtained for standard wide-flange shapes by Ketter (1962), and Lu and Kamalvand (1968) in the form of interaction curves between the axial and lateral loads. Unfortunately, these results cannot be used for plating since items 1 and 4 were not considered. Another complication is that the wide-flange sections are doubly symmetrical, whereas the section shown in Fig. 4.33 is singly symmetrical with a very large top flange.

This means, for example, that although it was possible to nondimensionalize the results for wide-flange sections in terms of L/r and make them applicable with a very small error to any wide-flange section, the unsymmetrical section of the stiffened panel must be treated as a special case for every combination of relative proportions. Nomographs for the ultimate strengths of stiffened plates with a yield point of 47 ksi and the ranges of geometrical and loading parameters commonly encountered in ship structures are given by Vojta and Ostapenko (1967).

4.5 BUCKLING OF ORTHOTROPIC PLATES

Problems related to rectangular plates with stiffeners parallel to one or both pairs of sides can be solved approximately by methods applicable to orthotropic plate theory. An orthotropic plate is one whose material properties are orthogonally anisotropic; a uniformly stiffened plate is reduced to this case by effectively “smearing” the stiffness characteristics of its stiffeners over the domain of the plate. Clearly, the theory is best applicable when the spacing of the stiffeners is small.

The calculation of buckling strength of orthotropic plates is based on the solution of the following differential equation governing the small deflection $w(x, y)$ of the buckled plate:

$$D_1 \frac{\partial^4 w}{\partial x^4} + 2D_3 \frac{\partial^4 w}{\partial x^2 \partial y^2} + D_2 \frac{\partial^4 w}{\partial y^4} + N_x \frac{\partial^2 w}{\partial x^2} + N_y \frac{\partial^2 w}{\partial y^2} + 2N_{xy} \frac{\partial^2 w}{\partial x \partial y} = 0 \quad (4.61)$$

where

$$D_1 = \frac{(EI)_x}{1 - \nu_x \nu_y}$$

$$D_2 = \frac{(EI)_y}{1 - \nu_x \nu_y}$$

$$D_3 = \frac{1}{2}(\nu_y D_1 + \nu_x D_2) + 2(GI)_{xy}$$

in which N_x , N_y , and N_{xy} are in-plane forces per unit width (Fig. 4.34), $(EI)_x$ and $(EI)_y$ are flexural stiffnesses, per unit width, of beam strips in the x and y directions, respectively; ν_x and ν_y are flexural Poisson ratios; and $2(GI)_{xy}$ is a measure of torsional stiffness.

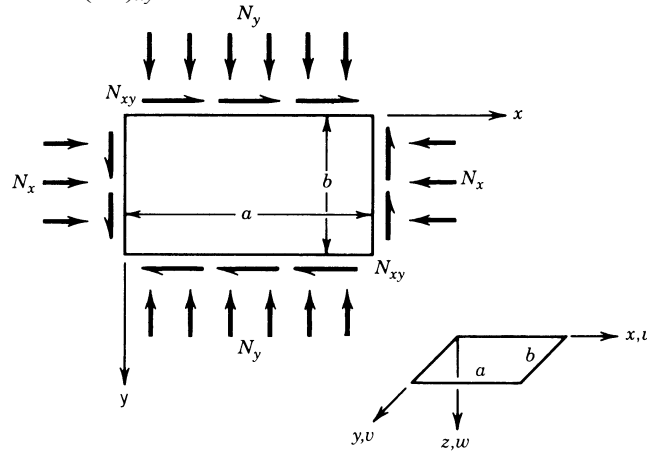


Fig. 4.34 Plate subjected to axial and shear stress.

Theoretical buckling data for several cases of rectangular plates with supported edges ($w = 0$), under uniform in-plane loadings, N_x , N_y , and N_{xy} , applied singly or in certain combinations, are presented. The following are some of the additional notations that will be employed: a and b are the lengths of plate in x and y directions, respectively (see Fig. 4.34); m (integer) is the number of buckles or half-waves in the x -direction when the buckle pattern is sinusoidal in that direction; and n (integer) is the number of buckles or half-waves in the y -direction when the buckle pattern is sinusoidal in the y -direction.

4.5.1 Compression

Uniaxial Compression in x-Direction, Loaded Edges Simply Supported, Unloaded Edges Elastically Restrained Against Rotation: For these conditions, referring to Fig. 4.34, N_x is the only loading, the edges $x = 0, a$ are simply supported, and the edges $y = 0, b$ are each elastically restrained against rotation by a restraining medium whose stiffness (moment per unit length per radian of rotation) is K . The quantity Kb/D_2 to be denoted by ε , will be used as a dimensionless measure of this stiffness. An exact solution leads to the following formula defining the value of N_x that can sustain a buckle pattern containing m sinusoidal half-waves in the x -direction:

$$\frac{N_x b^2}{\pi^2 D_3} = \left(\frac{b}{a/m} \right)^2 \frac{D_1}{D_3} + 2 + f_1 \left(\varepsilon, \left(\frac{a/m}{b} \right)^2 \frac{D_2}{D_3} \right) \quad (4.62)$$

where f_1 is the function plotted in Fig. 4.35. If $(a/mb)^2(D_2/D_3) > 0.4$, Eq. 4.62 can be very closely approximated by the formula

$$\frac{N_x b^2}{\pi^2 D_3} = \left(\frac{b}{a/m} \right)^2 \frac{D_1}{D_3} + 2 + f_2(\varepsilon) + \left(\frac{a/m}{b} \right)^2 \frac{D_2}{D_3} f_3(\varepsilon) \quad (4.63)$$

where f_2 and f_3 are the functions plotted in Fig. 4.36. The buckling load is the smallest N_x obtained by substituting different integer values of m ($m = 1, 2, 3, \dots$) into Eq. 4.62 or, if it applies, Eq. 4.63. In performing this minimization, one should take into account the fact that for most practical restraining media the stiffness K is not fixed but is a function of the half-wavelength a/m of the edge rotation. K may also depend on the axial load in the restraining medium, therefore on N_x , necessitating a trial-and-error calculation to determine N_x for any selected m . Negative values of K are physically possible but are excluded from consideration in Fig. 4.35 and Fig. 4.36. Unequal restraints along the edges $y = 0$ and b can be handled approximately by first assuming the $y = 0$ constraint to be present at both edges, then the $y = b$ constraint, and averaging the two values of N_x thus obtained.

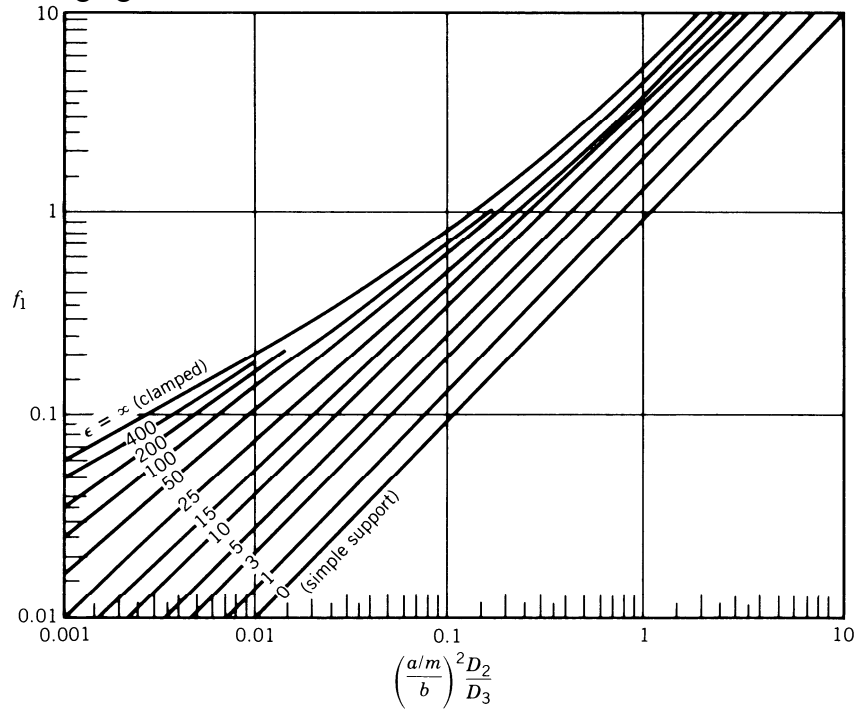


Fig. 4.35 Function f_1 in Eq. 4.5

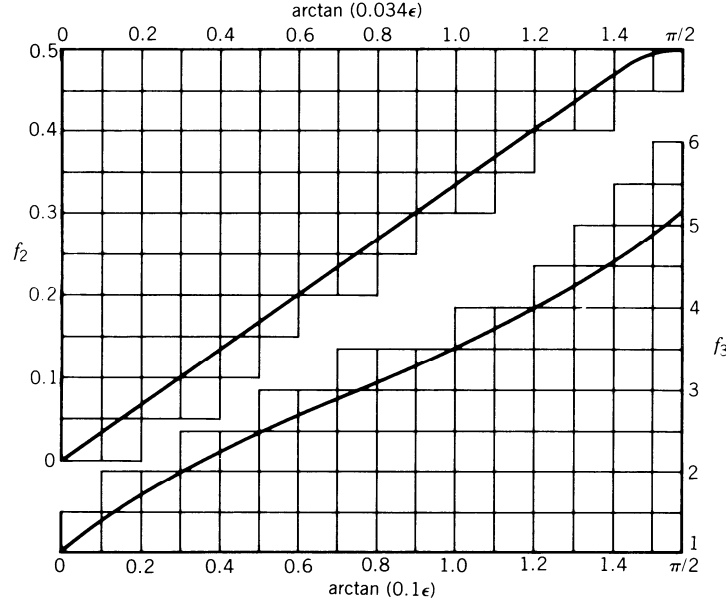


Fig. 4.36 Functions f_2 and f_3 in Eq. 4.52.

Uniaxial Compression, Loaded Edges Simply Supported, Unloaded Edges Clamped: Here N_x is the only loading, the edges $x = 0$ and a are simply supported, and the other two edges are clamped. The exact solution is contained in the condition $\varepsilon = \infty$ of the previous example. An approximate solution is given by Wittrick (1952) in the form

$$\frac{N_x b^2}{\pi^2 \sqrt{D_1 D_2}} = k - c \left(1 - \frac{D_3}{\sqrt{D_1 D_2}} \right) \quad (4.64)$$

where $c = 2.4$ and k is taken from curve (c) of Fig. 4.37. Equation 4.64 is virtually equivalent to Eq. 4.63 and must therefore be subject to the same restriction, [i.e., $(a/mb)^2 (D_2/D_3) > 0.4$].

Uniaxial Compression, All Edges Clamped: Wittrick (1952) gives an approximate solution for these conditions in the form of Eq. 4.64 with $c = 2.46$ and k taken from curve (d) of Fig. 4.37.

4.5.2 Biaxial compression

Biaxial Compression, All Edges Simply Supported: When all four edges are simply supported, combinations of N_x and N_y that can sustain a buckle pattern of m sinusoidal half-waves in the x -direction and n sinusoidal half-waves in the y -direction are defined exactly by the interaction equation

$$\frac{1}{n^2} \frac{N_x b^2}{\pi^2 D_3} + \frac{1}{m^2} \frac{N_y a^2}{\pi^2 D_3} = \left(\frac{b/n}{a/m} \right)^2 \frac{D_1}{D_3} + 2 + \left(\frac{a/m}{b/n} \right)^2 \frac{D_2}{D_3} \quad (4.65)$$

In using Eq. 4.53, one must substitute different combinations of m and n until that combination is found which minimizes N_x for a given N_y , N_y for a given N_x , or N_x and N_y simultaneously for a given ratio between them. It can be shown (Libove, 1983) that these minima will occur with at least one of the two integers equal to unity. Therefore, only the combinations $m = 1; n = 1, 2, 3, \dots$ and $n = 1; m = 2, 3, \dots$ need to be tried. The condition

$$\frac{N_y b^2}{\pi^2 D_2} < 1 \quad (4.66)$$

is sufficient to ensure that $n = 1$ will govern. In that case, with N_y regarded as given, Wittrick (1952) has shown that the N_x required for buckling is defined by

$$\frac{N_x b^2}{\pi^2 D_3} = 2 + (k - 2) \left[\frac{D_1 D_2}{D_3^2} \left(1 - \frac{N_y b^2}{\pi^2 D_2} \right) \right]^{1/2} \quad (4.67)$$

where k is the function plotted as curve (a) in Fig. 4.37. The case of the infinitely long plate ($a/b = \infty$) is of interest as the limiting case of a very long plate. For that case it can be deduced from Eq. 4.65 that if $N_x b^2 / \pi^2 D_3 \leq 2$, the longitudinal compression N_x is too small to sustain a multilobed buckle pattern, and the plate will buckle in a cylindrical mode (i.e., as a wide plate-column of length b) when $N_y b^2 / \pi^2 D_2 = 1$. On the other hand, if $N_x b^2 / \pi^2 D_3 > 2$, the buckle pattern will be sinusoidally lobed in the x -direction with a half-wave length-to-width ratio of

$$\frac{a/m}{b} = \left[\frac{D_2}{D_1} \left(1 - \frac{N_y b^2}{\pi^2 D_2} \right) \right]^{-1/4} \quad (4.68)$$

and the buckling will occur when N_x and N_y satisfy Eq. 4.67 with k set equal to 4. The interaction curve of Fig. 4.38 summarizes the results just given for the case $a/b = \infty$.

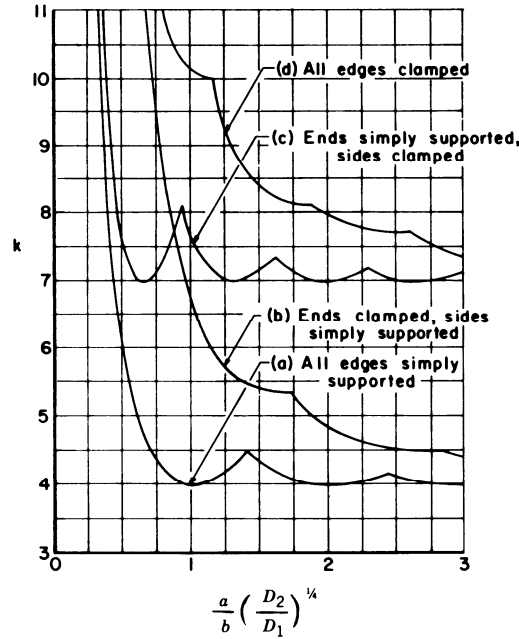


Fig. 4.37 Buckling coefficients for orthotropic plates.

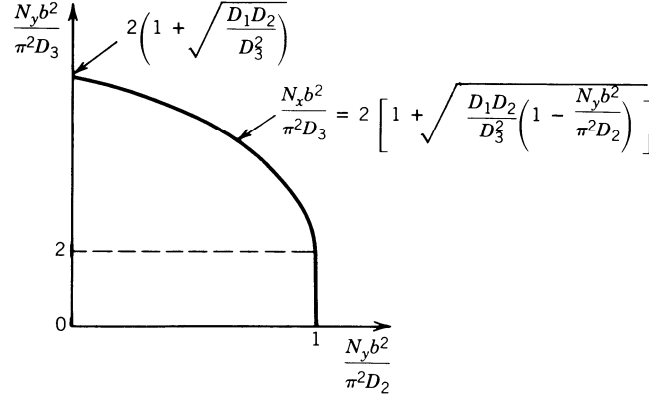


Fig. 4.38 Interaction curve for orthotropic plates.

Compression in x-Direction Applied to Clamped Edges, Limited Compression in y-Direction Applied to Simply Supported Edges: Referring to Fig. 4.34, and considering the case in which the edges $x = 0, a$ are clamped, the edges $y = 0, b$ are simply supported, N_{xy} is absent, and N_y satisfies the inequality (Eq. 4.66). Then, with N_y regarded as given, the value of N_x required to cause buckling is defined by Eq. 4.67 with k taken from curve (b) of Fig. 4.37 (Wittrick, 1952).

4.5.3 Shear

Shear, Various Boundary Conditions: Theoretical data for the shear flow N_{xy} required to cause buckling of rectangular orthotropic plates have been collected by Johns (1971). Three of his graphs are reproduced in Fig. 4.39. They apply, respectively, to the boundary conditions of (a) all edges simply supported; (b) edges $y = 0$ and $y = b$ simply supported, the other two edges clamped; and (c) all edges clamped. In Fig. 4.39, k_s stands for $N_{xy} b^2 / \pi^2 D_1^{1/4} D_2^{3/4}$.

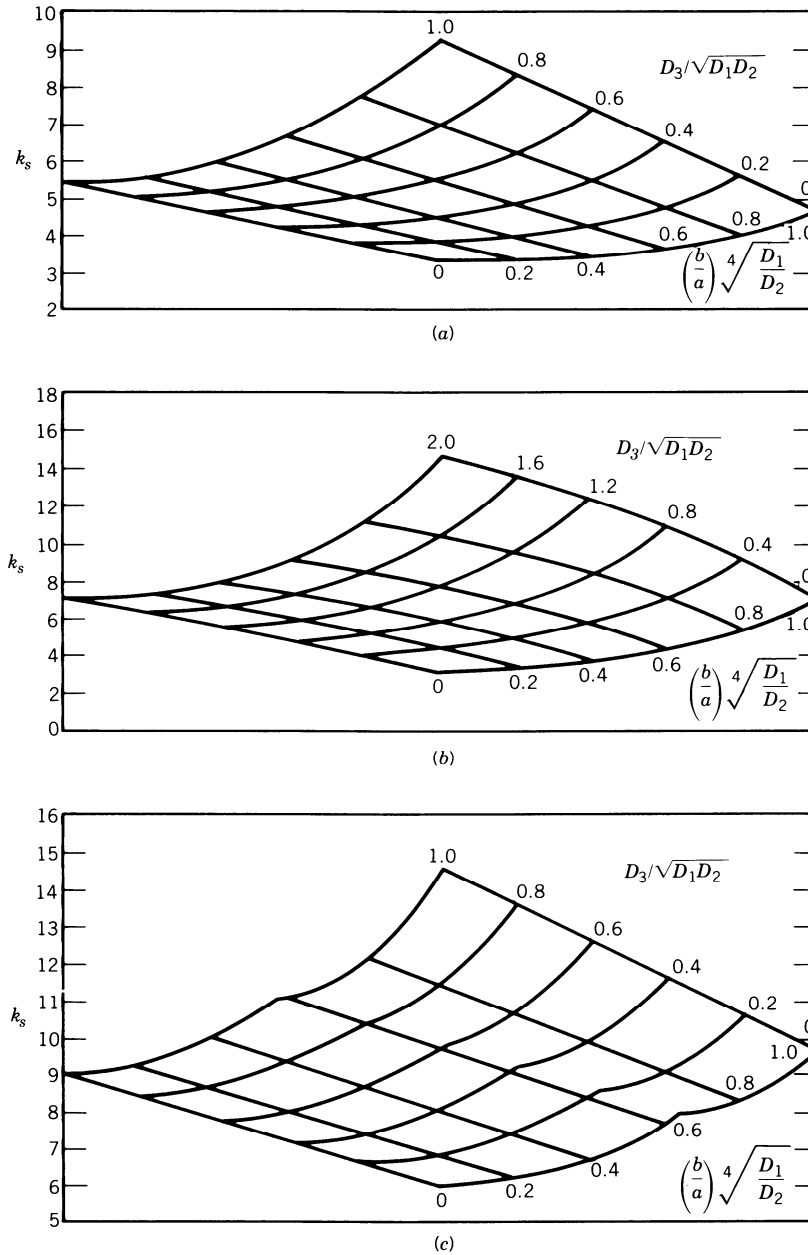


Fig. 4.39 Shear buckling coefficients for orthotropic plates. [Adapted from Johns (1971), printed with the permission of Her Majesty's Stationery Office.]

To make use of the buckling data presented above, one must of course, know the values of the elastic constants appearing in Eq. 4.61. These constants are best determined experimentally, by tests such as those described by Libove and Batdorf (1948) and Becker and Gerard (1963). If the plates are of a simple enough construction, the constants can also be evaluated theoretically. For example, for a sheet of thickness t and shear modulus G orthogonally stiffened by x -wise stiffeners of torsional stiffness C_1 spaced a distance b_1 apart, and y -wise stiffeners of torsional stiffness C_2 spaced a distance a_1 apart, $(EI)_x$ may be taken as the flexural stiffness of the composite beam consisting of one x -wise stiffener and its associated width b_1 of sheet, divided by b_1 , while $(EI)_y$ is computed in an analogous manner using a y -wise stiffener and

its associated width a_1 of sheet. For such plates, v_x and v_y may usually be taken as zero with little error, and then

$$D_3 = 2(GI)_{xy} = \frac{Gt^3}{6} + \frac{1}{2} \left(\frac{C_1}{b_1} + \frac{C_2}{a_1} \right) \quad (4.69)$$

(The factor $\frac{1}{2}$ in this formula is sometimes erroneously omitted.) Plates with integral wafflelike stiffening may also be modified as orthotropic plates, provided that the ribbings are so oriented as to create axes of elastic symmetry parallel to the plate edges; formulas for estimating the elastic constants of such plates are derived by Dow et al. (1954). Corrugated-core sandwich plates with the corrugations parallel to the x or y axis can similarly be treated as orthotropic plates, and formulas for their elastic constants are developed by Libove and Hubka (1951); however, for such sandwich plates, deflections due to transverse shear, neglected in the present discussion, may sometimes be important. It is common practice to treat a corrugated plate also as an orthotropic plate, and the appropriate elastic constants when the profile of the plate is sinusoidal are discussed by Lau (1981). However, there are indications (Perel and Libove, 1978) that modelling the corrugated plate as an orthotropic plate may lead to an underestimate of its shear buckling strength.

The orthotropic plate model has an additional shortcoming when applied to stiffened plates, namely its neglect of any coupling between in-plane forces and out-of-plane deflections. That is, underlying Eq. 4.61 is the tacit assumption that there exists a reference plane in which the forces N_x , N_y , and N_{xy} can be applied without producing any curvatures or twist. In the case of a sheet with identical stiffening on both sides, there does of course exist such a plane—it is the middle surface of the sheet. If the stiffening is one-sided, however, it is usually not possible to find a reference plane that will eliminate completely the coupling between in-plane forces and out-of-plane deflections. It has been shown (Whitney and Leissa, 1969; Jones, 1975) that such coupling, occurring in the context of composite laminated plates, can have a marked effect on the buckling loads. Therefore, it is very likely that in metal plates with one-sided stiffening it can also have a marked effect on the buckling loads. A thorough investigation of this effect, using an appropriately generalized orthotropic plate theory, would be a worthwhile subject for future research and some work has preceded in this direction (Mikami and Niwa 1996).

Finally, orthotropic plate theory is incapable of modeling local buckling, that is, buckling in which the buckle wavelengths are of the same order as the stiffener spacings or the widths of the plate elements of which the stiffeners are composed. Wittrick and Horsington (1984) have developed more refined approaches that can account for local buckling and modes of buckling in which local and overall deformations appear in conjunction. Their methods are applicable to plates with unidirectional stiffening possessing certain boundary conditions and subjected to combinations of shear and biaxial compression.

4.6 INTERACTION BETWEEN PLATE ELEMENTS

In the preceding sections, attention has been confined to the behavior of a single plate element supported along one or both of its longitudinal edges with or without stiffeners. The structural sections employed in practice (Fig. 4.1) are composed of plate elements arranged in a variety of configurations. It is clear that the behavior of an assembly of plates would be governed by an interaction between the plate components. In this section the mechanics of such an interaction and its implication in design are discussed briefly.

4.6.1 Buckling Modes of a Plate Assembly

Unlike a single plate element supported along the unloaded edges, a plate assembly can buckle in one of several possible modes. For the case of axial compression, the buckling mode can take one of the following forms:

- *Mode I / local.* This is the purely local buckling mode discussed earlier. The mode involves out-of-plane deformation of the component plates with the junctions remaining essentially straight, and it has a half-wavelength of the same order of magnitude as the widths of the plate elements.
- *Mode II / distortional.* The buckling process may involve in-plane bending of one or more of the constituent plates as well as out-of-plane bending of all the elements, as in a purely local mode. Such a buckling mode is referred to as a *distortional buckling mode*, *stiffener buckling mode*, *local torsional mode*, or *orthotropic mode*, depending on the context. The associated wavelengths are considerably greater than those of mode I (local buckling) but there is a half-wavelength at which the critical stress is a minimum.
- *Mode III / global.* The plate structure may buckle as a column in flexural or flexural-torsional mode with or without interaction of local buckling.

The three modes are illustrated for an I-beam in major axis bending in Fig. 4.40, based on the finite strip analysis results of Hancock (1978). Finite strip analysis has become a popular alternative to shell finite element analysis for this problem with several programs available for this analysis (Papangelis and Hancock 1995; Schafer and Adany 2006). Another alternative seeing significant recent attention is generalized beam theory (Silvestre and Camotim 2002). Attention in this section is primarily on the mode I / local type of buckling. Global buckling (mode III) and interaction between local and global modes of buckling, as well as mode II / distortional type of buckling and its interaction with the other modes are treated in detail in Chapter 13 and elsewhere in this guide.

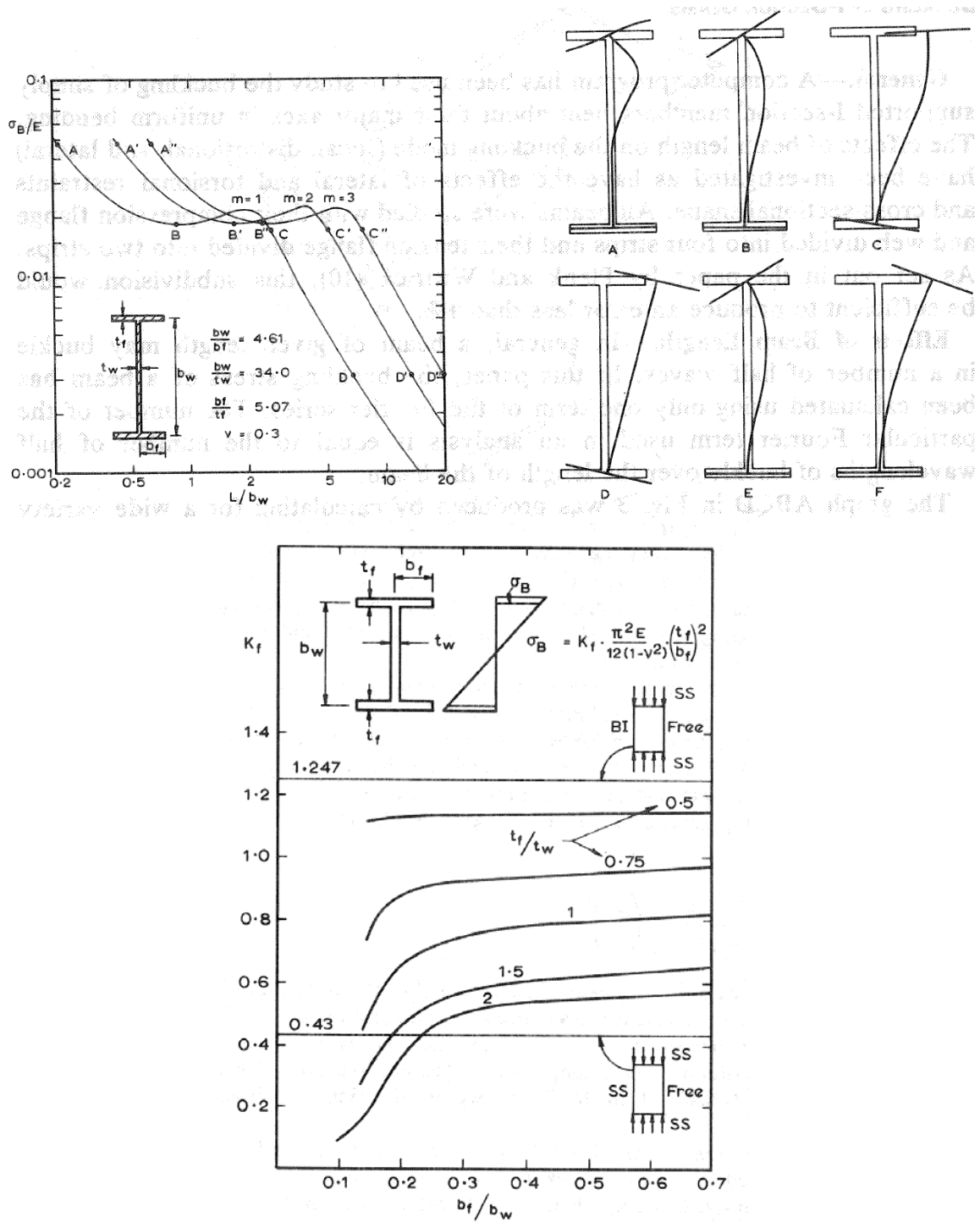


Fig. 4.40 Stability response of an I-beam in major axis bending using the finite strip method (a) half-wavelength vs. buckling stress, (b) buckling mode shapes, (c) plate buckling coefficient (Hancock 1978)

4.6.2 Local Buckling of a Plate Assembly

A prismatic plate structure is often viewed simply as consisting of *stiffened* and *unstiffened* plate elements. The former are plate elements supported on both of their longitudinal edges by virtue of their connection to adjacent elements, while the latter are those supported only along one of their longitudinal edges. Thus, the critical local buckling stress of a plate assembly may be taken as the smallest of the critical stresses of the plate elements, each treated as simply supported along its junctions with other plates. This stress will be conservative because the element providing the lower bound will be restrained by the more stable adjoining plate elements if longitudinal edge joints provide effective continuity. More complete information on k -factors as influenced by the interaction between plate components can be found in a number of classic references (Bleich, 1952); (Stowell et al., 1952; Gerard and Becker, 1957/1958; Timoshenko and Gere, 1961). However, such a calculation must be used with caution for the following reasons:

1. The results can be unduly conservative when the plate structure consists of elements with widely varying slenderness. This is the result of neglecting the rotational restraints at the functions.
2. The results are inapplicable unless it is ensured that all the plate elements buckle locally (i.e., the junctions remain essentially straight). If, on the other hand, mode II or III type of buckling is critical, the result of such a simplified calculation would be on the unsafe side.

The intervention of distortional, or stiffener buckling (mode II) may be averted in practice by designing “out” the stiffener buckling mode by the provision of stiffeners (edge or intermediate) of adequate rigidity. This may be advantageous because of the limited post-buckling resistance associated with the mode II type of buckling. However, it is not always practical or economical, designs where distortional buckling must be considered are discussed further in Chapter 13.

Figure 4.18 gives the variations of the local buckling coefficients k_w for a wide-flange I-section, a box section and a Z- or channel section, respectively, with respect to the geometrical properties of the member. Each of these charts is divided into two portions by a dashed line running across it (Kroll et al., 1943). In each portion, buckling of one of the elements dominates over the other, but the proportions exactly on the dashed line represent the case where the buckling stress of the elements are equal. Additional charts and related information may be found in the references such as the Japanese *Handbook of Structural Stability* (CRCJ, 1971). In addition, free or low-cost computational tools (Papangelis and Hancock 1995; Schafer and Adany 2006; Silvestre and Camotim 2002); are now readily available and able to provide similar results.

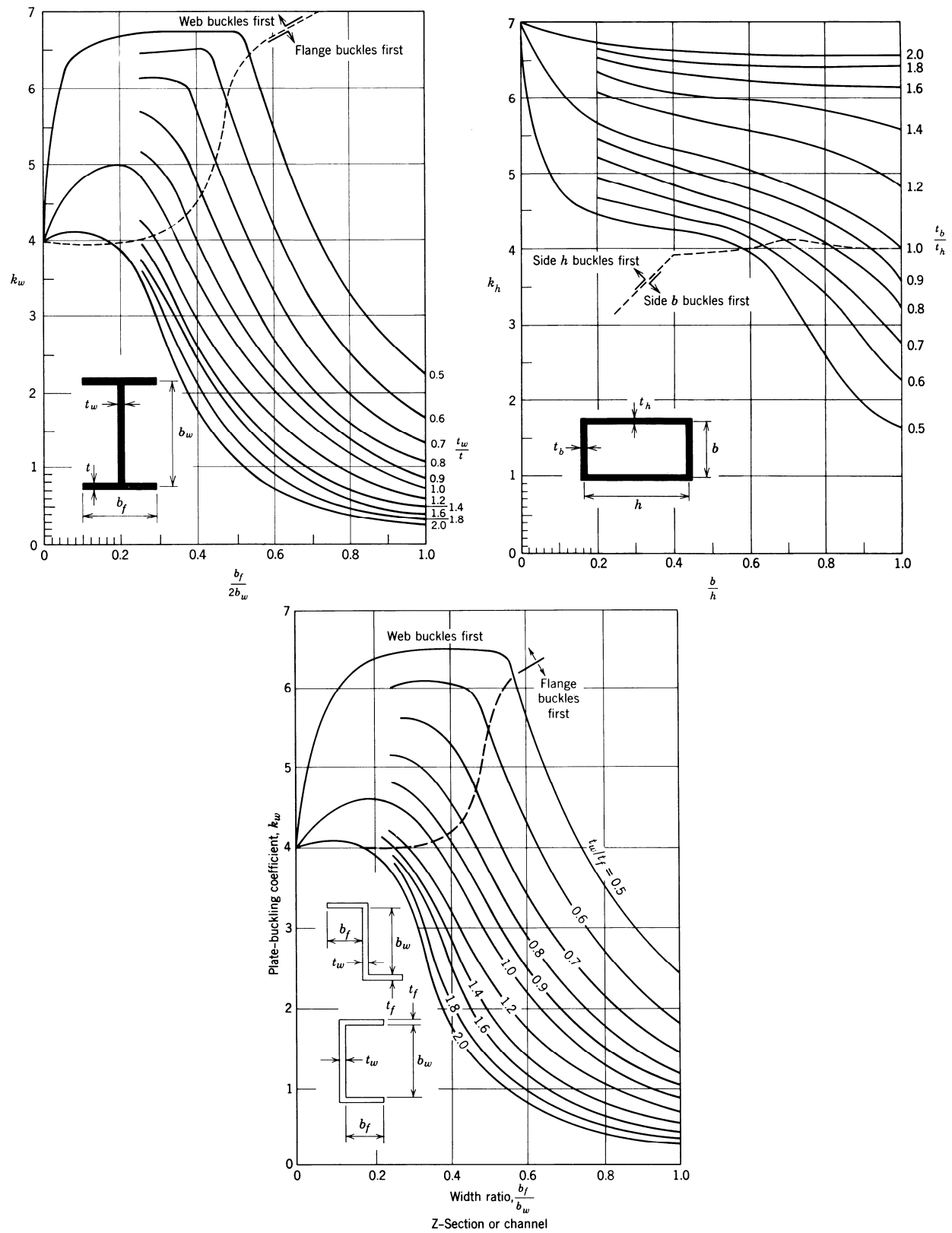


Fig. 4.41 Plate buckling coefficients for plate assemblies (Kroll et al., 1943)

4.6.3 Post-buckling of a Plate Assembly

Interaction between the elements of a plate assembly is inescapable because of the equilibrium and compatibility conditions that must be satisfied at the junction. In the case of local buckling it is possible to simplify these conditions considerably, as has been shown by Benthem (1959). The smallness of the in-plane displacements in comparison to the out-of-plane displacements makes it possible to assume that normal displacements are zero for each plate element meeting at a corner. Also, because of the smallness of the bending rigidity in comparison to the extensional rigidity, it is possible to assume that the in-plane membrane meets another plate element at an angle (Walker, 1964; Graves-Smith, 1968; Rhodes and Harvey, 1971; Tien and Wang, 1979).

In the post-buckling range in-plane displacements and membrane stresses dominate the behavior of the buckled plates. The interactions between plate elements along the junctions become very complex. The problem is compounded when interaction between global and local buckling is considered, or when interaction between distortional and the other modes is considered. Suffice to say post-buckling and strength of plate assemblies considering all possible instabilities (modes I – III) remains a topic of considerable interest in research.

The earlier references on interaction of local and overall buckling in the post-buckling range include those by Bijlaard and Fisher (1952), Cherry (1960), Graves-Smith (1969), Klöppel et al. (1969), Sharp (1970), and Škaloud and Zornerova (1970). Research in this field has also been carried out by Rhodes and Harvey (1976), Graves-Smith and Sridharan (1978, 1980), Kalyanaraman (1978), Thomasson (1978), Little (1979), Rhodes and Loughlan (1980), Hancock (1980, 1981), Sridharan and Graves-Smith (1981), Fukumoto and Kubo (1982), Sridharan (1982) and Bradford and Hancock (1984). Using the concept of effective width, the problem has been investigated by DeWolf et al. (1974), Wang and Pao, (1981), and Desmond et al. (1981a and b).

As design methods for local-overall buckling (modes I and III) mature, recent research attentions has been focused on mode II: distortional buckling. Lau and Hancock (1987) provided analytical formula for predicting elastic distortional buckling and later Hancock, Kwon et al. (1994) provided empirical formulas for predicting the ultimate strength in distortional buckling for a variety of different cold-formed steel cross-sections. Bradford (1992) has examined the distortional mode in the context of hot-rolled steel I-beams, while Schafer and Peköz (2002; 1999) examined local, distortional, and global buckling of cold-formed steel beams and columns in developing the methods currently used in the AISI (2007) Specification. The application aspect of this subject is discussed further for thin-walled members in Chapter 13.

4.7 REFERENCES

- AA (1994), *Aluminum Design Manual*, Aluminum Association, Washington, D.C.
- Abdel-Sayed, G. (1969), "Effective Width of Thin Plates in Compression," *ASCE J. Struct. Div.*, Vol. 95, No. ST10, pp. 2183–2204.
- AISC (1993), *Load and Resistance Factor Design for Structural Steel Buildings*, American Institute of Steel Construction, Chicago.
- AISI (1996), *Specification for the Design of Cold-Formed Steel Structural Members*, American Iron and Steel Institute, Washington, D.C.
- Allen, H. G., and Bulson, P. S. (1980), *Background to Buckling*, McGraw-Hill, Maidenhead, Berkshire, England.
- Aluminum Company of America (1960), *Alcoa Structural Handbook* (also *Handbook of Design Stresses for Aluminum*), Alcoa, Pittsburgh, Pa.
- Azhari, M., and Bradford, M. A. (1993), "Inelastic Initial Load Buckling of Plates with and Without Residual Stresses," *J. Eng. Struct.*, Vol. 15, No. 1, 1993, pp. 31–39.
- Batdorf, S. B., and Houbolt, J. C. (1946), "Critical Combinations of Shear and Transverse Direct Stress for an Infinitely Long Flat Plate with Edges Elastically Restrained Against Rotation," *NACA Rep. No. 847*.
- Batdorf, S. B., and Stein, M. (1947), "Critical Combinations of Shear and Direct Stress for Simply Supported Rectangular Flat Plates," *NACA Tech. Note No. 1223*.
- Becker, H., and Gerard, G. (1963), "Measurement of Torsional Rigidity of Stiffened Plates," *NASA Tech. Note No. D-2007*.
- Benthem, J. P. (1959), "The Reduction in Stiffness of Combinations of Rectangular Plates in Compression After Exceeding the Buckling Load," *NLL-TR S-539*.
- Bergman, S., and Reissner, H. (1932), "Über die Knickung von rechteckigen Platten bei Schubbeanspruchung," *Z. Flugtech Motorluftschiffahrt*, Vol. 23, p. 6.
- Bijlaard, P. P. (1949), "Theory and Tests on Plastic Stability of Plates and Shells," *J. Aeronaut. Sci.*, Vol. 16, pp. 529–541.
- Bijlaard, P. P. (1950), "On the Plastic Buckling of Plates," *J. Aeronaut. Sci.*, Vol. 17, p. 493.
- Bijlaard, P. P. (1957), "Buckling of Plates Under Nonhomogeneous Stress," *ASCE J. Eng. Mech. Div.*, Vol. 83, No. EM3, Proc. Paper 1293.
- Bijlaard, P. P., and Fisher, G. P. (1952), "Column Strength of H Sections and Square Tubes, in Post Buckling Range of Component Plates," *NACA Tech. Note No. 2994*.
- Bleich, F. (1952), *Buckling Strength of Metal Structures*, McGraw-Hill, New York.
- Bleich, F., and Ramsey, L. B. (1951), *A Design Manual on the Buckling Strength of Metal Structures*, Society of Naval Architects, Washington, D.C.
- Brockenbrough, R. L., and Johnston, B. G. (1974), *U.S. Steel Design Manual*, 2nd ed., U.S. Steel Corporation, Pittsburgh, Pa.
- Brown, C. J. (1990), "Elastic Buckling of Perforated Plates Subjected to Concentrated Loads," *J. Comput. Struct.*, Vol. 36, No. 6, pp. 1103–1109.
- Bryan, G. H. (1891), "On the Stability of a Plane Plate Under Thrusts in Its Own Plane, with Applications to the 'Buckling' of the Sides of a Ship," *Proc. London Math. Soc.*, Vol. 22.
- Bulson, P. S. (1970), *Stability of Flat Plates*, American Elsevier, New York.
- Cherry, S. (1960), "The Stability of Beams with Buckled Compression Flanges," *Struct. Eng.*, Vol. 38, No. 9.
- Chwalla, E. (1936a), "Beitrag zur Stabilitätstheorie des Stegbleches vollwandiger Träger," *Stahlbau*, Vol. 9, p. 81.
- Chwalla, E. (1936b), "Die Bemessung der waagrecht ausgesteiften Stegbleche vollwandiger Träger," *Prelim Publ. IABSE, 2nd Cong.*, Berlin-Munich, p. 957.
- Clark, J. W., and Rolf, R. L. (1966), "Buckling of Aluminum Columns, Plates and Beams," *ASCE J. Struct. Div.*, Vol. 92, No. ST3, pp. 17–38.

- Conley, W. F., Becker, L. A., and Allnutt, R. B. (1963), "Buckling and Ultimate Strength of Plating Loaded in Edge Compression: Progress Report 2. Unstiffened Panels," *David Taylor Model Basin Rep. No.* 1682.
- Cook, I. T., and Rokey, K. C. (1963), "Shear Buckling of Rectangular Plates with Mixed Boundary Conditions," *Aeronaut. Q.*, Vol. 14.
- CRCJ (Column Research Committee of Japan) (1971), *Handbook of Structural Stability*, Corona Publishing Co., Tokyo.
- Crisfield, M. A. (1975), "Full Range Analysis of Steel Plates and Stiffened Plating Under Uniaxial Compression," *Proc. Inst. Civ. Eng.*, Part 2, pp. 1249–1255.
- CSA (1974, 1984), *Cold Formed Steel Structural Members*, CSA Standard S136, Canadian Standards Association, Rexdale, Ontario, Canada.
- CSA (1983), *Strength Design in Aluminum*, CAN3-S157-M83, Canadian Standards Association, Rexdale, Ontario, Canada.
- Dawe, J. L., and Kulak, G. L. (1984), "Local Buckling of W-Shaped Columns and Beams," *ASCE J. Struct. Eng.*, Vol. 110, No. 6, pp. 1292–1304.
- Dawe, J. L., and Kulak, G. L. (1986), "Local Buckling of Beam-Columns," *ASCE J. Struct. Eng.*, Vol. 112, No. 11, pp. 2447–2461.
- Dawson, R. G., and Walker, A. C. (1972), "Post-buckling of Geometrically Imperfect Plates," *ASCE J. Struct. Div.*, Vol. 98, No. ST1, pp. 75–94.
- Desmond, T. P., Peköz, T., and Winter, G. (1981a), "Edge Stiffeners for Thin-Walled Members," *ASCE J. Struct. Div.*, Vol. 107, No. ST2, Proc. Pap. 16056, pp. 329–354.
- Desmond, T. P., Peköz, T., and Winter, G. (1981b), "Intermediate Stiffeners for Thin Walled Members," *ASCE J. Struct. Div.*, Vol. 107, No. ST4, Proc. Pap. 16194, pp. 627–648.
- DeWolfe, J. T., Peköz, T., and Winter, G. (1974), "Local and Overall Buckling of Cold Formed Members," *ASCE J. Struct. Div.*, Vol. 100, No. ST10, pp. 2017–2306.
- Dow, N. F., Libove, C., and Hubka, R. E. (1954), "Formulas for the Elastic Constants of Plates with Integral Waffle-like Stiffening," *NACA Rep. No.* 1195.
- Dwight, J. B. (1971), "Collapse of Steel Compression Panels," *Proc. Conf. Dev. Bridge Des. Constr.*, Crosby Lockwood, London.
- Dwight, J. B., and Little, G. H. (1976), "Stiffened Steel Compression Flanges, a Simpler Approach," *Struct. Eng.*, Vol. 54, No. 12, pp. 501–509.
- Dwight, J. B., and Moxham, K. E. (1969), "Welded Steel Plates in Compression," *Struct. Eng.*, Vol. 47, No. 2.
- Dwight, J. B., and Ratcliffe, A. T. (1968), "The Strength of Thin Plates in Compression," in *Thin-Walled Steel Structures* (ed. K. C. Rokey and H. V. Hill), Crosby Lockwood, London.
- Elangovan, P. T., and Prinsze, M. (1992), "Critical Shear Stress of Flat Rectangular Plates with Free Edges," *J. Thin-Walled Struct.*, Vol. 13, No. 5, pp. 409–425.
- Elsharkawi, K., and Walker, A. C. (1980), "Buckling of Multibay Stiffened Plate Panels," *ASCE J. Struct. Div.*, Vol. 106, No. ST8, pp. 1695–1716.
- Fok, W. C., Walker, A. C., and Rhodes, J. (1977), "Buckling of Locally Imperfect Stiffeners in Plates," *ASCE J. Eng. Mech. Div.*, Vol. 103, No. EM5, pp. 895–911.
- Fujita, Y., Yoshida, K., and Arai, H. (1970), "Instability of Plates with Holes," 3rd Rep., *J. Soc. Nav. Archit. Jpn.*, Vol. 127, pp. 161–169.
- Fukamoto, Y., and Kubo, M. (1982), "Buckling in Steel U Shaped Beams," *ASCE J. Struct. Div.*, Vol. 108, No. ST5, pp. 1174–1190.
- Fukamoto, Y., Usami, T., and Yamaguchi, K. (1977), "Inelastic Buckling Strength of Stiffened Plates in Compression," *IABSE Period. 3/1977, IABSE Proc.* p-8/77, pp. 1–15.
- Gerard, G., and Becker, H. (1957/1958), "Handbook of Structural Stability," six parts, *NACA Tech. Notes Nos.* 3781–3786.
- Graves-Smith, T. R. (1968), "The Postbuckled Behavior of Thin Walled Columns," *8th Cong. IABSE*, New York, pp. 311–320.

- Graves-Smith, T. R. (1969), "The Ultimate Strength of Locally Buckled Columns of Arbitrary Length," in *Thin-Walled Steel Structures* (ed. K. C. Roakey and H. V. Hill), Crosby Lockwood, London.
- Graves-Smith, T. R., and Sridharan, S. (1978), "A Finite Strip Method for the Buckling of Plate Structures Under Arbitrary Loading," *Int. J. Mech. Sci.*, Vol. 20, pp. 685–693.
- Graves-Smith, T. R., and Sridharan, S. (1980), "The Local Collapse of Elastic Thin-Walled Columns," *J. Struct. Mech.*, Vol. 13, No. 4, pp. 471–489.
- Grosskurth, J. F., White, R. N., and Gallagher, R. H. (1976), "Shear Buckling of Square Perforated Plates," *ASCE J. Eng. Mech. Div.*, Vol. 102, No. EM6, Proc. Pap. 12641, pp. 1025–1040.
- Hancock, G. J. (1980), "Design Methods for Thin-Walled Box Columns," *Rep. No. 359*, University of Sydney, Sydney, Australia.
- Hancock, G. J. (1981), "Interaction Buckling of I-Section Columns," *ASCE J. Struct. Div.*, Vol. 107, No. ST1, pp. 165–181.
- Harris, H. G., and Pifko, A. B. (1969), "Elastic-Plastic Buckling of Stiffened Rectangular Plates," *Proc. Symp. Appl. Finite Elem. Methods Div. Eng.*, Vanderbilt University, Nashville, Tenn., Nov.
- Horne, M. R., and Narayanan, R. (1975), "An Approximate Method for the Design of Stiffened Steel Compression Panels," *Proc. Inst. Civ. Eng.*, Part 2, Vol. 59, pp. 501–514.
- Horne, M. R., and Narayanan, R. (1977), "Design of Axially Loaded Stiffened Plates," *ASCE J. Struct. Div.*, Vol. 103, No. ST11, pp. 2243–2257.
- Iguchi, S. (1938), "Die Knickung der rechteckigen Platte durch Schubkräfte," *Ing. Arch.*, Vol. 9, p. 1.
- Inoue, T., and Kato, B. (1993), "Analysis of Plastic Buckling of Steel Plates," *Int. J. Solids Struct.*, Vol. 30, No. 6, pp. 835–856.
- Isami, T., and Hidenori, K. (1990), "New Strength Prediction Method for Biaxially Compressed Plates," *Proc. 39th Jpn. Nat. Congr. Appl. Mech. Theor. Appl. Mech.*, Vol. 39, University of Tokyo Press, Tokyo, pp. 109–118.
- Johns, D. J. (1971), "Shear Buckling of Isotropic and Orthotropic Plates: A Review," *Tech. Rep. R&M No. 3677*, British Aeronautical Research Council, London.
- Johnson, A. E., Jr. (1957), "Charts Relating the Compressive and Shear Buckling Stress of Longitudinally Supported Plates to the Effective Deflectional Stiffness," *NACA Tech. Note No. 4188*.
- Johnson, A. L., and Winter, G. (1966), "Behavior of Stainless Steel Columns and Beams," *ASCE J. Struct. Div.*, Vol. 92, No. ST5, p. 97.
- Jombock, J. R., and Clark, J. W. (1962), "Post-buckling Behavior of Flat Plates," *Trans. Am. Soc. Civ. Eng.*, Vol. 127, Part I, pp. 227–240.
- Jombock, J. R., and Clark, J. W. (1968), "Bending Strength of Aluminum Formed Sheet Members," *ASCE J. Struct. Div.*, Vol. 94, No. ST2, pp. 511–528.
- Jones, R. M. (1975), *Mechanics of Composite Materials*, Scripta, Silver Spring, Md., pp. 264–267.
- Kalyanaraman, V., and Peköz, T. (1978), "Analytical Study of Unstiffened Elements," *ASCE J. Struct. Div.*, Vol. 104, No. ST9, pp. 1507–1524.
- Kalyanaraman, V., Peköz, T., and Winter, G. (1977), "Unstiffened Compression Elements," *ASCE J. Struct. Div.*, Vol. 103, No. ST9, pp. 1833–1848.
- Kawai, T., and Ohtsubo, H. (1968), "A Method of Solution for the Complicated Buckling Problems of Elastic Plates with Combined Use of Raleigh–Ritz Procedure in the Finite Element Method," *Proc. 2nd Air Force Conf. Matrix Methods Struct. Mech.*, Oct.
- Kemp, A. R. (1996), "Inelastic Local and Lateral Buckling in Design Codes," *ASCE J. Struct. Eng.*, Vol. 122, No. 4, pp. 374–382.
- Ketter, R. L. (1962), "Further Studies on the Strength of Beam-Columns," *Trans. ASCE*, Vol. 127, No. 2, p. 224.
- Klitchieff, J. M. (1949), "On the Stability of Plates Reinforced by Ribs," *J. Appl. Mech.*, Vol. 16, No. 1.
- Klöppel, K., Schmied, R., and Schubert, J. (1969), "Ultimate Strength of Thin Walled Box Shaped Columns Under Concentric and Eccentric Loads: Post Buckling Behavior of Plate Elements and Large Deformations Are Considered," *Stahlbau*, Vol. 38, pp. 9–19, 73–83.

- Koiter, W. T. (1963), "Introduction to the Post-buckling Behavior of Flat Plates," *Int. Colloq. Comportement Postcritiques Plaques Utilisée Constr. Metall.*, Institute of Civil Engineering, Liege, Belgium.
- Kroll, W. D., Fisher, G. P., and Heimerl, G. J. (1943), "Charts for the Calculation of the Critical Stress for Local Instability of Columns with I, Z, Channel and Rectangular Tube Sections," *NACA Wartime Rep. No. L-429*.
- Kuhlmann, U. (1989), "Definition of Flange Slenderness Limits on the Basis of Rotation Capacity Values," *J. Constr. Steel Res.*, Vol. 14, No. 1, pp. 21–40.
- Kumai, T. (1952), "Elastic Stability of a Square Plate with a Central Circular Hole Under Edge Thrust," *Rep. Inst. Appl. Mech. Kyusyn Univ.*, Vol. 1, No. 2, p. 1.
- Kusuda, T. (1959), "Buckling of Stiffened Panels in Elastic and Strain-Hardening Range," *Rep. No. 39*, Transportation Technical Research Institute (Unyn-Gijutsu Kenkyujo Mejiro, Toshima-Ku), Tokyo.
- LaBoube, R. A., and Yu, W. W. (1982), "Bending Strength of Webs of Cold-Formed Steel Beams," *ASCE J. Struct. Div.*, Vol. 108, No. ST7, pp. 1589–1604.
- Lau, J. H. (1981), "Stiffness of Corrugated Plate," *ASCE J. Eng. Mech. Div.*, Vol. 17, No. EM1, pp. 271–275.
- Lau, S. C. W., and Hancock, G. J. (1989), "Inelastic Buckling Analysis of Beams, Columns and Plates Using the Spline Finite Strip Method," *J. Thin-Walled Struct.*, Vol. 7, No. 3–4, pp. 213–238.
- Lay, M. G. (1965), "Flange Local Buckling in Wide-Flange Shapes," *ASCE J. Struct. Div.*, Vol. 91, No. ST6, pp. 49–66.
- Legget, D. M. A. (1941), "The Buckling of a Square Panel in Shear When One Pair of Opposite Edges Is Clamped and the Other Pair Simply Supported," *Tech. Rep. R&M No. 1991*, British Aeronautical Research Council, London.
- Levy, S., Wolley, R. M., and Knoll, W. D. (1947), "Instability of Simply Supported Square Plate with Reinforced Circular Hole in Edge Compression," *J. Res. Natl. Bur. Stand.*, Vol. 39, pp. 571–577.
- Libove, C. (1983), "Buckle Pattern of Biaxially Compressed Simply Supported Orthotropic Rectangular Plates," *J. Compos. Mater.*, Vol. 17, No. 1, pp. 45–48.
- Libove, C., and Batdorf, S. B. (1948), "A General Small-Deflection Theory for Flat Sandwich Plates," *NACA Rep. No. 899*.
- Libove, C., and Hubka, R. E. (1951), "Elastic Constants for Corrugated-Core Sandwich Plates," *NACA Tech. Note No. 2289*.
- Lind, N. C. (1973), "Buckling of Longitudinally Stiffened Sheets," *ASCE J. Struct. Div.*, Vol. 99, No. ST7, pp. 1686–1691.
- Lind, N. C., Ravindra, M. K., and Schorn, G. (1976), "Empirical Effective Width Formula," *ASCE J. Struct. Div.*, Vol. 102, No. ST9, pp. 1741–1957.
- Little, G. H. (1976), "Stiffened Steel Compression Panels: Theoretical Failure Analysis," *Struct. Eng.*, Vol. 54, No. 12, pp. 489–500.
- Little, G. H. (1979), "The Strength of Square Steel Box-Columns: Design Curves and Their Theoretical Basis," *Struct. Eng.*, Vol. 57.
- Lu, L. W., and Kamalvand, H. (1968), "Ultimate Strength of Laterally Loaded Columns," *ASCE J. Struct. Div.*, Vol. 94, No. ST6, pp. 1505–1524.
- May, I. M., and Ganaba, T. H. (1988), "Elastic Stability of Plates with and Without Openings," *J. Eng. Comput.*, Vol. 5, No. 1, pp. 50–52.
- McKenzie, K. I. (1964), "The Buckling of Rectangular Plate Under Combined Biaxial Compression, Bending and Shear," *Aeronaut. Q.*, Vol. 15, No. 3, pp. 239–246.
- Merrison Committee (1973), "Inquiry into the Basis of Design and Method of Erection of Steel Box Girder Bridges (Interior Design and Workmanship Rules)," Merrison Committee, London.
- Michael, M. E. (1960), "Critical Shear Stress for Webs with Holes," *J. R. Aeronaut. Soc.*, Vol. 64, p. 268.
- Moheit, W. (1939), "Schubbeulung rechteckiger Platten mit eingespannten Rändern," Thesis, Technische Hochschule Darmstadt, Leipzig, Germany.

- Murray, J. M. (1946), "Pietzker's Effective Breadth of Flange Reexamined," *Engineering*, Vol. 161, p. 364.
- Murray, N. W. (1973), "Buckling of Stiffened Panel Loaded Axially and in Bending," *Struct. Eng.*, Vol. 51, No. 8, pp. 285–301.
- Murray, N. W. (1975), "Analysis and Design of Stiffened Plates for Collapse Load," *Struct. Eng.*, Vol. 53, No. 3, pp. 153–158.
- Nemeth, J. and Michael, P. (1990), "Buckling and Post-buckling Behavior of Compression-Loaded Isotropic Plates with Cutouts," *Proc. 31st Struct. Dyn. Mater. Conf.*, April 2–4 Part 2, American Institute of Aeronautics and Astronautics, New York, pp. 862–876.
- Newell, J. S. (1930), "The Strength of Aluminum Alloy Sheets," *Airway Age*, Vol. 11, p. 1420; Vol. 12, p. 1548.
- Nguyen, R. P., and Yu, W. W. (1982), "Longitudinally Reinforced Cold-Formed Steel Beam Webs," *ASCE J. Struct. Div.*, Vol. 108, No. ST11, pp. 2423–2442.
- Pavlovic, M. N., and Baker, G. (1989), "Effect of Non-uniform Stress Distribution on the Stability of Biaxially Compressed Plates," *Int. J. Struct. Mech. Mater. Sci.*, Vol. 28, No. 1–4, pp. 69–89.
- Perel, D., and Libove, C. (1978), "Elastic Buckling of Infinitely Long Trapezoidally Corrugated Plates in Shear," *Trans. ASME J. Appl. Mech.*, Vol. 45, pp. 579–582.
- Peters, R. W. (1954), "Buckling of Long Square Tubes in Combined Compression and Torsion and Comparison with Flat-Plate Buckling Theories," *NACA Tech. Note No. 3184*.
- Ramberg, W., McPherson, A. E., and Levy, S. (1939), "Experiments on Study of Deformation and of Effective Width in Axially Loaded Sheet-Stringer Panels," *NACA Tech. Note No. 684*.
- Redwood, R. G., and Uenoya, M. (1979), "Critical Loads for Webs with Holes," *ASCE J. Struct. Div.*, Vol. 105, No. ST10, pp. 2053–2068.
- Rhodes, J., and Harvey, J. M. (1971), "Effects of Eccentricity of Load or Compression on the Buckling and Post-buckling Behavior of Flat Plates," *Int. J. Mech. Sci.*, Vol. 13, pp. 867–879.
- Rhodes, J., and Harvey, J. M. (1976), "Plain Channel Section Struts in Compression and Bending Beyond the Local Buckling Load," *Int. J. Mech. Sci.*, Vol. 8, pp. 511–519.
- Rhodes, J., and Harvey, J. M. (1977), "Examination of Plate Post Buckling Behavior," *ASCE J. Eng. Mech. Div.*, Vol. 103, No. EM3, pp. 461–480.
- Rhodes, J., and Loughlan, J. (1980), "Simple Design Analysis of Lipped Simple Columns," *Proc. 5th Int. Spec. Conf. Cold-Formed Steel Struct.*, St. Louis, Mo.
- Rockey, K. C. (1980), "The Buckling and Post-buckling Behavior of Shear Panels Which Have a Central Circular Cut Out," in *Thin Walled Structures* (ed. J. Rhodes and A. C. Walker), Granada, London.
- Rockey, K. C., Anderson, R. G., and Cheung, Y. K. (1969), "The Behavior of Square Shear Webs Having a Circular Hole," in *Thin-Walled Steel Structures* (ed. K. C. Rockey and H. V. Hill), Crosby Lockwood, London.
- Roorda, J., and Venkataramaiah, K. R. (1979), "Effective Width of Stiffened Cold-Formed Steel Plates," *Can J. Civ. Eng.*, Vol. 6, No. 3.
- Schlack, A. L. (1964), "Elastic Stability of Pierced Square Plates," *Exp. Mech.*, p. 167.
- Schuman, L., and Back, G. (1930), "Strength of Rectangular Flat Plates Under Edge Compression," *NACA Tech. Rep. No. 356*.
- Seide, P., and Stein, M. (1949), "Compressive Buckling of Simply Supported Plates with Longitudinal Stiffeners," *NACA Tech. Note No. 1825*.
- Seydel, E. (1933), Über das Ausbeulen von rechteckigen isotropen oder orthogonalanisotropen Platten bei Schubbeanspruchung," *Ing. Arch.*, Vol. 4, p. 169.
- Sharp, M. L. (1966), "Longitudinal Stiffeners for Compression Members," *ASCE J. Struct. Div.*, Vol. 92, No. ST5, pp. 187–212.
- Sharp, M. L. (1970), "Strength of Beams or Columns with Buckled Elements," *ASCE J. Struct. Div.*, Vol. 96, No. ST5, pp. 1011–1015.
- Sherbourne, A. N., Marsh, C., and Lian, C. Y. (1971), "Stiffened Plates in Uniaxial Compression," *IABSE Publ.*, Vol. 31-I, Zurich, pp. 145–178.

- Škaloud, M., and Zornerova, M. (1970), "Experimental Investigation into the Interaction of the Buckling of Compressed Thin-Walled Columns with the Buckling of Their Plate Elements," *Acta Technica CSAV* No. 4.
- Southwell, R. V., and Skan, S. (1924), "On the Stability Under Shearing Force of a Flat Elastic Strip," *Proc. R. Soc.*, Vol. A105.
- Sridharan, S. (1982), "A Semi-analytical Method for the Post-Local-Torsional Buckling Analysis of Prismatic Plate Structures," *Int. J. Numer. Methods Eng.*, Vol. 18, pp. 1685–1607.
- Sridharan, S., and Graves-Smith, T. R. (1981), "Post-buckling Analysis with Finite Strips," *ASCE J. Eng. Mech. Div.*, Vol. 107, No. EM5, pp. 869–888.
- Stein, O. (1936), "Stabilität ebener Rechteckbleche unter Biegung und Schub," *Bauingenieur*, Vol. 17, p. 308.
- Stein, M. (1959), "The Phenomenon of Change in Buckle Pattern in Elastic Structures," *NACA Tech. Note No. R-39*.
- Stein, M. (1989), "Effect of Transverse Shearing Flexibility on Post-buckling on Plates in Shear," *AIAA J.*, Vol. 27, No. 5, pp. 652–655.
- Stowell, E. Z. (1948), "A Unified Theory of Plastic Buckling of Columns and Plates," *NACA Tech. Note No. 1556*.
- Stowell, E. Z. (1949), "Plastic Buckling of a Long Flat Plate Under Combined Shear and Longitudinal Compression," *NACA Tech. Note No. 1990*.
- Stowell, E. Z., Heimerl, G. J., Libove, C., and Lundquist, E. E. (1952), "Buckling Stresses for Flat Plates and Sections," *Trans. Am. Soc. Civ. Eng.*, Vol. 117, pp. 545–578.
- Supple, W. J. (1980), "Buckling of Plates Under Axial Load and Lateral Pressures," in *Thin Walled Structures* (ed. J. Rhodes and A. C. Walker), Granada, London.
- Thomasson, P.-O. (1978), "Thin-Walled C-Shaped Panels in Axial Compression," *Document D.I. 1978*, Swedish Council for Building Research, Stockholm.
- Tien, Y. L., and Wang, S. T. (1979), "Local Buckling of Beams Under Stress Gradient," *ASCE J. Struct. Div.*, Vol. 105, No. ST8, pp. 1571–1588.
- Timoshenko, S. (1910), "Einge Stabilitätsprobleme der Elastizitätstheorie," *Z. Math. Phys.*, Vol. 58, pp. 337.
- Timoshenko, S. (1934), "Stability of the Webs of Plate Girders," *Engineering*, Vol. 138, p. 207.
- Timoshenko, S. P., and Gere, J. M. (1961), *Theory of Elastic Stability*, 2nd ed., McGraw-Hill, New York.
- Troitsky, D. S. C. (1976), *Stiffened Plates, Bending, Stability and Vibrations*, Elsevier, New York.
- Tsien, H. S. (1942), "Buckling of a Column with Nonlinear Lateral Supports," *J. Aeronaut. Sci.*, Vol. 9, No. 4.
- Tvergaard, V. (1973), "Imperfection-Sensitivity of a Wide Integrally Stiffened Panel Under Compression," *Int. J. Solids Struct.*, Vol. 9, pp. 177–192.
- Usami, T. (1982), "Post Buckling of Plates in Compression and Bending," *ASCE J. Struct. Div.*, Vol. 108, No. ST3, pp. 591–609.
- Usami, T., and Fukumoto, Y. (1982), "Local and Overall Buckling of Welded Box Columns," *ASCE J. Struct. Div.*, Vol. 108, No. ST3, pp. 525–542.
- Vojta, J. F., and Ostapenko, A. (1967), "Ultimate Strength Design Curves for Longitudinally Stiffened Plate Panels with Large b/t ," *Fritz Eng. Lab. Rep. No. 248.19*, Lehigh University, Bethlehem, Pa.
- von Kármán, T., Sechler, E. E., and Donnell, L. H. (1932), "Strength of Thin Plates in Compression," *Trans. A.S.M.E.*, Vol. 54, No. APM-54-5, p. 53.
- Walker, A. C. (1964), "Thin Walled Structural Forms Under Eccentric Compressive Load Actions," Doctoral thesis, University of Glasgow, Glasgow, Scotland.
- Wang, S. T. (1969), "Cold-Rolled Austenitic Stainless Steel: Material Properties and Structural Performance," *Cornell Univ. Dept. Struct. Eng. Rep. No. 334*.
- Wang, S. T., and Pao, H. Y. (1981), "Torsional-Flexural Buckling of Locally Buckled Columns," *Int. J. Comput. Struct.*, Vol. 11.

- Wang, S. T., Errera, S. J., and Winter, G. (1975), "Behavior of Cold Rolled Stainless Steel Members," *ASCE J. Struct. Div.*, Vol. 101, No. ST11, pp. 2337–2357.
- Wang, S. T., Yost, M. I., and Tien, Y. L. (1977), "Lateral Buckling of Locally Buckled Beams Using Finite Element Techniques," *Int. J. Comput. Struct.*, Vol. 7.
- Way, S. (1936), "Stability of Rectangular Plates Under Shear and Bending Forces," *J. Appl. Mech. ASME*, Dec. Vol. 3, No. 4, pp. A131–A135.
- Webb, S. E., and Dowling, P. J. (1980), "Large Deflection Elasto-plastic Behavior of Discretely Stiffened Plates," *Proc. Inst. Civ. Eng.*, Part 2, Vol. 69, pp. 375–401.
- Whitney, J. M., and Leissa, A. W. (1969), "Analysis of Heterogeneous Anisotropic Plates," *Trans. ASME J. Appl. Mech.*, Vol. 36, pp. 261–266.
- Winter, G. (1947), "Strength of Thin Steel Compression Flanges," *Trans. ASCE*, Vol. 112, p. 527.
- Winter, G. (1983), "Commentary on the 1968 Edition of the Specification for the Design of Steel Structural Members," in *Cold-Formed Steel Design Manual*, American Iron and Steel Institute, Washington, D.C.
- Winter, G., Lansing, W., and McCalley, R. B. (1950), "Four Papers on the Performance of Thin Walled Steel Structures," *Eng. Exp. Strn. Rep. No. 33*, Cornell University, Ithaca, N.Y., pp. 27–32, 51–57.
- Wittrick, W. H. (1952), "Correlation Between Some Stability Problems for Orthotropic and Isotropic Plates Under Bi-axial and Uniaxial Direct Stress," *Aeronaut. Q.*, Vol. 4, pp. 83–99.
- Wittrick, W. H. (1968), "A Unified Approach to the Initial Buckling of Stiffened Panels in Compression," *Aeronaut. Q.*, Vol. 19, p. 265.
- Wittrick, W. H., and Horsington, R. W. (1984), "Buckling and Vibration of Composite Folded Plate Structures of Finite Length in Combined Shear and Compression," *Proc. R. Soc. London*, Vol. A392, pp. 107–144.
- Yamaki, N. (1959/1960), "Post-buckling Behavior of Rectangular Plates with Small Initial Curvature Loaded in Edge Compression," *J. Appl. Mech. ASME*, Vol. 26, pp. 407–414; Vol. 27, pp. 335–342.
- Yang, H. T. Y. (1969), "A Finite Element Formulation for Stability Analysis of Doubly Curved Thin Shell Structures," Doctoral thesis, Cornell University, Ithaca, N.Y.
- Yoshizuka, J., and Naruoka, M. (1971), "Buckling Coefficient of Simply Supported Rectangular Plates Under Combined Bending and Compressive Stresses in Two Perpendicular Directions," *Stahlbau*, Vol. 40, p. 217.
- Yu, W. W., and Davis, C. S. (1973), "Cold Formed Steel Members with Perforated Elements," *ASCE J. Struct. Div.*, Vol. 99, No. ST10, p. 2061.
- Zender, W., and Hall, J. B., Jr. (1960), "Combinations of Shear Compressive Thermal and Compressive Load Stresses for the Onset of Permanent Buckles in Plates," *NASA Tech. Note No. D-384*.

New references

- AA (2005), *Aluminum Design Manual*, Aluminum Association, Washington, D.C.
- AISC (2005) *Specification for Structural Steel Buildings*, American Institute of Steel Construction, Chicago, IL, AISC 360-05.
- AISC (2005b) *Seismic Provisions for Structural Steel Buildings*, American Institute of Steel Construction, Chicago, IL, AISC 341-05.
- AISI (2007) *Specification for the Design of Cold-Formed Steel Structural Members*, American Iron and Steel Institute, Washington, D.C., AISI-S100-07.
- Brown, C.J., and Yettram, A.L. (2000). "Factors influencing the elastic stability of orthotropic plates containing a rectangular cut-out." *Journal of Strain Analysis for Engineering Design*, 35(6), 445–458.
- El-Sawy, K.M., and Nazmy, A.S. (2001). "Effect of aspect ratio on the elastic buckling of uniaxially loaded plates with eccentric holes." *Thin-Walled Structures*, 39(12), 983–998.

- Kesti, J. (2000). "Local and Distortional Buckling of Perforated Steel Wall Studs," Dissertation/Thesis, Helsinki University of Technology, Espoo, Finland.
- Miller, T.H., and Peköz, T. (1994). "Unstiffened strip approach for perforated wall studs." *ASCE Journal of Structural Engineering*, 120(2), 410-421.
- Moen, C., Schafer, B.W. (2008). "Simplified Methods for Predicting Elastic Buckling of Cold-Formed Steel Structural Members with Holes" *Proceedings of the 19th International Specialty Conference on Cold-Formed Steel*, St. Louis, MO. pp 17-32.
- Moen, C.D., and Schafer, B.W. (2006). "Impact of holes on the elastic buckling of cold-formed steel columns with applications to the Direct Strength Method." Eighteenth International Specialty Conference on Cold-Formed Steel Structures, Orlando, FL, 269-283.
- Tovar, J., and Sposito, T. (2005). "Application of direct strength method to axially loaded perforated cold-formed steel studs: Distortional and local buckling." *Thin-Walled Structures*, 43(12), 1882-1912.
- Vann, P.W. (1971). "Compressive buckling of perforated plate elements." First Specialty Conference on Cold-formed Structures, Rolla, Missouri, 58-64.

More new references

- Bambach, M. R. (2008). "Inclined yield lines in flange outstands." *Structural Engineering and Mechanics*, 29(6), 623-642.
- Bambach, M. R., and Rasmussen, K. J. R. (2004a). "Design provisions for sections containing unstiffened elements with stress gradient." *Journal of Structural Engineering*, 130(10), 1620-1628.
- Bambach, M. R., and Rasmussen, K. J. R. (2004b). "Effective widths of unstiffened elements with stress gradient." *Journal of Structural Engineering*, 130(10), 1611-1619.
- Bradford, M. A. (1992). "Lateral-Distortional buckling of steel I-Section members." *Journal of Constructional Steel Research*, 23(1-3), 97-116.
- Bradford, M. A., and Azhari, M. (1995). "Inelastic local buckling of plates and plate assemblies using bubble functions." *Engineering Structures*, 17(2), 95-103.
- Bradford, M. A., and Hancock, G. J. (1984). "Elastic interaction of local and lateral buckling in beams." *Thin-Walled Structures*, 2(1), 1-25.
- Brown, C. J., and Yettam, A. L. (1986). "The elastic stability of square perforated plates under combinations of bending, shear and direct load." *Thin-Walled Structures*, 4(3), 239-246.
- Caccese, V., Elgaaly, M., and Chen, R. (1993). "Experimental study of thin steel-plate shear walls under cyclic load." *Journal of structural engineering New York, N.Y.*, 119(2), 573-587.
- Davidson, J. S., Ballance, S. R., and Yoo, C. H. (1999). "Analytical model of curved I-girder web panels subjected to bending." *Journal of Bridge Engineering*, 4(3), 204-212.
- Earls, C. J. (1999). "On the inelastic failure of high strength steel I-shaped beams." *Journal of Constructional Steel Research*, 49(1), 1-24.
- Elgaaly, M. (1998). "Thin steel plate shear walls behavior and analysis." *Thin-Walled Structures*, 32(1-3), 151-180.
- Elgaaly, M., Caccese, V., and Du, C. (1993). "Postbuckling behavior of steel-plate shear walls under cyclic loads." *Journal of structural engineering New York, N.Y.*, 119(2), 588-605.
- Featherston, C. A., and Ruiz, C. (1998). "Buckling of curved panels under combined shear and compression." *Proceedings of the Institution of Mechanical Engineers, Part C: Journal of Mechanical Engineering Science*, 212(3), 183-196.
- Ghavami, K. (1994). "Experimental study of stiffened plates in compression up to collapse." *Journal of Constructional Steel Research*, 28(2), 197-221.
- Gioncu, V., and Petcu, D. (1997). "Available Rotation Capacity of Wide-Flange Beams and Beam-Columns: Part 1. Theoretical Approaches." *Journal of Constructional Steel Research*, 43(1-3), 161-217.
- Goncalves, R., and Camotim, D. (2007). "Thin-walled member plastic bifurcation analysis using generalised beam theory." *Advances in Engineering Software*, 38(8-9), 637-646.

- Grondin, G. Y., Chen, Q., Elwi, A. E., and Cheng, J. J. (1998). "Stiffened Steel Plates under Compression and Bending." *Journal of Constructional Steel Research*, 45(2), 125-148.
- Grondin, G. Y., Elwi, A. E., and Cheng, J. J. R. (1999). "Buckling of stiffened steel plates - A parametric study." *Journal of Constructional Steel Research*, 50(2), 151-175.
- Hancock, G. J. (1978). "LOCAL, DISTORTIONAL, AND LATERAL BUCKLING OF I-BEAMS." *ASCE J Struct Div*, 104(11), 1787-1798.
- Hancock, G. J., Kwon, Y. B., and Stefan Bernard, E. (1994). "Strength design curves for thin-walled sections undergoing distortional buckling." *Journal of Constructional Steel Research*, 31(2-3), 169-186.
- Hitaka, T., and Matsui, C. (2003). "Experimental study on steel shear wall with slits." *Journal of Structural Engineering*, 129(5), 586-595.
- Kosteski, N., Packer, J. A., and Puthli, R. S. (2003). "A finite element method based yield load determination procedure for hollow structural section connections." *Journal of Constructional Steel Research*, 59(4), 453-471.
- Kwon, Y. B., and Hancock, G. J. (1991). "A nonlinear elastic spline finite strip analysis for thin-walled sections." *Thin-Walled Structures*, 12(4), 295-319.
- Lau, S. C. W., and Hancock, G. J. (1986). "Buckling of thin flat-walled structures by a spline finite strip method." *Thin-Walled Structures*, 4(4), 269-294.
- Lau, S. C. W., and Hancock, G. J. (1987). "DISTORTIONAL BUCKLING FORMULAS FOR CHANNEL COLUMNS." *Journal of structural engineering New York, N.Y.*, 113(5), 1063-1078.
- Lau, S. C. W., and Hancock, G. J. (1989). "Inelastic buckling analyses of beams, columns and plates using the spline finite strip method." *Thin-Walled Structures*, 7(3-4), 213-238.
- Libove, C., Ferdman, S., and Reusch, J. J. (1949). "Elastic buckling of a simply supported plate under a compressive stress that varies linearly in the direction of loading." *NACA Technical Note No. 1891*, 1891.
- Lubell, A. S., Prion, H. G. L., Ventura, C. E., and Rezai, M. (2000). "Unstiffened steel plate shear wall performance under cyclic loading." *Journal of structural engineering New York, N.Y.*, 126(4), 453-460.
- Mikami, I., and Niwa, K. (1996). "Ultimate compressive strength of orthogonally stiffened steel plates." *Journal of Structural Engineering*, 122(6), 674-681.
- Paik, J. K., Thayamballi, A. K., and Lee, J. M. (2004). "Effect of Initial Deflection Shape on the Ultimate Strength Behavior of Welded Steel Plates Under Biaxial Compressive Loads." *Journal of Ship Research*, 48(1), 45-60.
- Papangelis, J. P., and Hancock, G. J. (1995). "Computer analysis of thin-walled structural members." *Computers and Structures*, 56(1), 157-176.
- Peköz, T. (1987). "DEVELOPMENT OF A UNIFIED APPROACH TO THE DESIGN OF COLD-FORMED STEEL MEMBERS." American Iron and Steel Institute.
- Roberts, T. M., and Sabouri-Ghomi, S. (1992). "Hysteretic characteristics of unstiffened perforated steel plate shear panels." *Thin-Walled Structures*, 14(2), 139-151.
- Sabouri-Ghomi, S., and Roberts, T. M. (1992). "Nonlinear dynamic analysis of steel plate shear walls including shear and bending deformations." *Engineering Structures*, 14(5), 309-317.
- Schafer, B. W. (2002). "Local, distortional, and Euler buckling of thin-walled columns." *Journal of Structural Engineering*, 128(3), 289-299.
- Schafer, B. W., and Adany, S. "Buckling analysis of cold-formed steel members using CUFSM: Conventional and constrained finite strip methods." *Eighteenth International Specialty Conference on Cold-Formed Steel Structures*, Orlando, FL, United States, 39-54.
- Schafer, B. W., and Peköz, T. (1998). "Cold-formed Steel Members with Multiple Longitudinal Intermediate Stiffeners." *Journal of Structural Engineering*, 124(10), 1175-1181.
- Schafer, B. W., and Peköz, T. (1999). "Laterally braced cold-formed steel flexural members with edge stiffened flanges." *Journal of Structural Engineering*, 125(2), 118-126.

- Shahwan, K. W., and Waas, A. M. (1998). "Buckling of unilaterally constrained infinite plates." *Journal of Engineering Mechanics*, 124(2), 127-136.
- Sheikh, I. A., Elwi, A. E., and Grondin, G. Y. (2003). "Stiffened steel plates under combined compression and bending." *Journal of Constructional Steel Research*, 59(7), 911-930.
- Shi, Y. J., Chan, S. L., and Wong, Y. L. (1996). "Modeling for moment-rotation characteristics for end-plate connections." *Journal of Structural Engineering*, 122(11), 1300-1306.
- Silvestre, N., and Camotim, D. (2002). "Second-order generalised beam theory for arbitrary orthotropic materials." *Thin-Walled Structures*, 40(9), 791-820.
- Smith, S. T., Bradford, M. A., and Oehlers, D. J. (1999). "Local buckling of side-plated reinforced-concrete beams. I: Theoretical study." *Journal of Structural Engineering*, 125(6), 622-633.
- Yu, C., and Schafer, B. W. (2006). "Effect of longitudinal stress gradient on the ultimate strength of thin plates." *Thin-Walled Structures*, 44(7), 787-799.
- Yu, C., and Schafer, B. W. (2007). "Effect of longitudinal stress gradients on elastic buckling of thin plates." *Journal of Engineering Mechanics*, 133(4), 452-463.